Optimization in cognitive radio systems with successive interference cancellation and relaying

Marwa Chami

le cnam

École doctorale Informatique, Télécommunications et Électronique

Centre d'Études et de Recherche en Informatique et Communications

THÈSE DE DOCTORAT

présentée par : **Marwa CHAMI**

soutenue le : **12 mai 2016**

pour obtenir le grade de : **Docteur du Conservatoire National des Arts et Métiers**

Spécialité : **Radiocommunications**

Optimization in cognitive radio systems with successive interference cancellation and relaying

THÈSE DIRIGÉE PAR

M. LE RUYET Didier	*Professeur des Universités, CNAM Paris*

RAPPORTEURS

M. GORCE Jean-Marie	*Professeur des universités, CITI lab, Insa Lyon, Inria*
M. HELARD Jean-François	*Professeur des Universités, INSA Rennes*

PRÉSIDENT

M. DUHAMEL Pierre	*Directeur de recherches, CNRS, LSS*

EXAMINATEURS

Mme. PISCHELLA Mylène	*Maître de conférences, CNAM Paris*
M. BADER Carlos Faouzi	*Professeur adjoint, CentraleSupelec, Rennes*
M. KOUNTOURIS Marios	*Associate professor, SUPÉLEC*

Optimisation des systèmes cognitifs avec annulation successive d'interférence et relayage

Marwa CHAMI

le cnam

To Ali

Acknowledgment

First and foremost, I would like to thank God, whose many blessings have made me who I am today.

I wish to express my sincere gratitude to the persons who helped to make my three-year's PhD a valuable experience and a pleasing journey that I will never forget.

I am truly grateful to my thesis advisor, Prof. Didier Le Ruyet, and to my supervisor, Dr. Mylène Pischella, for all their help throughout my PhD studies. Their guidance helped me in all the time of research and writing of this dissertation.

I would like to thank the jury members, Prof. Jean-Marie Gorce, Prof. Jean-François Hélard, Prof. Pierre Duhamel, Dr. Carlos Faouzi Bader, Dr. Marios Kountouris, for reviewing and discussing my dissertation.

My thanks also goes to all my colleagues and friends, with whom I passed many years of enriching interaction. I mention Fatima, Nour, Salma, Hanen, Iness, Imad, Ali Kabalan, Wosen, Juwendo, Ali Dziri, Hmaied and Félix for their help and support.

A very special thanks goes to two special persons who left us last year, My uncle Ali El Chami and My dear friend Ali Fayyad, for their support and love.

Last but not least, my sincere feelings of gratitude to my parents, Mohamad and Zeinab, my brothers, Toufic and Bassel, and my sister, Maya for their love, patience and encouragement throughout my life.

Finally, I would like to express my deep love to the person who stood by my side and taught me many things through these years. You make my life complete.

Abstract

Cognitive Radio (CR) is a promising technique for efficient spectrum utilization. It was introduced due to the scarcity of frequency spectrum in view of the evolution of wireless communication technologies. The CR technology permits an unlicensed user called Secondary User (SU) to coexist with the licensed user called Primary User (PU) without degrading his performance. In a CR system, the SU has the ability to sense and adapt to his environment in order to detect possible frequency holes in the wireless spectrum and transmit in it under some constraints so as to increase the total data rate. Besides, resource allocation in CR systems is one of the most common studied scenarios especially for multi-carrier transmissions, with the aim to maximize the system throughput.

In this thesis, we investigate the resource allocation problem for an uplink multi-user underlay CR system where the SU is allowed to coexist with the PU provided that the interference caused to the PU is below a predefined threshold. We apply two decoding techniques, Successive Interference Cancellation (SIC) and Superposition Coding (SC), at the SU in order to maximize the secondary rate.

In a first step, the single-user scenario is studied, assuming perfect channel state information (CSI) at the SU. We evaluate the performance of the system by proposing an adaptive decoding algorithm where the SU can either treat the interference as noise or perform SIC or SC. We investigate the power allocation problem taking into account the power budget and the interference threshold constraints. A general solution for the power optimization problem in an uplink underlay CR system is proposed. Both theoretical analysis and simulation results show that the proposed algorithm achieves higher sum rate than classical algorithms, providing high-enough data rates for the secondary system at the expense of a very low degradation of the primary system's rate.

Then, the secondary multi-user scenario is investigated, where multiple users are allowed to exist in the secondary cell. Power and subcarrier allocation problems are detailed in order to maximize the secondary rate. We highlight the benefits of the proposed multi-user adaptive algorithm which encompasses three phases. The first step includes the adaptive selection of the decoding strategy at the secondary receiver. The second step describes the subcarrier allocation among the different users. Finally, the third step details the optimal distribution of the available power budget on the users.

However, perfect channel knowledge requires perfect channel measurements at the receiver and a perfect feedback link to send this channel information to the transmitter, which may be

impractical to implement. Thus, we also study the single-user scenario assuming that only statistical CSI of channel gains between the primary transmitter and both primary and secondary receivers is available at the SU. We detail the analytical expressions for the outage probabilities and then we solve the non-convex optimization problem using a sequential approximation algorithm. Simulations show that the proposed algorithm is efficient and robust with statistical CSI. This work can be easily extended to the multi-user case.

Finally, we propose a new system model where the secondary receiver acts as a Full-Duplex (FD) relay node in order to maximize the primary rate and thus the total system rate. The proposed scenario is first studied for single-carrier modulation scheme for both Amplify-and-Forward (AF) and Decode-and-Forward (DF) relaying protocols. The constraints to apply Successive Interference Cancellation (SIC) and to relay are determined and the new achievable rates are specified such that the relay node relays whenever the new achievable rate is better than the one achieved without relying. Furthermore, the performance of the DF relaying scheme in the FD mode is evaluated for multi-carrier modulation. The performance of the proposed system model is evaluated via simulations and an important improvement of the primary achievable rate and thus of the total system rate is shown.

Keywords— Cognitive radio, Underlay, Optimization, Maximum sum-rate, OFDM, Multiuser, Imperfect CSI, Relay, Full-Duplex.

Résumé

La Radio Cognitive (CR pour Cognitive Radio) est une technique prometteuse pour assurer une utilisation efficace du spectre. Elle a été introduite en raison de la rareté du spectre des fréquences, compte tenu de l'évolution des technologies des communications sans fil. La CR permet à un utilisateur non licencié appelé utilisateur secondaire (SU pour Secondary User) de coexister avec un utilisateur agréé appelé utilisateur primaire (PU pour Primary User) sans dégrader les performances du dernier. Dans un système de CR, le SU a la capacité de détecter et de s'adapter à son environnement afin de détecter des trous de fréquences possibles dans le spectre sans fil et transmettre dans ces trous sous certaines contraintes de manière à augmenter le débit total. Par ailleurs, l'allocation des ressources dans les systèmes CR forme l'un des scénarios étudiés les plus courantes en particulier pour des transmissions à porteuses multiples, dans le but de maximiser le débit du système.

Dans cette thèse, nous étudions le problème d'allocation des ressources pour un système CR à multi-utilisateur pour une transmission de liaison montante. On considère le scénario underlay où le SU est autorisé à coexister avec le PU à condition que l'interférence causé au PU soit inférieure à un seuil prédéfini. Nous appliquons deux techniques de décodage, l'annulation successive d'interférence (SIC pour Successive Interference Cancellation) et le codage à superposition (SC pour Superposition Coding), au SU afin de maximiser le débit secondaire.

Dans une première étape, le scénario mono-utilisateur est étudié, en supposant que les informations d'état de canal sont connues parfaitement au SU. Nous évaluons la performance du système en proposant un algorithme de décodage adaptatif où le SU peut soit traiter l'interférence venant du primaire comme du bruit, ou bien appliquer le SIC ou SC. Nous étudions le problème d'allocation de puissance en tenant compte du budget de puissance et des contraintes de seuil d'interférence. Une solution générale pour le problème d'optimisation de puissance dans un système de liaison montante pour un système underlay CR est proposée. L'analyse des simulations et les résultats théoriques montrent que l'algorithme proposé assure une augmentation sur le débit total du système, en se comparant aux algorithmes classiques.

Ensuite, le scénario multi-utilisateurs secondaires est étudié, où plusieurs utilisateurs sont autorisés à exister dans la cellule secondaire. Les problèmes d'allocation de puissance et de sous-porteuses sont détaillés dans le but de maximiser le débit secondaire. Nous mettons en évidence les avantages de l'algorithme adaptatif dans le cas multi-utilisateur, qui comprend trois phases. La première étape comprend la sélection adaptative de la stratégie de décodage au niveau du récepteur secondaire. La deuxième étape décrit l'attribution de sous-porteuses parmi

les différents utilisateurs. Enfin, la troisième étape détaille la répartition optimale du budget de puissance disponible sur les utilisateurs.

Cependant, la connaissance parfaite du canal nécessite des mesures de canal parfait au niveau du récepteur et un lien de rétroaction parfaite pour envoyer ces informations à l'émetteur, ce qui peut être impossible à mettre en œuvre. Ainsi, nous étudions aussi le scénario mono-utilisateur en supposant que juste la connaissance statistique des gains de canaux primaires est disponible au SU. Nous détaillons les expressions analytiques pour les probabilités de panne et nous résolvons le problème d'optimisation non-convexe en utilisant un algorithme d'approximation séquentielle. Les simulations montrent que l'algorithme proposé est efficace et robuste avec la connaissance statistique des canaux. Ce travail peut être facilement étendu au cas multi-utilisateur.

Enfin, nous proposons un nouveau modèle de système où le récepteur secondaire peut agir comme un nœud de relayage Full-Duplex (FD) afin de maximiser le débit primaire et donc le débit total du système. Le scénario proposé est d'abord étudié pour un schéma de modulation à mono-porteuse dans les deux cas Amplify-and-Forward (AF) et Decode-and-Forward (DF). Les contraintes pour appliquer le SIC et pour le relayage sont déterminés et les nouveaux débits réalisables sont spécifiés de telle sorte que le nœud de relayage relaie à chaque fois que le nouveau débit atteignable est meilleur que celui obtenu sans relayage. En outre, les performances du système de transmission en mode FD avec le protocole DF sont évaluées avec la modulation multi-porteuse. Les performances du modèle de système proposé sont évaluées par le biais de simulations et une amélioration importante sur le débit primaire et donc le débit total du système est affiché.

Mots Clés— Radio Cognitive, Underlay, Optimisation, Débit maximal, OFDM, Multi-utilisateurs, Relayage.

Table des matières

Table des figures

Liste des tableaux

Notation

General notations

$\mathbf{R}^n$	The set of vectors of length n with real elements
$\mathbf{R}_+^n$	The set of vectors of length n with positive elements
$\log(.)$	The natural logarithm
$\log_2(.)$	The base 2 logarithm
$\mathbf{L}$	Lagrangian of an optimization problem
∇f	The gradient of function f
$(.)^T$	The transpose operator
$\mathcal{CN}(a, b)$	The circularly symmetric complex Gaussian distribution with mean a and variance b

Thesis specific notations

x_i^k	Channel input within subcarrier k for user i
y_i^k	Channel output within subcarrier k for user i
R_i^k	Achievable rate within subcarrier k for user i
z_i^k	The additive white Gaussian noise at receiver i
L	Total number of subcarriers
B	Total available bandwidth
n_0	Noise power in band B
N_0	Spectral density of the AWGN noise
$P_{\max}$	Maximum power
P_{out}	Outage probability
m	discrete time index
I_{th}	Interference threshold
h_{ij}	complex channel coefficient between transmitter j and receiver i
h_r	complex channel coefficient between relay node and receiver

Specific notations for Section 3.9

$s_{u_{[k]}}$	The activated SU within subcarrier k
$R_{s_{u_{[k]}}}$	The achievable rate of the activated SU within subcarrier k

$P_{s_{u_{[k]}}}$	The transmit power of the activated SU within subcarrier k

Abreviations and acronyms

List of Acronyms

AF	Amplify-and-Forward
AWGN	Additive White Gaussian Noise
BS	Base Station
BC	Broadcast Channel
CDMA	Code Division Multiple Access
CF	Compress-and-Forward
CR	Cognitive Radio
CSI	Channel State Information
D2D	Device-to-Device
DF	Decode-and-Forward
DSA	Dynamic Spectrum Access
DTV	Digital Television
EPA	Equal Power Allocation
FCC	Federal Communications Commission
FD	Full-Duplex
FFT	Fast Fourier Transform
G-IFC	Gaussian Interference Channel
HD	Half-Duplex
IFFT	Inverse Fast Fourier Transform
ISI	Inter-Symbol Interference
KKT	Karush-Kuhn-Tucker
LTE	Long-Term Evolution
MAC	Multiple Access Channel
MIMO	Multiple-Input Multiple-Output
OFDM	Orthogonal Frequency Division Multiplexing
PU	Primary User
SC	Superposition Coding
SCA	Successive Convex Approximation
SDR	Software-Defined Radio
SIC	Successive Interference Cancellation

SNR	Signal-to-Noise Ratio
SU	Secondary User
WRAN	Wireless Regional Area Network

Résumé Détaillé de la Thèse

0.1 Introduction

Avec la multiplication des différentes technologies de réseau sans fil, la demande de spectre radioélectrique est en augmentation considérable. Ce spectre est réglementé par un organisme gouvernemental qui alloue le spectre en attribuant des licences exclusives pour les utilisateurs d'exploiter leurs réseaux dans différentes régions géographiques. Cependant, le spectre radioélectrique est de plus en plus encombré, bien que les mesures de spectre indiquent que le spectre attribué est sous-utilisé, c'est à dire, à n'importe quel temps et endroit données, une grande partie du spectre est non utilisée. D'où l'idée de la radio cognitive apparait comme une solution prometteuse à ce problème.

La radio cognitive est une forme de communication sans fil dans laquelle un système peut détecter intelligemment les canaux de communication qui sont en cours d'utilisation et ceux qui ne le sont pas, et peut se déplacer dans les canaux inutilisés. Ceci permet d'optimiser l'utilisation des fréquences radio disponibles du spectre tout en minimisant les interférences avec d'autres utilisateurs. Dans d'autres mots, la radio cognitive permet à un utilisateur non licencié qu'on appelle secondaire de coexister dans la même bande de fréquence avec l'utilisateur primaire licencié é condition de ne pas gêner ce dernier.

Dans la pratique, on a différentes approches d'implémentation pour la radio cognitive : Overlay, Underlay et Interweave.

— La radio cognitive Overlay (Fig. ??) :

Cette vision de la radio cognitive part de la notion de coopération entre le système primaire et secondaire. On considère dans la radio cognitive overlay que le système secondaire connaît au préalable les spécifications des transmissions primaires. Cette connaissance a priori des signaux du primaire peut être exploitée aussi bien pour améliorer les transmissions primaires tout en atténuant les interférences provenant du secondaire vers le primaire, ou encore pour annuler les perturbations des émetteurs primaires sur les récepteurs secondaires.

— La radio cognitive Underlay (Fig. ??) :

Cette approche propose de transmettre simultanément sur les mêmes bandes de fréquence, les signaux primaires et secondaires, tout en respectant une contrainte de puissance imposée aux émetteurs secondaires. On suppose donc qu'en dessous d'un certain seuil de puissance des émetteurs secondaires, aucune dégradation significative n'est ob-

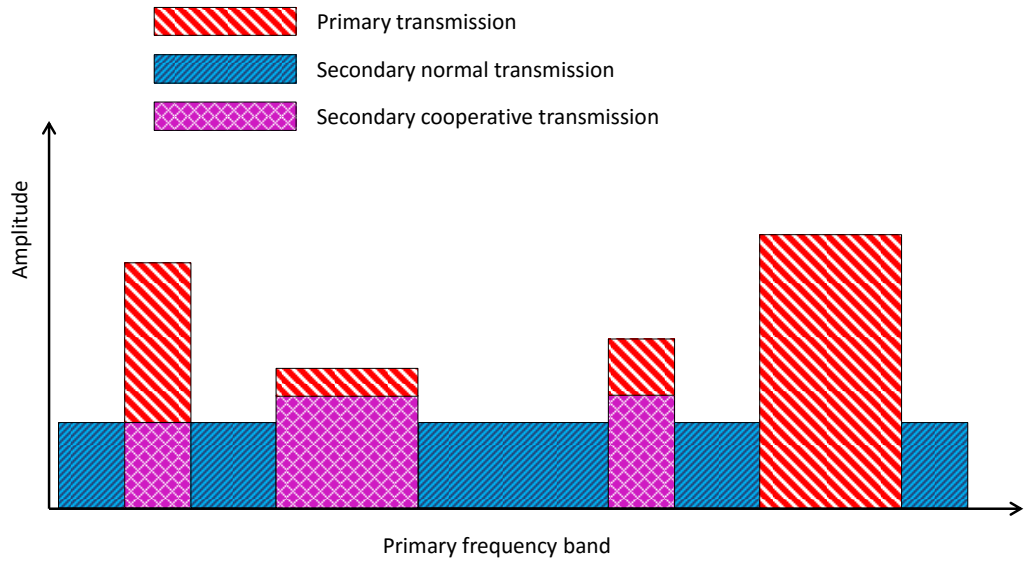
Primary transmission
Secondary normal transmission
Secondary cooperative transmission
Amplitude
Primary frequency band

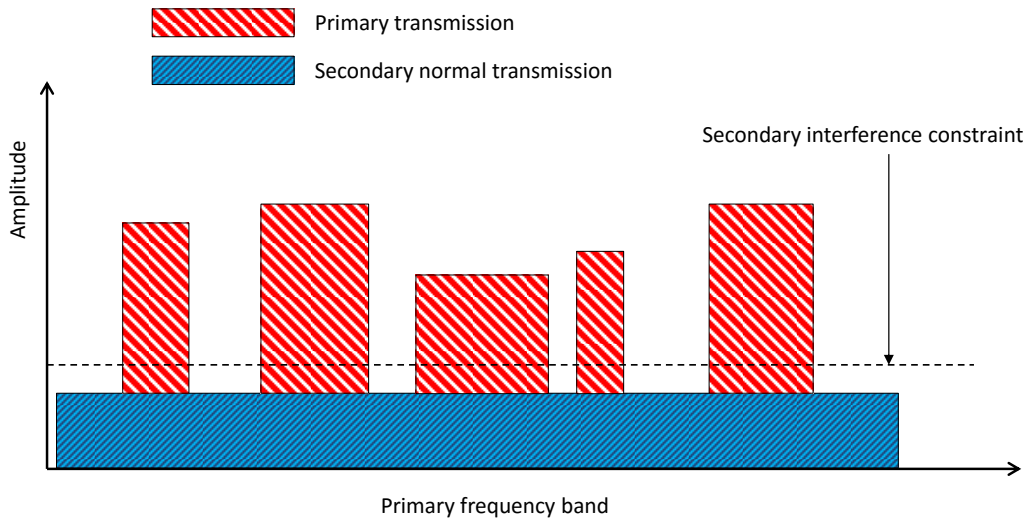
Primary transmission
Secondary normal transmission
Secondary interference constraint
Amplitude
Primary frequency band

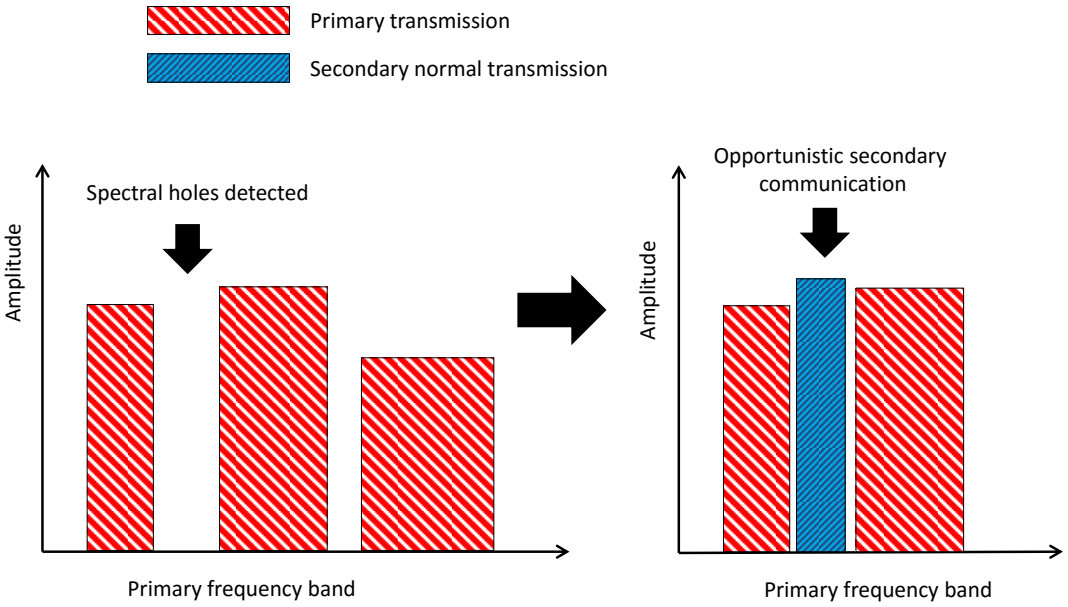

servée sur les transmissions primaires.

— La radio cognitive InterWeave :

Comme illustré dans la Fig. ??, on constate de façon générale que la majeure partie des ressources radio allouée aux utilisateurs primaires n'est pas constamment utilisée par ceux-ci. Cela implique une disponibilité de trou spectral qui peut être exploité de façon opportuniste pour l'émission des signaux secondaires.

Dans le présent manuscrit, nous proposons un algorithme de décodage adaptatif au niveau de l'utilisateur secondaire, dans le but de maximiser son débit sans dégrader les performances du système primaire.

0.2 Scénario étudié

Dans le scénario étudié, on considère une cellule primaire et une cellule secondaire de même taille. On étudie les performances de l'underlay dans un système radio cognitif avec une transmission de liaison montante et en utilisant l'OFDM. Nous supposons que toutes les transmissions sont parfaitement synchrones. Le système primaire occupe une bande passante B qui est divisée en L sous-porteuses adjacentes parallèles. La station de base (BS) secondaire est située é une distance d_{sec} de la BS primaire.

Nous commençons par définir les paramètres du modèle de système pour le cas mono-utilisateur, c'est-à-dire où un seul utilisateur existe dans chaque cellule. Ces paramètres seront utilisés tout au long de cette thèse. Cependant, certains paramètres liés aux terminaux mobiles secondaires seront modifiés pour le cas multi-utilisateur. Dans le cas mono-utilisateur, l'indice p se réfère au système primaire, tandis que l'indice s fait référence au système secondaire. Les signaux primaires et secondaires reçus dans chaque sous-porteuse $k \in \{1, \ldots, L\}$ peuvent être écrits comme (voir Fig. 3.1)

$$y_p^k = h_{pp}^k x_p^k + h_{ps}^k x_s^k + z_p^k$$
$$y_s^k = h_{sp}^k x_p^k + h_{ss}^k x_s^k + z_s^k$$

où y_i^k est la sortie du canal et x_i^k est l'entrée du canal correspondant é des données s_i^k avec une puissance P_i^k pour la sous-porteuse k et l'utilisateur i. $P_{i,\max}$ est la puissance d'émission maximale de l'émetteur i. h_{ij}^k, qui est une variable gaussienne complexe circulaire de moyenne nulle, désigne le gain de canal entre l'émetteur j et le récepteur i. Les gains de canaux sont supposés constants pendant un intervalle de temps de transmission. z_i^k désigne le bruit additif blanc Gaussien (AWGN) au niveau du récepteur i. La variance de bruit $n_i^k = n_0$ est la même sur chaque sous-porteuse k.

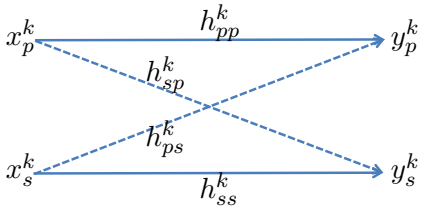

FIGURE 1 – Canal à interférence à deux utilisateurs pour chaque sous-porteuse $k \in \{1, \ldots, L\}$

0.3 Connaissance parfaite des canaux au niveau de l'utilisateur secondaire

Dans cette partie, on considère que l'utilisateur secondaire connait toutes les informations de canaux parfaitement. On étudie premièrement le cas mono-utilisateur, puis on traite le cas où plusieurs utilisateurs secondaires coexistent dans la cellule secondaire.

0.3.1 Algorithme de décodage adaptatif

Dans le scénario étudié, l'utilisateur primaire traite toujours l'interférence qu'il reçoit du secondaire comme du bruit, sans adapter sa stratégie de décodage. L'algorithme proposé est itératif et dépend de la puissance calculée à l'itération précédente $n-1$. Ainsi, le débit primaire atteignable à l'itération n et sur la sous-porteuse k est donné par

$$R_{p,n}^k = \frac{B}{L} \log_2 \left(1 + \frac{| h_{pp}^k |^2 P_{p,n}^k}{n_0 + | h_{ps}^k |^2 P_{s,n}^k} \right) \quad (1)$$

Par contre, l'utilisateur secondaire peut adapter sa stratégie de décodage selon la quantité d'interférence et certaines contraintes liées aux méthodes d'annulation successive d'interférence, tout en gardant une transmission au-dessous d'un seuil d'interférence I_{th} prédéfini au niveau du primaire. Ce seuil est calculé de façon à ce que le débit primaire en présence de l'interférence du secondaire reste au-dessus d'un pourcentage de dégradation en le comparant au rate du primaire maximum (sans interférence) donné par $R^k_{p,n,\max} = \frac{B}{L}\log_2\left(1+\frac{|h^k_{pp}|^2 P^k_{p,n}}{n_0}\right)$. Ainsi, la dégradation Δ est donnée par

$$(1-\Delta)\, R^k_{p,n,\max} = \frac{B}{L}\log_2\left(1+\frac{|h^k_{pp}|^2 P^k_{p,n}}{n_0 + I^k_{th}}\right)$$

Dans ce qui suit, nous résumons les étapes de l'algorithme adaptatif proposé, selon les différentes contraintes :

1. Si le transmetteur primaire n'émet pas, le récepteur secondaire décode son propre signal sans interférence. Son débit est donc calculé par

$$R^k_{s,n} = \frac{B}{L}\log_2\left(1+\frac{|h^k_{ss}|^2 P^k_{s,n}}{n_0}\right) \tag{2}$$

2. Si l'interférence au niveau du récepteur secondaire est faible, i.e., $|h^k_{sp}|^2 \leqslant |h^k_{ss}|^2$, le récepteur secondaire traite cette interférence comme du bruit. Dans ce cas, son débit atteignable est donné par

$$R^k_{s,n} = \frac{B}{L}\log_2\left(1+\frac{|h^k_{ss}|^2 P^k_{s,n}}{|h^k_{sp}|^2 P^k_{p,n-1} + n_0}\right) \tag{3}$$

3. Si l'interférence au niveau du récepteur secondaire est forte, i.e., $|h^k_{sp}|^2 > |h^k_{ss}|^2$, le canal vu par le récepteur secondaire est un canal multi-accès (MAC). Plusieurs cas sont possibles :

   (a) Le récepteur secondaire essaie de décoder le signal du primaire pour le retrancher en appliquant le SIC. Pour le faire, il faut que le débit du primaire vu par par le récepteur primaire soit inférieur ou égale au même débit vu par le récepteur secondaire. Cette condition peut être donnée par

$$a^k P^k_s \geqslant c^k \tag{4}$$

   où

$$a^k = |h^k_{sp}|^2 |h^k_{ps}|^2 - |h^k_{pp}|^2 |h^k_{ss}|^2$$
$$c^k = n_0\left(|h^k_{pp}|^2 - |h^k_{sp}|^2\right)$$

   Dans ce cas, le récepteur secondaire décode son propre signal sans interférence, et le

débit primaire atteignable est donné par

$$R_{s,n}^k = \frac{B}{L}\log_2\left(1+\frac{|h_{ss}^k|^2 P_{s,n}^k}{n_0}\right) \tag{5}$$

(b) Si le récepteur secondaire est incapable de faire du SIC, on test la capacité d'appliquer les SC en décomposant le signal secondaire en deux signaux dépendant de α^k qui doit être compris entre 0 et 1. Avec cette stratégie, le décodage se fait sur trois étapes et les contraintes pour faire du SC sont données par

$$\begin{cases} \frac{\left(|h_{pp}^k|^2-|h_{sp}^k|^2\right)}{|h_{ps}^k|^2|h_{sp}^k|^2} < \frac{P_s^k}{n_0} \\ P_s^k a^k < c^k \end{cases} \tag{6}$$

qui sont détaillé dans le Tableau 3.1. Dans ce cas, le débit secondaire atteignable est donné par

$$R_{s,n}^k = \frac{B}{L}\log_2\left(1+\frac{\alpha^k|h_{ss}^k|^2 P_{s,n}^k}{n_0}\right) + \frac{B}{L}\log_2\left(1+\frac{(1-\alpha^k)|h_{ss}^k|^2 P_{s,n}^k}{\alpha^k|h_{ss}^k|^2 P_{s,n}^k + |h_{sp}^k|^2 P_{p,n-1}^k + n_0}\right) \tag{7}$$

où

$$\alpha^k = \frac{(|h_{sp}^k|^2 - |h_{pp}^k|^2)n_0 + |h_{ps}^k|^2|h_{sp}^k|^2 P_{s,n}^k}{|h_{pp}^k|^2|h_{ss}^k|^2 P_{s,n}^k} \tag{8}$$

(c) Si aucune de ces stratégies de décodage ne peut être appliquée, le transmetteur secondaire s'éteint.

		c^k	
		Positive	Negative
a^k	Positive	$\frac{P_s^k}{n_0} > \frac{\|h_{pp}^k\|^2-\|h_{sp}^k\|^2}{\|h_{ps}^k\|^2\|h_{sp}^k\|^2}$ $P_s^k < \frac{c^k}{a^k}$	Impossible
	Negative	$\frac{P_s^k}{n_0} > \frac{\|h_{pp}^k\|^2-\|h_{sp}^k\|^2}{\|h_{ps}^k\|^2\|h_{sp}^k\|^2}$	$P_s^k > \frac{c^k}{a^k}$

TABLE 1 – Les conditions du codage à superposition

L'algorithme de décodage adaptatif proposé peut être présenté par la Fig. 3.4, pour $P_{p,n-1}^k \neq 0$.

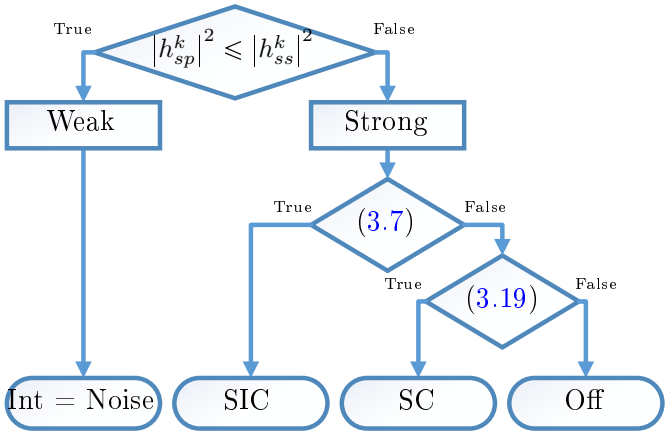

FIGURE 2 – Stratégies de Décodage pour l'utilisateur secondaire à la sous-porteuse k

0.3.2 Optimisation des puissances

Une fois la stratégie de décodage est choisie pour chaque sous-porteuse, on procède à l'étape de l'optimisation des puissances primaire et secondaire, dans le but de maximiser les débites primaire et secondaire, respectivement. L'algorithme d'allocation de puissance est décrit pas la Fig. 3.7.

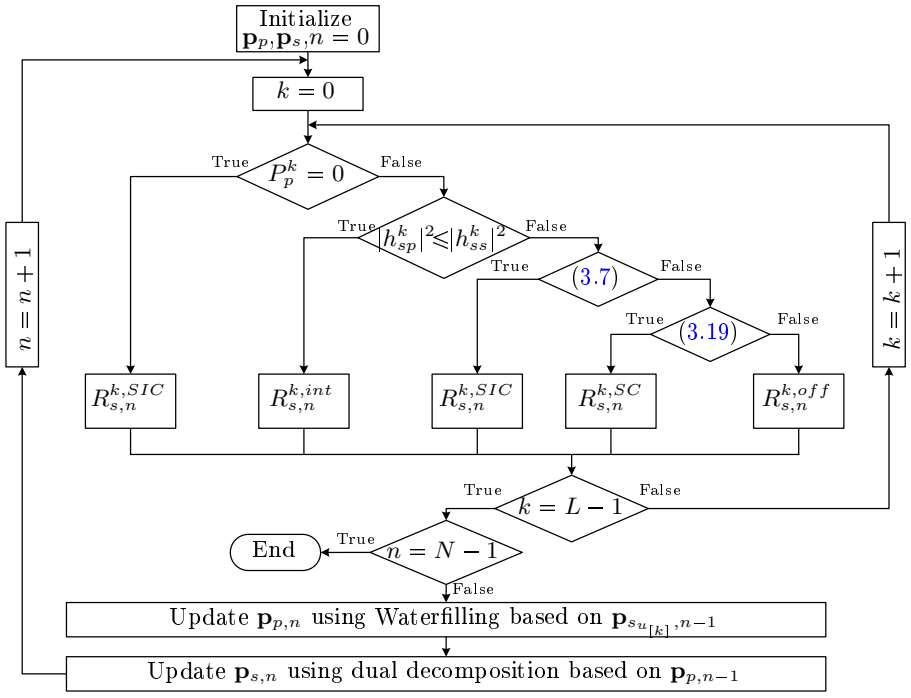

FIGURE 3 – Allocation de puissance

A l'itération n, le problème d'allocation de puissance au niveau de l'utilisateur secondaire

est donné par

$$\max_{\mathbf{p}_{s,n}} R_{s,n} \tag{9a}$$

$$\text{s.t. } \sum_{k=1}^{L} P_{s,n}^{k} \leqslant P_{s,max} \tag{9b}$$

$$\text{s.t. } P_{s,n}^{k} \geqslant 0 \, \forall \, k \in \{1, \ldots, L\} \tag{9c}$$

$$\text{s.t. } |h_{ps}^{k}|^2 P_{s,n}^{k} \leqslant I_{th}^{k} \, \forall \, k \notin \mathcal{S}_1 \tag{9d}$$

$$\text{s.t. } (3.7), \forall \, k \in \mathcal{S}_3 \tag{9e}$$

$$\text{s.t. } (3.19), \forall \, k \in \mathcal{S}_4 \tag{9f}$$

oé $R_{s,n} = \sum_{k \in \mathcal{S}_2} R_{s,n}^{k,int} + \sum_{k \in \mathcal{S}_1 \cap \mathcal{S}_3} R_{s,n}^{k,SIC} + \sum_{k \in \mathcal{S}_4} R_{s,n}^{k,SC}$

Comme ce problème est séparable selon les différentes contraintes, on peut le décomposer en trois sous-problèmes :

$$C_{int} : \max_{\{P_{s,n}^{k}\}_{k \in \mathcal{S}_2}} \sum_{k \in \mathcal{S}_2} R_{s,n}^{int} - \mu_{s,n} \sum_{k \in \mathcal{S}_2} P_{s,n}^{k} \tag{10a}$$

$$|h_{ps}^{k}|^2 P_{s,n}^{k} \leqslant I_{th}^{k}, \forall k \in \mathcal{S}_2$$

$$C_{SIC} : \max_{\{P_{s,n}^{k}\}_{k \in \mathcal{S}_3}} \sum_{k \in \mathcal{S}_3} R_{s,n}^{SIC} - \mu_{s,n} \sum_{k \in \mathcal{S}_3} P_{s,n}^{k} \tag{10b}$$

$$|h_{ps}^{k}|^2 P_{s,n}^{k} \leqslant I_{th}^{k}, \forall k \in \mathcal{S}_3$$

$$a^{k} P_{s,n}^{k} \geqslant c^{k}, \forall k \in \mathcal{S}_3$$

$$C_{SC} : \max_{\{P_{s,n}^{k}\}_{k \in \mathcal{S}_4}} \sum_{k \in \mathcal{S}_4} R_{s,n}^{SC} - \mu_{s,n} \sum_{k \in \mathcal{S}_4} P_{s,n}^{k} \tag{10c}$$

$$|h_{ps}^{k}|^2 P_{s,n}^{k} \leqslant I_{th}^{k}, \forall k \in \mathcal{S}_4$$

$$\frac{\left(|h_{pp}^{k}|^2 - |h_{sp}^{k}|^2\right)}{|h_{ps}^{k}|^2 |h_{sp}^{k}|^2} < \frac{P_{s,n}^{k}}{n_0}, \forall k \in \mathcal{S}_4$$

$$a^{k} P_{s,n}^{k} < c^{k} \, \forall k \in \mathcal{S}_4$$

Les deux sous-problèmes C_{int} et C_{SIC} sont convexes et leurs solutions peuvent être données en appliquant le Lagrangien. Alors que le troisième sous-problème n'est pas convexe et on doit donc appliquer un algorithme d'approximation séquentielle afin de le transformer en un problème convexe. La solution du problème (3.37) est donné par le Tableau 3.2, et les coefficients du problèmes sont donnés par le Tableau 3.3.

TABLE 2 – Valeurs optimales de $P_{s,n}^k$

Conditions	Decoding strategies	$P_{s,n}^k$
$P_{p,(n-1)}^k = 0$ any value for a^k and c^k	Interweave	$\left[\frac{1}{\mu_{s,n}} - \frac{1}{b_{s,(n-1)}^k}\right]^+$
$P_{p,(n-1)}^k \neq 0$ $\left\{a^k = 0; c^k = 0\right\}$	Int = Noise	$\min\left\{\left[\frac{1}{\mu_{s,n}} - \frac{1}{b_{s,(n-1)}^k}\right]^+ ; \frac{I_{\text{th}}^k}{\left\|h_{ps}^k\right\|^2}\right\}$
$P_{p,(n-1)}^k \neq 0$ $\left\{a^k < 0; c^k > 0\right\}$	SIC	0
	SC	$\min\left\{\max\left\{\left[\frac{1}{\hat{\mu_{s,n}}} - \frac{1}{b_{s,(n-1)}^k}\right]^+ ; \frac{n_0(\left\|h_{pp}^k\right\|^2 - \left\|h_{sp}^k\right\|^2)}{\left\|h_{sp}^k\right\|^2 \left\|h_{ps}^k\right\|^2}\right\} ; \frac{I_{\text{th}}^k}{\left\|h_{ps}^k\right\|^2}\right\}$
$P_{p,(n-1)}^k \neq 0$ $\left\{a^k > 0; c^k < 0\right\}$	SIC	$\min\left\{\left[\frac{1}{\mu_{s,n}} - \frac{1}{b_{s,(n-1)}^k}\right]^+ ; \frac{I_{\text{th}}^k}{\left\|h_{ps}^k\right\|^2}\right\}$
	SC	0
$P_{p,(n-1)}^k \neq 0$ $\left\{a^k < 0; c^k < 0\right\}$	SIC	$\min\left\{\frac{c^k}{a^k}; \left[\frac{1}{\mu_{s,n}} - \frac{1}{b_{s,(n-1)}^k}\right]^+ ; \frac{I_{\text{th}}^k}{\left\|h_{ps}^k\right\|^2}\right\}$
	SC	$\min\left\{\max\left\{\left[\frac{1}{\hat{\mu_{s,n}}} - \frac{1}{b_{s,(n-1)}^k}\right]^+ ; \frac{n_0(\left\|h_{pp}^k\right\|^2 - \left\|h_{sp}^k\right\|^2)}{\left\|h_{sp}^k\right\|^2 \left\|h_{ps}^k\right\|^2}; \frac{c^k}{a^k}\right\} ; \frac{I_{\text{th}}^k}{\left\|h_{ps}^k\right\|^2}\right\}$
$P_{p,(n-1)}^k \neq 0$ $\left\{a^k > 0; c^k > 0\right\}$	SIC if $\frac{c^k}{a^k} \leqslant \frac{I_{\text{th}}^k}{\left\|h_{ps}^k\right\|^2}$	$\min\left\{\max\left\{\left[\frac{1}{\mu_{s,n}} - \frac{1}{b_{s,(n-1)}^k}\right]^+ ; \frac{c^k}{a^k}\right\} ; \frac{I_{\text{th}}^k}{\left\|h_{ps}^k\right\|^2}\right\}$
	otherwise	0
	SC	$\min\left\{\max\left\{\left[\frac{1}{\hat{\mu_{s,n}}} - \frac{1}{b_{s,(n-1)}^k}\right]^+ ; \frac{n_0(\left\|h_{pp}^k\right\|^2 - \left\|h_{sp}^k\right\|^2)}{\left\|h_{sp}^k\right\|^2 \left\|h_{ps}^k\right\|^2}\right\} ; \frac{c^k}{a^k}; \frac{I_{\text{th}}^k}{\left\|h_{ps}^k\right\|^2}\right\}$

TABLE 3 – Coefficients d'optimisation pour le problème (3.39)

Cases	$b^k_{s,(n-1)}$
$P^k_{p,(n-1)} \neq 0$ and $\left\|h^k_{sp}\right\|^2 \leqslant \left\|h^k_{ss}\right\|^2$	$\frac{\left\|h^k_{ss}\right\|^2}{n_0+\left\|h^k_{sp}\right\|^2 P^k_{p,(n-1)}}$
$P^k_{p,(n-1)} \neq 0$ and $\left\|h^k_{sp}\right\|^2 > \left\|h^k_{ss}\right\|^2$	$\frac{\left\|h^k_{ss}\right\|^2}{n_0}$
$P^k_{p,(n-1)} = 0$	$\frac{\left\|h^k_{ss}\right\|^2}{n_0}$
Cases	a^k
$P^k_{p,(n-1)} \neq 0$ and $\left\|h^k_{sp}\right\|^2 \geqslant \left\|h^k_{ss}\right\|^2$	$\left\|h^k_{sp}\right\|^2 \left\|h^k_{ps}\right\|^2 - \left\|h^k_{pp}\right\|^2 \left\|h^k_{ss}\right\|^2$
all other cases	0
Cases	c^k
$P^k_{p,(n-1)} \neq 0$ and $\left\|h^k_{sp}\right\|^2 \geqslant \left\|h^k_{ss}\right\|^2$	$n_0 \left(\left\|h^k_{pp}\right\|^2 - \left\|h^k_{sp}\right\|^2\right)$
all other cases	0

0.3.3 Scénario multi-utilisateurs secondaires

Dans cette partie, plusieurs utilisateurs secondaires peuvent coexister dans la cellule secondaire. On propose alors un algorithme d'allocation de ressources qui comportent plusieurs phases :

- Tout d'abord, pour chaque k, on choisit parmi tous les utilisateurs celui qui offre le meilleur rate, c'est-à-dire, sur chaque sous-porteuse un seul utilisateur sera actif.
- On applique les deux algorithmes de décodage adaptatif et d'allocation de puissance pour chaque utilisateur, sur ses sous-porteuses actives.

L'algorithme global est donné par la Fig. 3.9.

0.3.4 Simulations

Avec une connaissance parfaite des canaux, les gains de canaux h^k_{ij} prennent en compte la perte de chemin, le shadowing log-normale et le Rayleigh. Le modèle de perte de chemin est l'extension du modèle COST 231 à Hata à 800 MHz dans un environnement urbain dense, $L_{dB}(d) = 125.08+35.22\times\log_{10}(d)$, et l'écart type du shadowing est égale é 6 dB. Les deux cellules primaires et secondaires ont des antennes omnidirectionnelles avec le même rayon $d_P = d_s = 1$ km. La dégradation autorisée du débit primaire est $\Delta = 0,1$, ce qui signifie que 90 % du débit primaire sans interférence est garantie.

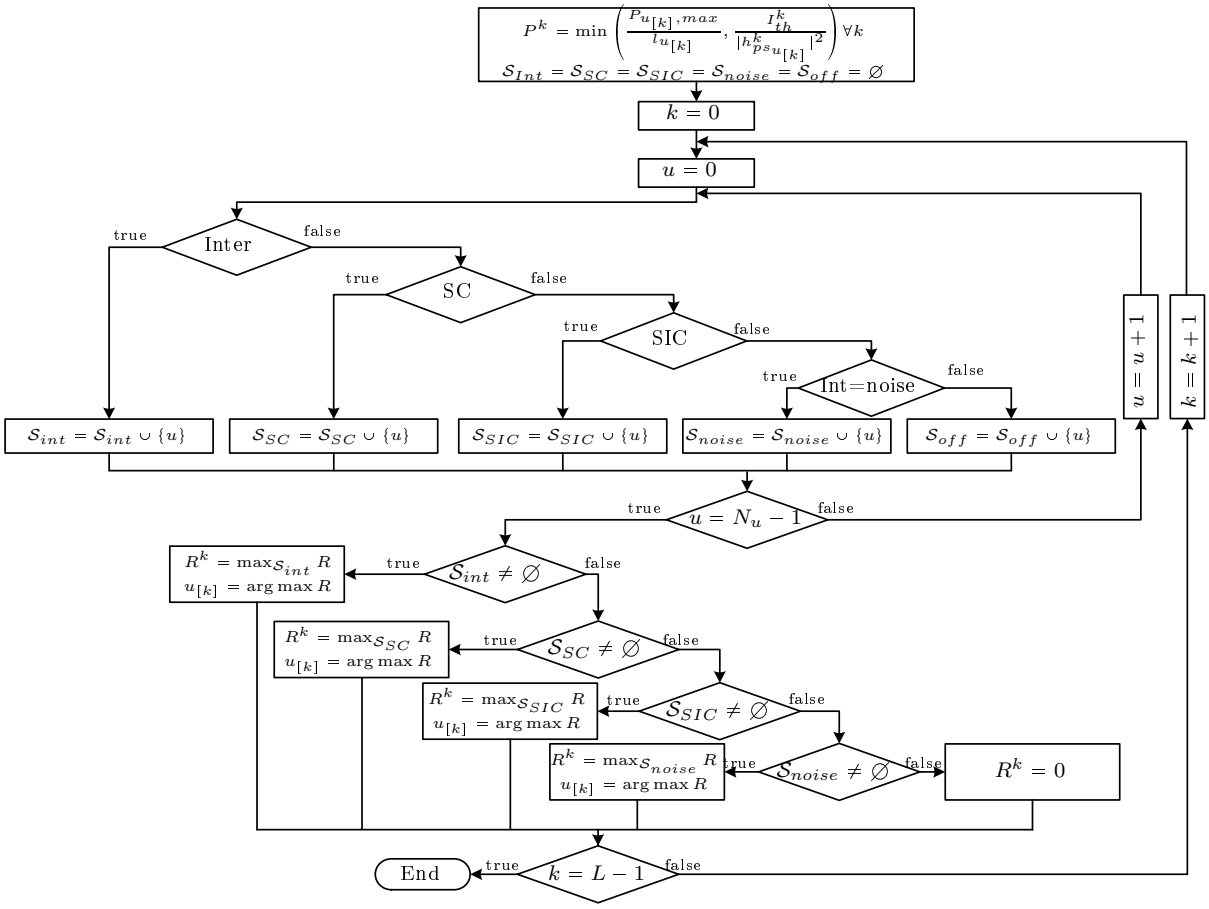

FIGURE 4 – Algorithme d'allocation de sous-porteuses

Débits atteignables par l'algorithme proposé dans le cas mono-utilisateur

L'impact de l'algorithme proposé sur les débits total, primaire et secondaire est représenté sur la Fig. 3.13 et la Fig. 3.14. En comparant la méthode proposée au scénario où juste le SIC est applicable au niveau du système secondaire, notée "SIC", la méthode proposée présente une amélioration due à l'application du SC. Une forte amélioration apportée par l'optimisation de puissance en présence de la stratégie SC est aussi mise en évidence.

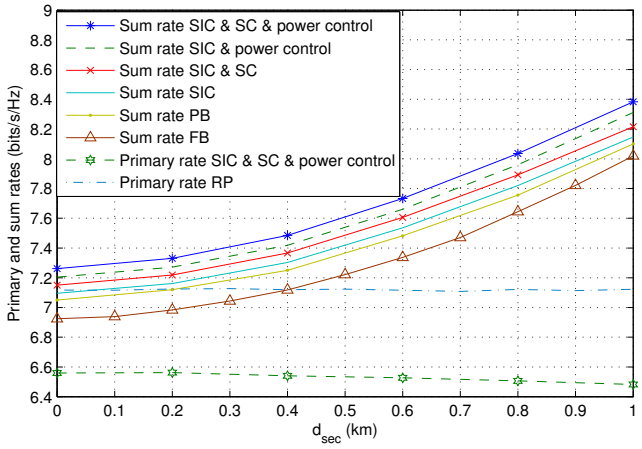

FIGURE 5 – Débits primaire et total comparés avec différentes méthodes

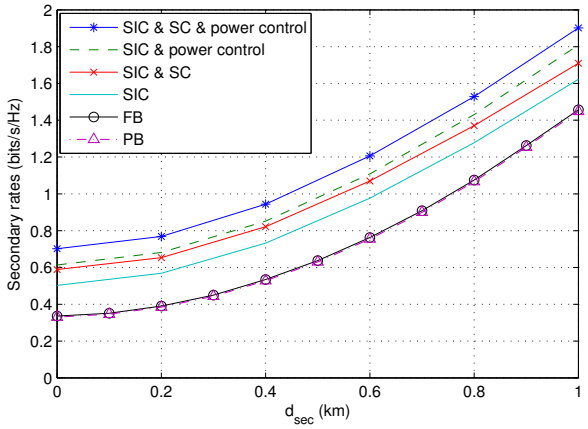

FIGURE 6 – Débit secondaire comparé avec différentes méthodes

Débits atteignables par l'algorithme proposé dans le cas multi-utilisateur

Dans cette partie, les performances de l'algorithme proposé est évaluée avec différent nombre d'utilisateurs dans la cellule secondaire. Dans la Fig. 3.15, les débits totaux atteignables avec deux utilisateurs secondaires sont comparés pour les différents algorithmes de décodage appliqués. On remarque que le gain obtenu par l'algorithme proposé est plus importante avec deux utilisateurs.

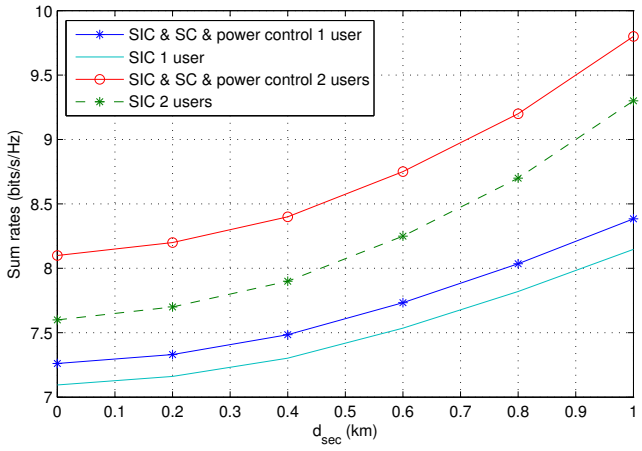

FIGURE 7 – Débits totaux atteignables avec deux utilisateurs secondaires

Dans la Fig. 3.16, les débits secondaires atteignables sont affichés selon le nombre des utilisateurs secondaires.

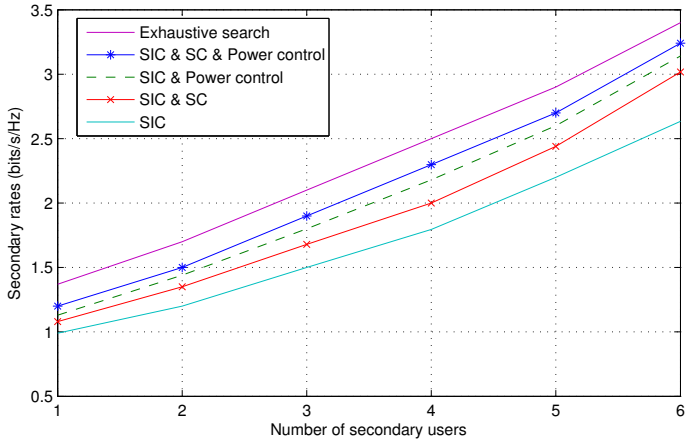

FIGURE 8 – Débits secondaires en fonction du nombre d'utilisateurs pour d_{sec}= 0.6 km

0.4 Connaissance Statistiques des Canaux

Dans cette partie, on considère que l'utilisateur secondaire possède juste une connaissance statistiques des canaux du système primaire $|h_{pp}^k|^2$ et $|h_{ps}^k|^2$. Pour résoudre le problème d'allocation de ressource dans ces conditions, il faut tout d'abord calculer les différentes probabilité d'outage sur les contraintes et les expressions des débits dépendants de $|h_{pp}^k|^2$ ou $|h_{ps}^k|^2$.

0.4.1 Allocation de puissance

Le problème d'allocation de puissance avec connaissance statistique des canaux est donné par (4.3), avec ϵ^k, θ^k, δ^k and γ^k les limites d'outage

$$\max_{\mathbf{p}_s} R_s \tag{11a}$$

$$\text{s.t.} \sum_{k=1}^{L} P_s^k \leqslant P_{s,\max} \tag{11b}$$

$$\text{s.t.} \; P_s^k \geqslant 0, \forall k \in \{1, \ldots, L\} \tag{11c}$$

$$\text{s.t.} \; \exp^{-\frac{I_{th}^k}{P_s^k \lambda_{ps}^k}} \leqslant \theta^k, \forall k \notin \mathcal{S}_1 \tag{11d}$$

$$\text{s.t.} \; \exp^{-\frac{\nu^k n_0}{\lambda_{pp}^k}} \frac{1}{1 + \frac{\lambda_{ps}^k}{\lambda_{pp}^k} \nu^k P_s^k} \leqslant \epsilon^k, \forall k \in \mathcal{S}_3 \tag{11e}$$

$$\text{s.t.} \; \exp^{-\frac{|h_{sp}^k|^2}{\lambda_{pp}^k}} \frac{1}{1 + \frac{|h_{sp}^k|^2 P_s^k \lambda_{ps}^k}{\lambda_{pp}^k n_0}} \leqslant \delta^k, \forall k \in \mathcal{S}_4 \tag{11f}$$

$$\text{s.t.} \; \exp^{-\frac{\nu^k n_0}{\lambda_{pp}^k}} \frac{1}{1 + \frac{\lambda_{ps}^k}{\lambda_{pp}^k} \nu^k P_s^k} \geqslant 1 - \gamma^k, \forall k \in \mathcal{S}_4 \tag{11g}$$

où

$$\nu^k = \frac{|h_{sp}^k|^2}{n_0 + |h_{ss}^k|^2 P_s^k} \tag{12}$$

and $R_s = \sum_{k \in \mathcal{S}_2} R_s^{k,int} + \sum_{k \in \mathcal{S}_1 \cap \mathcal{S}_3} R_s^{k,SIC} + \sum_{k \in \mathcal{S}_4} R_s^{k,SC}$.

Comme dans le cas de connaissance parfaite des canaux, le problème d'optimisation est décomposable en trois sous-problèmes, et on applique un algorithme d'approximation séquentiel sur les sous-problèmes non-convexes. La résolution du problème (4.3) résulte en une solution générale donnée par le Tableau 4.4, avec les paramètres présentés dans le Tableau 4.5.

TABLE 4 – Valeurs optimales de $P_{s,n}^k$

Conditions	Decoding strategies	$P_{s,n}^k$
$P_{p,(n-1)}^k = 0$	Interweave	$\left[\frac{1}{\mu_{s,n}} - \frac{1}{b_{s,(n-1)}^k}\right]^+$
$P_{p,(n-1)}^k \neq 0$	Int = Noise	$\min\left\{\left[\frac{1}{\mu_{s,n}} - \frac{1}{b_{s,(n-1)}^k}\right]^+ ; \frac{I_{th}^k}{\lambda_{ps}^k \log(\frac{1}{\theta^k})}\right\}$
$P_{p,(n-1)}^k \neq 0$ $\{E^k < 0; F^k > 0\}$	SIC	0
$P_{p,(n-1)}^k \neq 0$ $\{E^k > 0; F^k < 0\}$	SIC	$\min\left\{\left[\frac{1}{\mu_{s,n}} - \frac{1}{b_{s,(n-1)}^k}\right]^+ ; \frac{I_{th}^k}{\lambda_{ps}^k \log(\frac{1}{\theta^k})}\right\}$

$P^k_{p,(n-1)} \neq 0$ $\left\{E^k < 0; F^k < 0\right\}$	SIC	$\min\left\{\left[\frac{1}{\mu_{s,n}} - \frac{1}{b^k_{s,(n-1)}}\right]^+; \frac{I^k_{th}}{\lambda^k_{ps}\log(\frac{1}{\theta^k})}; \frac{F^k}{E^k}\right\}$
$P^k_{p,(n-1)} \neq 0$ $\left\{E^k > 0; F^k > 0\right\}$	SIC if $\frac{F^k}{E^k} \leqslant \frac{I^k_{th}}{\lambda^k_{ps}\log(\frac{1}{\theta^k})}$ otherwise	$\max\left\{\min\left\{\left[\frac{1}{\mu_{s,n}} - \frac{1}{b^k_{s,(n-1)}}\right]^+; \frac{I^k_{th}}{\lambda^k_{ps}\log(\frac{1}{\theta^k})}\right\}; \frac{E^k}{F^k}\right\}$ 0
$P^k_{p,(n-1)} \neq 0$ $\left\{G^k < 0; H^k > 0\right\}$ or $\left\{E^k > 0; J^k < 0\right\}$	SC	0
$P^k_{p,(n-1)} \neq 0$ $\left\{G^k > 0; H^k > 0\right\}$ and $\left\{E^k > 0; J^k > 0\right\}$	SC	$\max\left\{\min\left\{\left[\frac{1}{\hat{\mu}_{s,n}} - \frac{1}{b^k_{s,(n-1)}}\right]^+; \frac{I^k_{th}}{\lambda^k_{ps}\log(\frac{1}{\theta^k})}; \frac{J^k}{E^k}\right\}; \frac{H^k}{G^k}\right\}$
$P^k_{p,(n-1)} \neq 0$ $\left\{G^k > 0; H^k > 0\right\}$ and $\left\{E^k < 0; J^k > 0\right\}$	SC	$\max\left\{\min\left\{\left[\frac{1}{\hat{\mu}_{s,n}} - \frac{1}{b^k_{s,(n-1)}}\right]^+; \frac{I^k_{th}}{\lambda^k_{ps}\log(\frac{1}{\theta^k})}\right\}; \frac{H^k}{G^k}\right\}$
$P^k_{p,(n-1)} \neq 0$ $\left\{G^k > 0; H^k > 0\right\}$ and $\left\{E^k < 0; J^k < 0\right\}$	SC	$\max\left\{\min\left\{\left[\frac{1}{\hat{\mu}_{s,n}} - \frac{1}{b^k_{s,(n-1)}}\right]^+; \frac{I^k_{th}}{\lambda^k_{ps}\log(\frac{1}{\theta^k})}\right\}; \frac{H^k}{G^k}; \frac{J^k}{E^k}\right\}$
$P^k_{p,(n-1)} \neq 0$ $\left\{G^k > 0; H^k < 0\right\}$ and $\left\{E^k > 0; J^k > 0\right\}$	SC	$\min\left\{\left[\frac{1}{\hat{\mu}_{s,n}} - \frac{1}{b^k_{s,(n-1)}}\right]^+; \frac{I^k_{th}}{\lambda^k_{ps}\log(\frac{1}{\theta^k})}; \frac{J^k}{E^k}\right\}$
$P^k_{p,(n-1)} \neq 0$ $\left\{G^k > 0; H^k < 0\right\}$ and $\left\{E^k < 0; J^k > 0\right\}$	SC	$\min\left\{\left[\frac{1}{\hat{\mu}_{s,n}} - \frac{1}{b^k_{s,(n-1)}}\right]^+; \frac{I^k_{th}}{\lambda^k_{ps}\log(\frac{1}{\theta^k})}\right\}$
$P^k_{p,(n-1)} \neq 0$ $\left\{G^k > 0; H^k < 0\right\}$ and $\left\{E^k < 0; J^k < 0\right\}$	SC	$\max\left\{\min\left\{\left[\frac{1}{\hat{\mu}_{s,n}} - \frac{1}{b^k_{s,(n-1)}}\right]^+; \frac{I^k_{th}}{\lambda^k_{ps}\log(\frac{1}{\theta^k})}\right\}; \frac{J^k}{E^k}\right\}$
$P^k_{p,(n-1)} \neq 0$ $\left\{G^k < 0; H^k < 0\right\}$ and $\left\{E^k > 0; J^k > 0\right\}$	SC	$\min\left\{\left[\frac{1}{\hat{\mu}_{s,n}} - \frac{1}{b^k_{s,(n-1)}}\right]^+; \frac{I^k_{th}}{\lambda^k_{ps}\log(\frac{1}{\theta^k})}; \frac{J^k}{E^k}; \frac{H^k}{G^k}\right\}$
$P^k_{p,(n-1)} \neq 0$ $\left\{G^k < 0; H^k < 0\right\}$ and $\left\{E^k < 0; J^k > 0\right\}$	SC	$\min\left\{\left[\frac{1}{\hat{\mu}_{s,n}} - \frac{1}{b^k_{s,(n-1)}}\right]^+; \frac{I^k_{th}}{\lambda^k_{ps}\log(\frac{1}{\theta^k})}; \frac{H^k}{G^k}\right\}$
$P^k_{p,(n-1)} \neq 0$ $\left\{G^k < 0; H^k < 0\right\}$ and $\left\{E^k < 0; J^k < 0\right\}$	SC	$\max\left\{\min\left\{\left[\frac{1}{\hat{\mu}_{s,n}} - \frac{1}{b^k_{s,(n-1)}}\right]^+; \frac{I^k_{th}}{\lambda^k_{ps}\log(\frac{1}{\theta^k})}; \frac{H^k}{G^k}\right\}; \frac{J^k}{E^k}\right\}$

TABLE 5 – Valeurs du coefficient $b^k_{s,(n-1)}$ dans le Tableau 4.4

Cases	$b^k_{s,(n-1)}$
$P^k_{p,(n-1)} = 0$	$\frac{\left\|h^k_{ss}\right\|^2}{n_0}$
$P^k_{p,(n-1)} \neq 0$ and $\left\|h^k_{sp}\right\|^2 \leqslant \left\|h^k_{ss}\right\|^2$	$\frac{\left\|h^k_{ss}\right\|^2}{\left\|h^k_{sp}\right\|^2 P^k_{p,(n-1)} + n_0}$
$P^k_{p,(n-1)} \neq 0$ and $\left\|h^k_{sp}\right\|^2 > \left\|h^k_{ss}\right\|^2$ (SIC)	$\frac{\left\|h^k_{ss}\right\|^2}{n_0}$
$P^k_{p,(n-1)} \neq 0$ and $\left\|h^k_{sp}\right\|^2 > \left\|h^k_{ss}\right\|^2$ (SC)	$\frac{\lambda^k_{ps}}{n_0}$

0.4.2 Simulations

Dans cette partie, on utilise les mêmes paramètres utilisés dans la partie précédente avec connaissance parfaite des canaux. On considère que les limites d'outage θ^k, ϵ^k, δ^k and γ^k sont tous égaux et valent 0.01. on compare les performances de l'algorithme proposé dans les deux cas de connaissance parfaite et statistique des canaux et on remarque que l'algorithme est bien robuste malgré la manque d'information parfaite. Les débits secondaire et total atteignables avec la méthode proposée sont donnés dans les Fig. 4.1 et Fig. 4.2, respectivement.

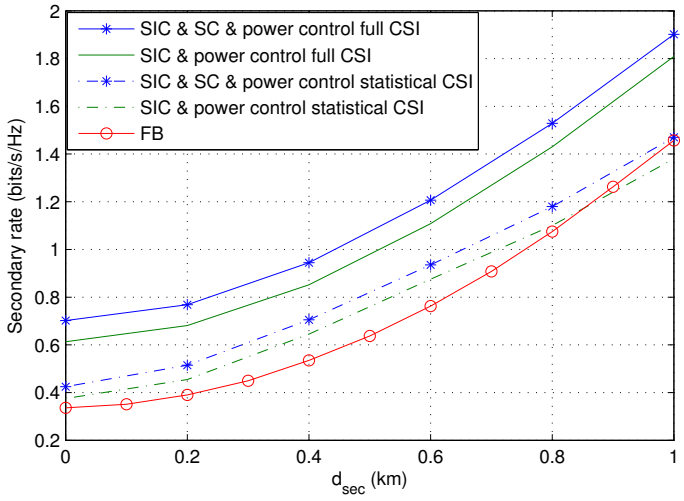

FIGURE 9 – Débits secondaires avec connaissance statistique des canaux

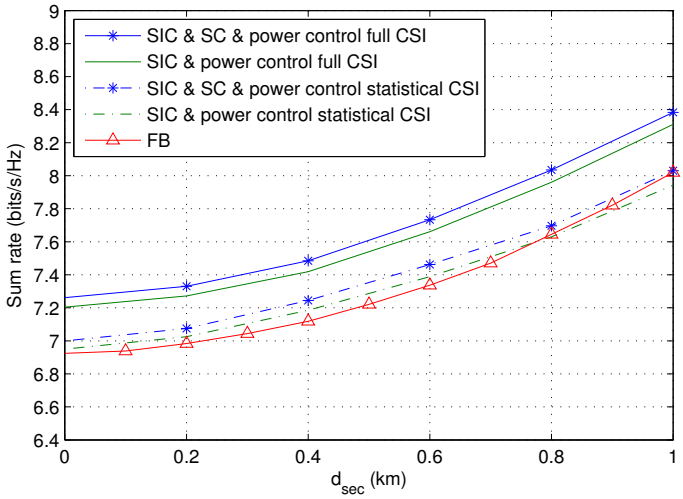

FIGURE 10 – Débits totaux avec connaissance statistique des canaux

0.5 Nouveau modèle proposé avec relayage au niveau du récepteur secondaire

Dans cette partie, on propose un nouveau modèle de système radio cognitif avec une transmission sur un liaison montante, dans lequel le récepteur secondaire peut agir comme un nœud de relayage, dans le but de maximiser le débit primaire comme présente la Fig. **??**. On se limite à l'application d'une partie de l'algorithme de décodage adaptatif, dans laquelle le récepteur secondaire peut appliquer le SIC ou bien traiter l'interférence venant du primaire comme du bruit. Dans tous les cas, on impose au récepteur secondaire de ne pas relayer que si le débit primaire obtenu après relayage est supérieur au celui obtenu sans relayage.

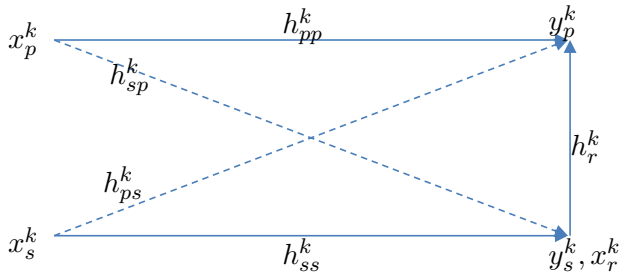

FIGURE 11 – Système radio cognitif avec relayage

Le modèle du système à la sous-porteuse k lorsque y_s^k relaie est donné par

$$y_p^k = h_{pp}^k x_p^k + h_{ps}^k x_s^k + h_r^k x_r^k + z_p^k \tag{13}$$

$$y_s^k = h_{sp}^k x_p^k + h_{ss}^k x_s^k + z_s^k \tag{14}$$

où x_r^k est le signal relayé qui dépend du protocole de relayage utilisé (AF ou DF). On étudie tout d'abord les débits atteignables avec AF et DF pour le cas mono-porteuse, puis on détaille l'allocation de ressources pour le cas multi-porteuses en appliquant le DF au récepteur secondaire.

0.5.1 Débits atteignable avec AF

Dans cette section, on considère que le récepteur secondaire peut agir comme un relais AF. Dans ce cas, le débit primaire atteignable est donné par

$$R_p^{k,AF} = \frac{B}{L}\log_2\left(1+\frac{|h_{pp}^k+\beta_{AF}^k h_r^k h_{sp}^k|^2 P_p^k}{|h_{ps}^k+\beta_{AF}^k h_r^k h_{ss}^k|^2 P_s^k+\beta_{AF}^k|h_r^k|^2 n_0+n_0}\right) \tag{15}$$

Pour le débit secondaire, plusieurs cas sont traités selon la possibilité de faire du SIC ou pas. On note qu'avec le relais AF, la contrainte du SIC est plus forte, parce qu'on compare le nouveau débit primaire après relayage avec le débit primaire vu par le secondaire).

0.5.2 Débits atteignable avec DF

Dans cette section, on considère que le récepteur secondaire peut agir comme un relais DF. Dans ce cas, le débit primaire atteignable est donné par

$$R_p^{k,DF} = \min\left\{\frac{B}{L}\log_2\left(1+\frac{|h_{sp}^k|^2 P_p^k}{|h_{ss}^k|^2 P_s^k+n_0}\right), \frac{B}{L}\log_2\left(1+\frac{|h_{pp}^k|^2 P_p^k+|h_r^k|^2 P_r^k}{|h_{ps}^k|^2 P_s^k+n_0}\right)\right\} \tag{16}$$

Par contre, le récepteur secondaire applique toujours le SIC dans ce cas, puisqu'il est capable de décoder le message du primaire. Par conséquence, son débit atteignable est donné par

$$R_s^k = \frac{B}{L}\log_2\left(1+\frac{|h_{ss}^k|^2 P_s^k}{n_0}\right) \tag{17}$$

0.5.3 Allocation de puissance pour le cas multi-porteuses avec DF

Dans cette partie, on résout le problème d'optimisation dans le cas multi-porteuses au niveau des systèmes primaire, secondaire et du relais. Le problème d'optimisation conjointe des puissances du primaire et du relais dans le but de maximiser le débit primaire est donné par l'équation (5.20).

$$\begin{aligned}
&\max_{\mathbf{p}_{p,n},\mathbf{p}_{r,n}} \sum_{k=1}^{L} R_{p,n}^{k,DF} \\
&\text{s.t.} \sum_{k=1}^{L} P_{p,n}^k + \sum_{k=1}^{L} P_{r,n}^k = P_{\text{total}} \\
&\text{s.t.} \; P_{p,n}^k \geqslant 0 \, \forall k \\
&\text{s.t.} \; P_{r,n}^k \geqslant 0 \, \forall k
\end{aligned} \tag{18}$$

où P_{total} présente la puissance totale maximale optimisée au niveau du transmetteur primaire et du relais. $P_{\text{total}} = P_{p,max} + P_{r,max}$, avec $P_{r,max}$ la puissance maximale transmise par le relais. Pour résoudre ce problème max-min, on définit $\overline{R_n^k} = \min\left(R_{p,n,1}^{k,DF}, R_{p,n,2}^{k,DF}\right)$. Le problème d'optimisation peut être écrit par

$$\max_{\mathbf{p}_{p,n},\mathbf{p}_{r,n},\overline{\mathbf{R}_n}} \sum_{k=1}^{L} \overline{R_n^k} \tag{19a}$$

$$\text{s.t. } \sum_{k=1}^{L} P_{p,n}^k + \sum_{k=1}^{L} P_{r,n}^k = P_{\text{total}} \tag{19b}$$

$$\text{s.t. } \overline{R_n^k} \leqslant R_{p,n,1}^{k,DF} \; \forall\, k \in \{1,\ldots,L\} \tag{19c}$$

$$\text{s.t. } \overline{R_n^k} \leqslant R_{p,n,2}^{k,DF} \; \forall\, k \in \{1,\ldots,L\} \tag{19d}$$

où $\overline{\mathbf{R}_n} = \left(\overline{R_n^1},\ldots,\overline{R_n^L}\right)$, $R_{p,n,1}^{k,DF} = \log_2\left(1 + A_{n-1}^k P_{p,n}^k\right)$, $R_{p,n,2}^{k,DF} = \log_2\left(1 + B_{n-1}^k P_{p,n}^k + C_{n-1}^k P_{r,n}^k\right)$, et

$$A_{n-1}^k = \frac{|h_{sp}^k|^2}{|h_{ss}^k|^2 P_{s,n-1}^k + n_0}$$

$$B_{n-1}^k = \frac{|h_{pp}^k|^2}{|h_{ps}^k|^2 P_{s,n-1}^k + n_0}$$

$$C_{n-1}^k = \frac{|h_r^k|^2}{|h_{ps}^k|^2 P_{s,n-1}^k + n_0}$$

On résout le problème et on déduit les expressions analytiques de $P_{p,n}^k$ et $P_{r,n}^k$ en fonctions des multiplicateurs de Lagrange. La puissance primaire transmise est donnée par

$$P_{p,n}^k = \frac{A_{n-1}^k C_{n-1}^k (1-\mu^k)}{\lambda (C_{n-1}^k - B_{n-1}^k)} \tag{20}$$

est la puissance transmise par le relais est égale à

$$P_{r,n}^k = \frac{\mu^k}{\lambda} - \frac{1 + B_{n-1}^k P_{p,n}^k}{C_{n-1}^k} \tag{21}$$

Les valeurs des multiplicateurs de Lagrange peuvent être calculées en utilisant la méthode de bissection.

De l'autre côté, le problème d'optimisation au niveau du secondaire est donné par le problème

(5.29).

$$\max_{\mathbf{P}_{s,n}} \sum_{k=1}^{L} \log_2 \left(1 + \frac{|h_{ss}^k|^2 P_{s,n}^k}{n_0}\right) \tag{22a}$$

$$\text{s.t. } \sum_{k=1}^{L} P_{s,n}^k = P_{s,\max} \tag{22b}$$

$$\text{s.t. } P_{s,n}^k \geqslant 0 \, \forall \, k \in \{1, \ldots, L\} \tag{22c}$$

$$|h_{ps}^k|^2 P_{s,n}^k \leqslant I_{th}^k \, \forall \, k \in \{1, \ldots, L\} \tag{22d}$$

Ce problème est résolu en utilisant la méthode du Lagrangien et la puissance transmise par le secondaire est donnée par le Tableau 3.2.

0.5.4 Simulations

Les résultats de simulations sont présentés en fonction de d_{sec}. Tout d'abord on compare les performances des protocoles AF et DF dans le cas mono-porteuse, et puis on analyse les performances du modèle proposé dans le cas multi-porteuses avec DF.

Mono-porteuse

Les débits primaire, secondaire et total atteignables par le relayage AF et DF sont comparés dans les Figures 5.13, 5.14 et 5.15, respectivement.

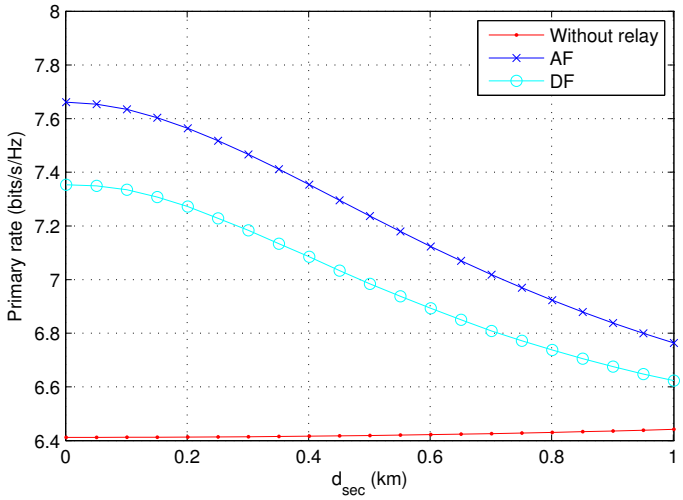

FIGURE 12 – Comparaison entre les débits primaires avec AF et DF

On remarque que le AF présente un gain primaire plus important que le DF dans le scénario proposé. On remarque aussi que le gain obtenu grâce à l'application du SIC se dégrade avec le AF parce que la nouvelle contrainte pour faire le SIC dans ce cas est plus forte.

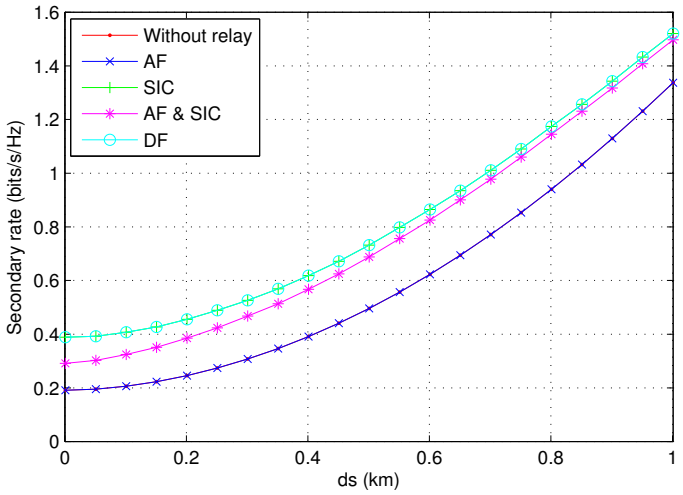

FIGURE 13 – Comparaison entre les débits secondaires avec AF et DF

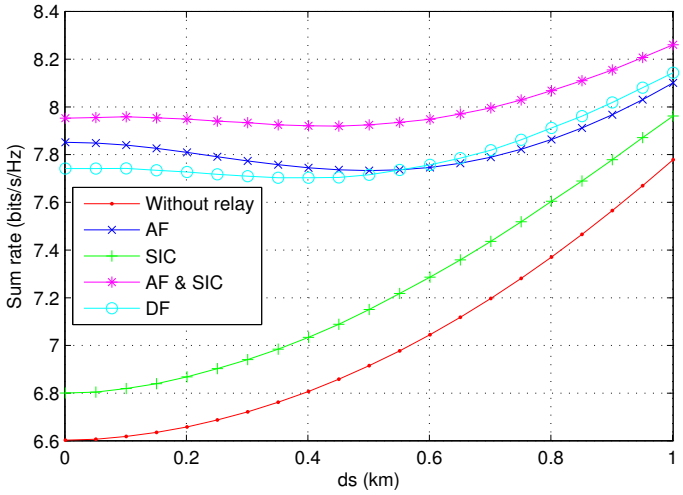

FIGURE 14 – Comparaison entre les débits totaux avec AF et DF

DF dans le scénario multi-porteuses

Dans cette partie, on considère 64 sous-porteuses pour chaque utilisateur. On compare les débits atteignables avec allocation de puissance. Les résultats de simulations pour les débits primaire et total sont donnés par 5.19 et 5.20, respectivement.

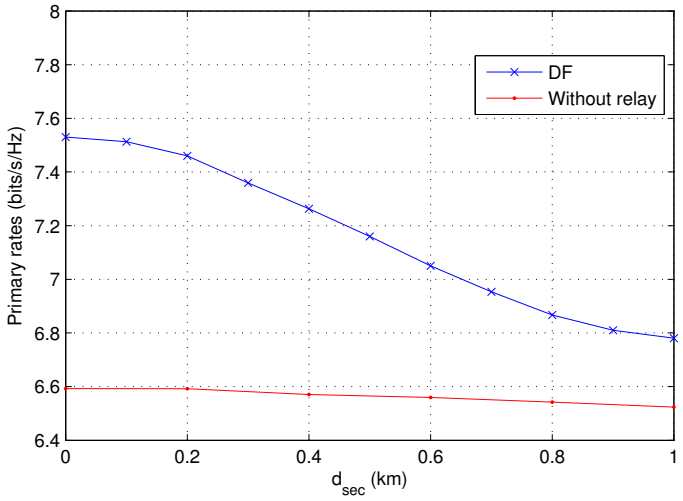

FIGURE 15 – Débit primaire avec DF dans le cas multi-porteuses

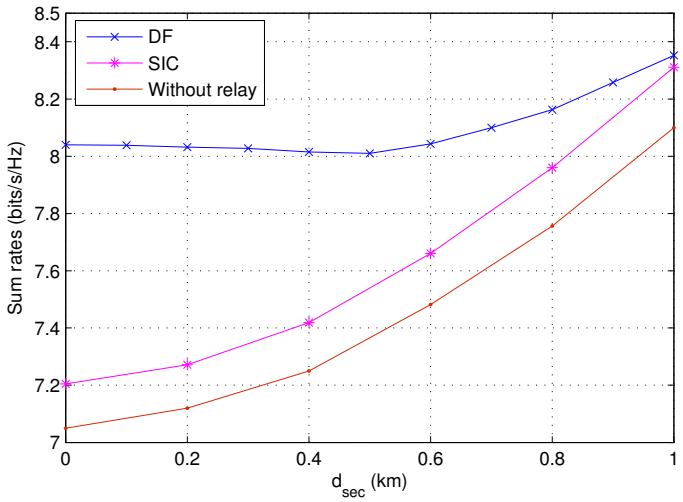

FIGURE 16 – Débit total avec DF dans le cas multi-porteuses

0.6 Conclusion

Cette thèse a étudié l'allocation des ressources dans un système de radio cognitive en underlay avec une transmission OFDM sur une liaison montante. Notre objectif était de maximiser les débits atteignables du système pour les deux utilisateurs primaire et secondaire. Un algorithme d'allocation dynamique des ressources, ainsi qu'un nouveau modèle basé sur un relais au niveau

du récepteur secondaire ont été proposés. Premièrement, nous avons présenté un algorithme de décodage adaptatif au niveau de l'utilisateur secondaire, lorsque un seul mobile secondaire est disponible dans la cellule secondaire. Avec l'algorithme proposé, l'utilisateur secondaire a pu soit traiter l'interférence de l'émetteur primaire comme du bruit, ou utiliser SIC ou SC. Nous avons étudié le problème d'allocation des ressources avec une connaissance parfaite ou statistique des canaux et une solution générale pour un système radio cognitif underlay avec une liaison montante et OFDM a été obtenu pour les deux scénarios.

Enfin, afin de maximiser le débit primaire, un nouveau modèle basé sur un nœud de relayage au récepteur secondaire a été proposé. Plus précisément, nous avons supposé que le récepteur secondaire peut agir comme un relais en FD afin d'aider la transmission primaire. Tout d'abord, nous avons considéré les deux protocoles de ralayage AF et DF dans le cas mono-porteuse. En outre, nous avons examiné le scénario multi-porteuses pour le cas DF. Les résultats de simulation ont montré une croissance importante du débit primaire atteignable comparant é des scénarios sans relais.

Chapitre 1

Introduction and Outline

1.1 Background and motivation

In early June 2009, the process of analog terrestrial broadcasting was shut down and the switch from analog to digital broadcast television known as the Digital Television (DTV) transition was completed [1]. This switch to all-digital broadcasting frees up some parts of the valuable broadcast spectrum for important services like advanced wireless and public safety communications. As advantage, DTV requires less spectrum space than its analog counterpart. The recent increase in wireless technology has further compounded the problem of spectrum scarcity. Moreover, observing an under-utilization of the licensed spectrum, the Federal Communications Commission (FCC) has allowed the unlicensed systems to operate within the spectrum band allocated to DTV services while ensuring that no harmful interference is caused to the DTV broadcasting, in order to improve the spectral efficiency in the TV bands [2]. More specifically, the FCC has recommended that wireless devices can coexist with the licensed users generating minimal interference while taking advantage of the available resources. This is called the Cognitive Radio (CR) technology, where the unlicensed user is called the cognitive user. In this context, the IEEE 802.22 working group has developed the so-called Wireless Regional Area Network (WRAN) standard which incorporates advanced CR capabilities including Dynamic Spectrum Access (DSA), spectrum sensing, coexistence for optimal use of the available spectrum, etc. [3].

According to the FCC definition, CR is a "radio or system that senses its operational electromagnetic environment and can dynamically and autonomously adjust its radio operating parameters to modify system operation, such as maximize throughput, mitigate interference, facilitate interoperability, access secondary markets". In other words, CR has the ability to sense the environment in which it operates and to adapt its transmission's parameters in order to maximize the spectrum use while minimizing the interference to the licensed users. In the

terminology of information theory, a CR is defined by the availability and utilization of network side information. It is an interference channel with asymmetric channel knowledge [4].

To achieve higher spectral efficiency, multiple access techniques can be employed such that licensed and unlicensed users can transmit data within the same frequency range [5]. Several multiple access techniques are proposed, including those based on Code Division Multiple Access (CDMA) [6, 7], spatial multiplexing [8], and OFDM [9, 10]. However, OFDM is known as a reliable transmission scheme for CR providing flexibility in allocating the radio resources in dynamic environment and assuring no mutual interference among the adjacent CR channels. Allocation of radio resources dynamically is a major challenge in CR systems. Many algorithms for resource allocation in OFDM based CR systems have been studied. These algorithms attempt to maximize the total throughput of the CR system subject to the total power constraint of the CR system and tolerable interference to the Primary User (PU).

1.2 Thesis objectives

In this thesis, we consider an OFDM-based CR cellular system composed of one primary cell and one secondary cell. We investigate the resource allocation problem, considering both single-user and multi-user cases in the secondary cell, in order to maximize the secondary achievable rate. The problem is faced either when perfect channel knowledge or when only statistical information of the primary channels is available at the SU. The relaying case is also considered.

The main objectives of the work performed in this thesis are :

— Determine an adaptive spectrum sharing algorithm, by allowing the SU to either treat the interference as noise or use SIC or SC, in order to maximize the secondary achievable rate.

— Investigate the power allocation problem to optimally allocate the transmit power under the maximum interference threshold allowed at the PU and the total power budget.

— Evaluate the performance of the proposed algorithm in the multi-user case, showing that multi-user diversity improves the system throughput. For this purpose, the subcarriers allocation problem is investigated and a general solution is proposed for both single and multiple user cases.

— Consider the same problem in both perfect and statistical CSI cases to prove the robustness of the proposed algorithm when only statistical channel knowledge of the primary's links is available at the SU.

— Maximize the primary achievable rate by considering that the secondary receiver can serve as a relay node with Amplify-and-Forward (AF) or DF relaying protocols.

1.3 Thesis outline

Resource allocation for an uplink OFDM-based underlay cognitive radio system is investigated from two perspectives : firstly, an adaptive decoding algorithm is proposed at the SU in order to maximize the secondary rate. This approach is detailed in chapters 3 and 4 for both

perfect and statistical CSI cases, respectively. And then, a relay-aided model is proposed where the secondary mobile terminal can help the primary transmission in order to maximize the primary rate. This proposition is described in Chapter 5. More specifically, the thesis is organized as follows :

In Chapter 2, we provide a technical background for the studied problem. General notions about OFDM, SIC and SC are described. Subsequently, capacity regions of the main multi-user channels from the information theoretic point of view are presented. Then, wireless radio channel models are detailed and the different relay-assisted channel models and protocols are discussed. Finally, convex optimization problems are introduced and both dual decomposition approach and Successive Convex Approximation (SCA) are detailed.

In Chapter 3, we consider two approaches to study the resource allocation problem for an underlay OFDM-based CR system when perfect channel knowledge is available at the different nodes. In the first approach, the single-user case is investigated where only one SU exists in the secondary cell. The adaptive decoding algorithm at the SU is detailed, where treating interference as noise, SIC and SC can be used. Furthermore, the power optimization problem is investigated and a general solution to the studied model is proposed using dual decomposition and SCA methods. In the second part of this chapter, multiple SUs are allowed to co-exist in the secondary cell and subcarrier allocation algorithm is proposed. Since only one user can be active at each time slot, the single-user general solution for the power optimization problem can be used once the activated users are selected within different subcarriers. Through extensive simulations, we show that our proposed algorithm outperforms some existing solutions.

In Chapter 4, the single-user scenario is studied when only statistical CSI about primary links is available at the SU. For that, the outage probabilities for different constraints are calculated and a general solution to the optimization problem is proposed. Simulation results prove the robustness of the proposed algorithm despite the lack of channel information.

In Chapter 5, in order to maximize the primary achievable rate and thus the total system rate, we exploit a new system model where the secondary receiver can act as a relay node. We focus on the Full-Duplex (FD) relay mode. For that, we investigate single-carrier scenario with both AF and DF protocols. Finally, we investigate the resource allocation procedure for DF in the multi-carrier scenario. The performance of this proposal is compared to previous results obtained in Chapter 3.

Finally, we conclude this thesis in the last chapter and provide some potential perspectives for future research activities.

1.4 List of publications

Journal paper

1. M. Chami, M. Pischella, D. Le Ruyet, "Resource Allocation for OFDM-based Multiuser Cooperative Underlay Cognitive Systems", submitted to IEEE Transactions on Cognitive Communications and Networking (TCCN), December 2015.

International Conferences

1. M. Chami, M. Pischella, D. Le Ruyet, "Resource Allocation with SIC under Statistical CSI in Multi-carrier based Cognitive Radio Networks", accepted in Proceedings of the IEEE Wireless Communications and Networking Conference (WCNC) 2016, April 2016.
2. M. Chami, M. Pischella, D. Le Ruyet, "Optimal power control for cooperative underlay cognitive system", in 11th International Symposium on Wireless Communications Systems (ISWCS) 2014, Aug 2014, pp. 558-562.
3. M. Chami, M. Pischella, D. Le Ruyet, "Adaptive Decoding Strategy with Superposition Coding for Cognitive Radio Systems", in Proceedings of European Wireless (EW) 2014 ; 20th European Wireless Conference, May 2014, pp. 1-6.

Chapitre 2

Technical Background

This chapter provides a technical background that is essential to the thesis where CR is the main issue with all related research subjects. This chapter summarizes the key concepts related to CR, OFDM, interference cancellation techniques, information theoretic concepts, capacity regions from the information theoretic point of view, wireless radio channel models, relay-assisted channel and convex optimization.

2.1 Cognitive Radio

Wireless communications have captured the attention in the last two decades, being the fastest growing segment of the communications industry. Many applications of wireless networking were developed for both analog and digital communications, with different generations trying to respond to the critical public policy issues : Spectrum access, efficiency, and reliability. In order to tend to more flexible and reconfigurable terminals, the idea of Software-Defined Radio (SDR) [11] was born out by replacing most of analog functions of radio transceivers by digital processing blocks. In an ideal software radio, all the aspects of the radio are defined in software on general-purpose processors, which cannot be practical. Therefore, the SDR compromises the software radio ideal in order to implement practical high-performance devices and infrastructure with current technology. However, even with these technologies, processing capacity still being wasted which motivates the development of the CR, which offers technology-based mechanisms including a degree of flexibility to the radios in a way that enhances the utilization of the radio spectrum.

In other words, the idea of CRs, which is a particular extension of SDR that employs model-based reasoning about the channel, users and communications context [12], was born out of the wireless spectrum's limitation. The original motivation of Mitola, who was the first to introduce this term in the late 90's, was the indication of measurements that even crowded spectrum is

not used across all time, space, and frequencies. For this purpose, advanced radio and signal processing technology along with novel spectrum allocation policies are used to support new wireless users operating in the existing spectrum without degrading the performance of licensed users called PUs [13]. More specifically, the CR technology permits to an unlicensed users called SUs to coexist with the PUs without degrading their performance. In a CR system, the SUs have the ability to sense and adapt to their environment in order to detect possible frequency holes in the wireless spectrum which therefore increase the spectral efficiency. Consequently, the CR technology is very appealing since it provides a low-cost and highly flexible alternative to the classic single-frequency band and single-protocol wireless communication [14].

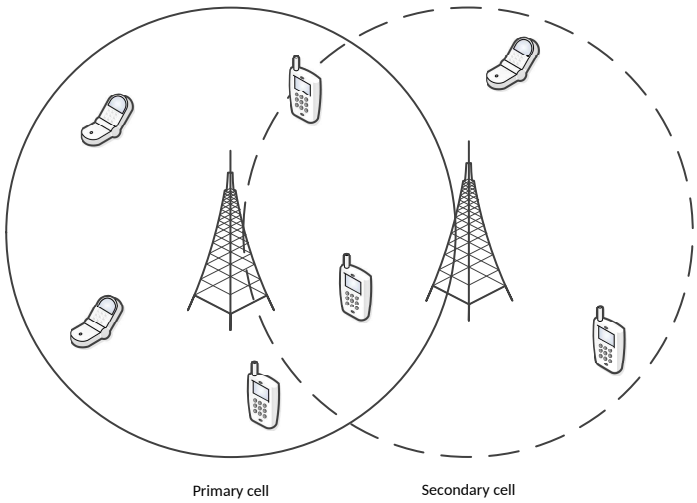

FIGURE 2.1 – Cognitive radio system

Based on the type of available network side information along with the regulatory constraints, three types of CR systems exist : interweave, underlay and overlay cognitive radio. Underlay and interweave CR are typically deployed in a bandwidth occupied by the primary system. In an interweave scenario, the SUs find and exploit spectral holes to avoid interfering with PUs. In other words, they adaptively sense the spectrum band and utilize it whenever it is not used by the PUs [15]. In the underlay case, the SUs are allowed to coexist with the PUs provided that the interference caused to the PUs is below a predefined threshold [15]. In other words, the spectrum is shared between both primary and secondary systems under some constraints. In this case, the interference constraint may be met via wideband signaling to maintain interference below the noise floor, or via multiple antennas and beamforming. In the later category, the SUs overhear and enhance noncognitive radio transmissions. More specifically, the secondary system has the knowledge of the primary system codebook, channel gains and transmitted information. A part of the SUs power can be used to retransmit the PUs message so that the SUs are able to maintain or improve the primary rate while achieving their own communication goals [15]. Both overlay and underlay scenarios are compared in [16].

2.2 Orthogonal frequency division mulotiplexing

Multi-carrier transmissions such as OFDM are largely used for CR networks due to their flexibility in allocating resources among SUs [17].

2.2.1 Basic conception

The main idea behind multi-carrier modulation is to divide the allocated spectrum band equally into multiple orthogonal subcarriers. Each subcarrier is modulated with a separate symbol and then the non-overlapping subcarriers are frequency-multiplexed, which helps to avoid spectral overlap of channels to eliminate inter-channel interference. OFDM is a special case of multi-carrier transmission and it was first introduced by Chang in 1966 [18]. It is based on Inverse Fast Fourier Transform (IFFT) at transmission and Fast Fourier Transform (FFT) at reception (Fig. 2.2). The transmission is achieved in parallel over different orthogonal subcarriers, each of them modulated with a conventional modulation scheme at a low symbol rate maintaining total data rates similar to conventional single-carrier modulation schemes in the same bandwidth. The low data rate on each of the subcarriers makes OFDM transmission very resilient to inter-symbol and inter-frame interference.

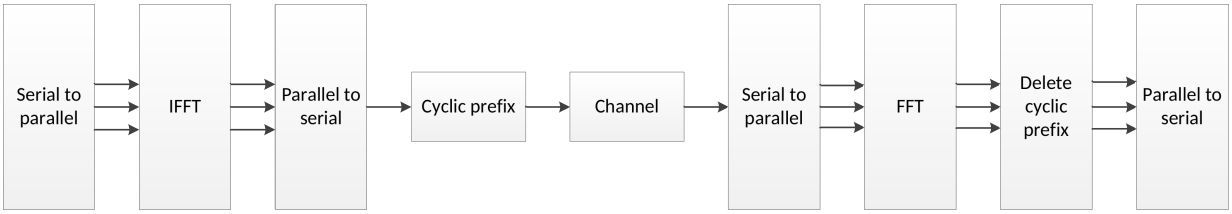

FIGURE 2.2 – Implementation of an OFDM system

After mapping the original data to be complex symbol and using the serial-to-parallel converter, the mapped symbols X which are the discrete frequency components of the transmitted signal $s(t)$, are distributed to L parallel subcarriers. The vector of L elements $[X[0], X[L-1]]$ is transmitted simultaneously by L subcarriers at each time slot. At transmission, IFFT is performed on all subsymbols $X[k]$ in order to generate the time domain signal as expressed in the following equation

$$x[n] = \frac{1}{\sqrt{L}} \sum_{k=0}^{L-1} X[k] e^{j2\pi nk/L},\ 0 \leqslant n \leqslant L-1 \tag{2.1}$$

A cyclic prefix of N_{CP} time samples is then appended to the L time samples (Fig. 2.3). It copies the N_{CP} last samples of each OFDM symbol and is then inserted at the beginning of the symbol. N_{CP} must be greater than the maximum multipath delay spread, therefore the useful data samples can be free of Inter-Symbol Interference (ISI). Finally, the baseband transmitted signal is upconverted to be the passband signal. At reception, N_{CP} is removed and FFT is applied on the received signal, which is the result of a circular convolution between $x[n]$ and the channel response, in order to retrieve the subsymbols.

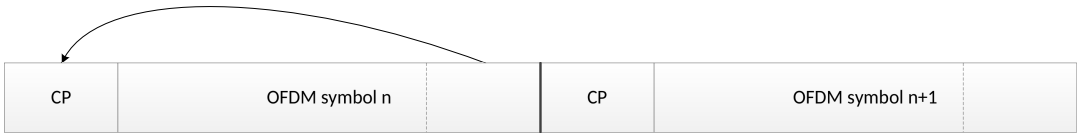

FIGURE 2.3 – Cyclic prefix

2.3 Interference cancellation techniques

As recent wireless systems are becoming increasingly interference-limited, the use of advanced interference mitigation techniques shows more interest to improve the network performance by increasing its capacity. Several concepts are studied for overcoming interference in wireless systems as network cooperation, interference cancellation receivers, etc. Interference cancellation detectors seek to remove interference by actually subtracting estimates of interfering signals from the received signal. This technique consists of an initial stage of matched-filters, followed by stages of interference cancellation [19]. Interference cancellation receivers typically come in two forms : parallel and successive. In parallel interference cancellation, all interfering signals are subtracted concurrently from the received signal. In the successive approach, signals are canceled serially in the descending order of estimated received power, from strongest to weakest. Two of these interference cancellation techniques are SIC and SC, which are both well-known capacity achieving coding schemes in wireless networks. Although SIC and SC are not always the optimal multiple access scheme in wireless networks [20–22], they are especially amenable to implementation [23, 24] and help to achieve full capacity in multi-user systems in several cases [21, 25, 26]. In this section, we will provide a brief description of both decoding strategies.

2.3.1 Successive Interference Cancellation

SIC is a promising technique to improve the efficiency of the wireless networks with relatively small additional complexity. It was first introduced by Cover [27] and it is defined as a physical layer capability [28] that allows a receiver to decode two or more signals that arrive simultaneously. Traditionally, if the receiver receives many packets, only the strongest signal can be decoded treating the other signals as interference. However, SIC allows recovery of the weaker signals by decoding the strongest signal first, subtracting it from the combined signal and then extracting the weaker ones from the residue. This can be an iterative process to recover multiple packets and hence it is termed *successive interference cancellation*. The flow chart of the process is shown in Fig. 2.4 [29]

At each iteration, all signals' powers are estimated and the signal with the largest power is selected. This one is estimated, then regenerated and removed from the buffered received signal. The remaining signals are now re-estimated and a new largest signal is selected. The process is continued until all the users' signals have been recovered or the maximum allowable number of cancellations is reached.

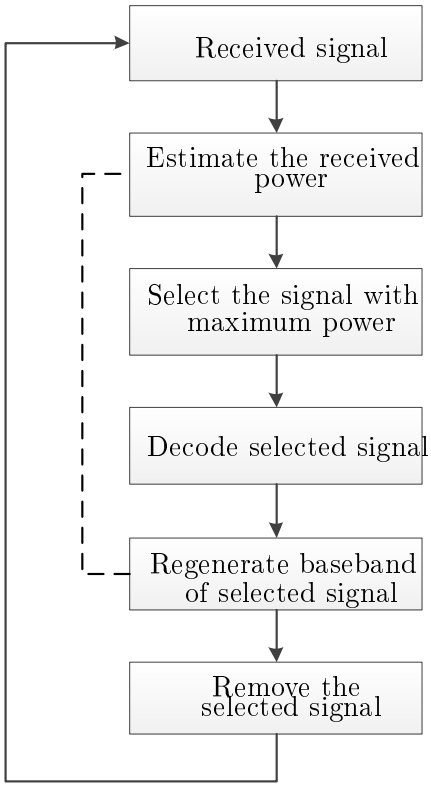

FIGURE 2.4 – Successive interference cancellation scheme

2.3.2 Superposition Coding

SC is a well-known capacity-achieving coding scheme in wireless network. This idea appeared first in [27] for Broadcast Channel (BC) and it was then adapted by Bergmans [30] to the general degraded BC. Actually, SC is largely used for MAC [31], interference channels [32–34], relay channels [35] and other channel models to achieve better performance than traditional orthogonal schemes (e.g., time, frequency, or code division). Specifically, SC is a physical layer technique by which a transmitter can simultaneously send independent messages to multiple receivers with asymmetric channel conditions.

Let us consider a two-receiver case, in which the transmitter decomposes the available power between the two receivers varying a parameter α between 0 and 1. In other words, it superimposes an additional message destined to a receiver 2 on a basic message destined for a receiver 1 which generates auxiliary codewords. The additional message appears as noise to receiver 1 ; the decoder at the secondary receiver extracts the additional message by applying SIC to first remove the interference caused by the basic message. This concept is illustrated in Fig. 2.5. However, there are two variants of SC scheme, which differ in how the codebooks are generated. The first variant, presented by Cover, has code clouds of the identical shape, while the second one given by Bergmans has code clouds of independently generated shapes [36].

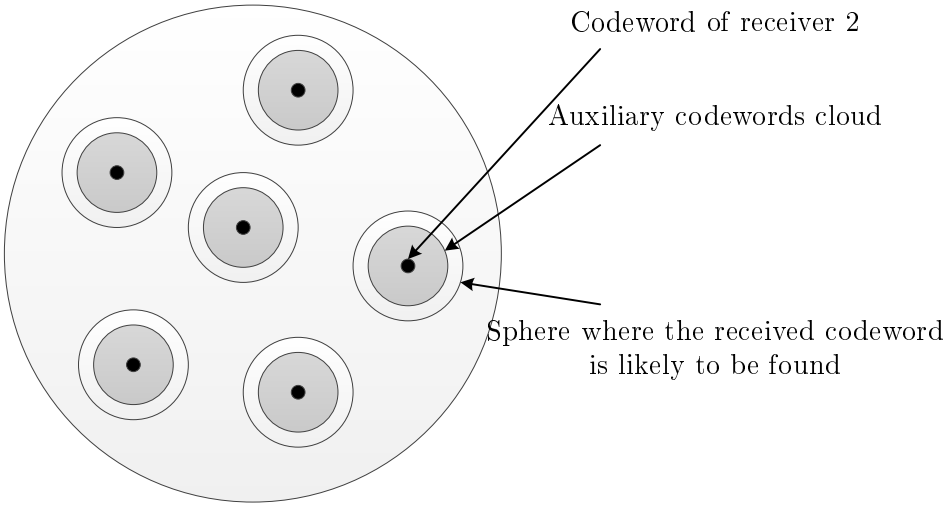

FIGURE 2.5 – Superposition coding scheme

2.4 Background on information theory

This section describes the information theory background useful for developing the capacity expressions given throughout this thesis. We detail the concept and properties of entropy, mutual information and typical sequences which will be used later to define different capacity regions. The concepts and definitions are taken from the book of Cover and Thomas [25].

2.4.1 Entropy and mutual information

In this section, the entropy and mutual information are defined as an introduction to the capacity expressions where these concepts are used.

The entropy represents the average of uncertainty of a random variable. It is the average number of bits required to describe a realization of the random variable [25]. The entropy of a random variable X with a probability mass function $p(x) = \Pr\{X = x\}$ is defined by

$$H(X) = -\sum_{x} p(x) \log_2 p(x) \tag{2.2}$$

The definition of the entropy of a single random variable can be extended to a pair of random variables (X, Y) which is called the joint entropy, and is defined as

$$H(X,Y) = -\sum_{x}\sum_{y} p(x,y) \log_2 p(x,y) \tag{2.3}$$

We can also define $H(X|Y)$ as the conditional entropy of two random variables X and Y, which represents the entropy of a random variable conditional on the knowledge of another random variable. The chain rule to describe the relation between entropy, mutual entropy and conditional

entropy is

$$H(X,Y) = H(X) + H(Y|X) \tag{2.4}$$

Furthermore, the mutual information $I(X;Y)$ is the reduction in uncertainty of X due to Y and it is defined by

$$\begin{aligned} I(X;Y) &= H(X) - H(X|Y) = \sum_{x,y} p(x,y) \log_2 \frac{p(x,y)}{p(x)p(y)} \\ &= H(Y) - H(Y|X) = H(X) + H(Y) - H(X,Y) \end{aligned} \tag{2.5}$$

$I(X;Y)$ measures the dependence between the two random variables.

2.4.2 Channel capacity

The notion of channel capacity was developed in order to derive the achievable limits of data transmission in a wireless communication system. Claude Shannon [37] was the first to talk about a communication with a strictly positive rate and a small error probability, without reducing the data rate, introducing the term of capacity as the maximum data rate that can be supported by the channel without error even with a noisy channel.

Let X and Y be the random variables representing the input and output of the channel, respectively. Let $I(X;Y)$ be the mutual information of X and Y and $p_X(x)$ the marginal distribution of X. The channel capacity is defined as

$$C = \sup_{P_X(x)} I(X;Y)$$

In this section, we will focus on the familiar Additive White Gaussian Noise (AWGN) channel defined at discrete time m by

$$y[m] = x[m] + z[m] \tag{2.6}$$

where $x[m]$ and $y[m]$ are complex input and output, respectively and $z[m]$ is $\mathcal{N}(0,\sigma^2)$ noise, independent over time. The capacity of the complex AWGN channel with power constraint P and noise variance σ^2 is

$$C_{AWGN} = \log_2 \left(1 + \frac{P}{\sigma^2}\right) \text{ bits per complex dimension} \tag{2.7}$$

which can be also expressed by

$$C_{AWGN} = \log_2 (1 + \text{SNR}) \text{ bits per complex dimension} \tag{2.8}$$

where $SNR = \frac{P}{\sigma^2}$ is the Signal-to-Noise Ratio (SNR). This capacity is a special case of Shannon's general theory applied to a specific channel.

Let us now consider a continuous-time Additive White Gaussian Noise (AWGN) channel with bandwidth B Hz, power constraint P Watts and additive white Gaussian noise with power spectral density $\frac{N_0}{2}$. Since the noise variance and the power constraint per real symbol are N_0 and $\frac{P}{2B}$ respectively, with $n_0 = N_0 B$, the capacity of the channel is $\frac{1}{2}\log_2\left(1+\frac{P}{N_0 B}\right)$ bits per real dimension or $\log_2\left(1+\frac{P}{N_0 B}\right)$ bits per complex dimension. Consequently, the capacity of the continuous-time AWGN channel is

$$C_{\text{AWGN}}(P,B) = B\log_2\left(1+\frac{P}{N_0 B}\right) \text{ bits/s} \tag{2.9}$$

2.5 Capacity region for multi-user channels

This section takes a fundamental look at the capacity of different multi-user channels. Firstly, we point out the expressions of the capacities for different models of the AWGN channel. Then, we introduce in Section 2.6 the fading channel, which will be used in the rest of the thesis.

2.5.1 Gaussian Multiple Access Channel

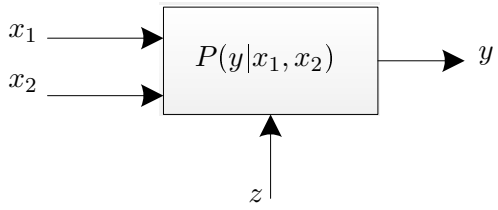

FIGURE 2.6 – Multiple Access Channel

In the independent-user MAC, the multiple users which are aware of each other's messages attempt to communicate independent information over the noisy channel to a single receiver. The channel capacity of MAC was found by Ahlswede [38] and Liao [39]. A proof of this capacity region was given by Cover et al. in [40]. To calculate the capacity region of Gaussian MAC presented in Fig. 2.6, we assume that the two encoders satisfy

$$p(x_1,x_2) = p_1(x_1)p_2(x_2)$$

For any two distributions $p_1(x_1)$ and $p_2(x_2)$, each sender j generates 2^{NR_j} independent codewords $\mathbf{x}_j(m_j), m_j \in \{1,2,\ldots,2^{NR_j}\}$ of length N. These codewords form the codebook which is revealed to the senders and the receiver. Thus, to send index m_j, sender j sends the codeword $\mathbf{x}_j(m_j)$.

At each word reception i, the receiver declares that $\hat{m}_{1_i} = m$ was sent from user 1 if and only if there exists one and only one m such that $(\mathbf{x}_1(m), \mathbf{y}(i))$ are jointly $\epsilon-$typical, i.e., $(\mathbf{x}_1(m), \mathbf{y}(i)) \in \mathcal{T}_\epsilon(\mathbf{x}_1, \mathbf{y}(i))$, where $\mathcal{T}_\epsilon$ is a typical set which is defined in Appendix A. According to jointly typical sequence properties, $\hat{m}_{1_i} = m_{1_i}$ with arbitrary small probability if

$$R_1 < I\left(X_1;Y\right) \tag{2.10}$$

if N is sufficiently large.

Assuming that m_{1_i} is decoded successfully at the receiver, it has now to decode m_{2_i} using the information it receives from second user. Then, $\hat{m}_{2_{i-1}} = m$ is declared to be the index sent in the previous transmission block if and only if there is a unique m such that $(\mathbf{x}_2, \mathbf{y}(i-1)) \in \mathcal{T}_\epsilon(\mathbf{x}_2, \mathbf{y}(i-1))$. Then, $\hat{m}_{2_{i-1}} = m_{2_{i-1}}$ if N is sufficiently large and if

$$R_1 < I\left(X_2; Y | X_1\right) \tag{2.11}$$

Consequently, the rate has to be

$$\begin{aligned} R &< R_1 + R_2 \\ &< I\left(X_1, X_2; Y\right) \end{aligned} \tag{2.12}$$

The capacity region of two-users MAC is then given by the convex closure of all (R_1, R_2) pairs satisfying

$$R_1 \leqslant I\left(X_1; Y | X_2\right) \tag{2.13}$$

$$R_2 \leqslant I\left(X_2; Y | X_1\right) \tag{2.14}$$

$$R_1 + R_2 \leqslant I(X_1, X_2; Y) \tag{2.15}$$

for $p(x_1, x_2, y) = p(x_1)p(x_2)p(y|x_1, x_2)$.

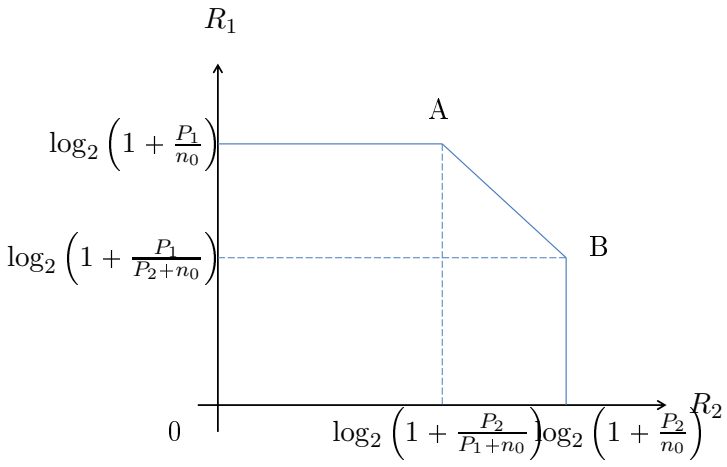

FIGURE 2.7 – Capacity region for MAC

More specifically, the capacity region of a two-user Gaussian MAC, presented in Fig. 2.7, is given by [25, 41] :

$$R_1 \leqslant \log_2\left(1 + \frac{P_1}{n_0}\right) \text{ bits per complex dimension} \tag{2.16}$$

$$R_2 \leqslant \log_2\left(1 + \frac{P_2}{n_0}\right) \tag{2.17}$$

$$R_1 + R_2 \leqslant \log_2\left(1 + \frac{P1 + P_2}{n_0}\right) \tag{2.18}$$

where P_1 and P_2 denote the allocated power to first and second users respectively. Note that the vertical line of the capacity region is achieved by SIC when signal 1 is first detected and removed. If the order of the signal detection is reversed and signal 2 is first detected, the horizontal line of the capacity region could be achieved by SIC. The titled line AB can be achieved by SC.

2.5.2 Broadcast channel

A BC [42] consists of a single transmitter that generates the channel input x, that will be communicated to many outputs y_i, and a probability transition function $p(y_1, y_2, \ldots, y_N|x)$. In this model, presented in Fig. 2.8 for two outputs, the transmission rate is limited by the worst channel.

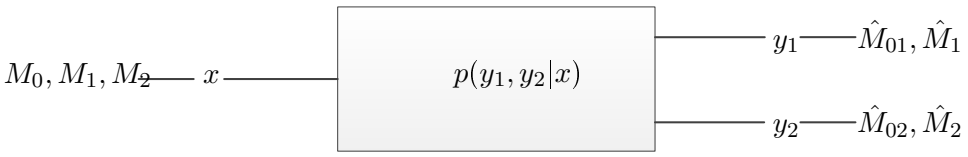

FIGURE 2.8 – Broadcast channel

To calculate the capacity region of a two-users BC, we consider an $((M_0, M_1, M_2), N)$ code. We define the rate (R_0, R_1, R_2) of an $((M_0, M_1, M_2), N)$ code by

$$\begin{aligned} R_0 &= \frac{1}{N}\log_2 M_0 \\ R_1 &= \frac{1}{N}\log_2 M_1 \\ R_2 &= \frac{1}{N}\log_2 M_2 \end{aligned}$$

all defined in bit per transmission, where R_1 and R_2 are the rates of transmission of independent information to receivers 1 and 2, respectively, and R_0 is the portion of the information common to both receivers. The rate (R_0, R_1, R_2) is said to be achievable by a BC if, for any $\epsilon > 0$ and for all N sufficiently large, there exists an $((M_0, M_1, M_2), N)$ code with

$$\begin{aligned} M_0 &\geqslant 2^{NR_0} \\ M_1 &\geqslant 2^{NR_1} \\ M_2 &\geqslant 2^{NR_2} \end{aligned}$$

such that the average probability of error is less than ϵ. On other words, if a rate pair (R_1, R_2) is achievable for private messages, then the rate triple $(R_0, R_1 - R_0, R_2 - R_0)$ is also achievable for the BC with common and private messages. The capacity of the BC is not known in general,

but is known for a special class as degraded broadcast channel.

A BC is said to be physically degraded if $X \rightarrow Y_1 \rightarrow Y_2$ forms a Markov chain, that is, Y_2 is a degraded version of Y_1 and $p(y_1, y_2|x) = p(y_1|x)p(y_2|x)$. The capacity region for sending independent information over the degraded BC is the convex hull of the closure of all (R_1, R_2) satisfying

$$R_1 \leqslant I(X; Y_1|U) \tag{2.19}$$

$$R_2 \leqslant I(Y_2; U) \tag{2.20}$$

$$\tag{2.21}$$

for some joint distribution $p(u)p(x|u)p(y_1, y_2|x)$, where the auxiliary random variable U has cardinality bounded by $|\mathrm{U}| \leqslant \min\{|X|, |Y_1|, |Y_2|\}$.

Besides, a BC is stochastically degraded BC if there exists another probability transition $\acute{p}(y_2|x)$ such that

$$p(y_2|x) = \sum_{\tilde{y_1}} p(\tilde{y_1}|x)\acute{p}(y_2|\tilde{y_1})$$

A stochastically degraded BC means that although $X \rightarrow Y_1 \rightarrow Y_2$ does not form a Markov chain, we can find an equivalent physical degraded BC with the same capacity such that $X \rightarrow \tilde{Y_1} \rightarrow Y_2$ forms a Markov chain. The Gaussian BC is a stochastically degraded BC with capacity region defined by

$$R_1 \leqslant \log_2\left(1 + \frac{\alpha P}{n_0}\right) \tag{2.22}$$

$$R_2 \leqslant \log_2\left(1 + \frac{(1-\alpha)P}{\alpha P + n_0}\right) \tag{2.23}$$

where α may be arbitrarily chosen ($0 \leqslant \alpha \leqslant 1$) to trade off rate R_1 for rate R_2 as the transmitter wishes.

SIC, SC and BC

The rate pairs which define the capacity region of a BC channel can be achieved by applying SC at the transmitter (encoding) with SIC at receivers (decoding). For the two-users case, the main idea is that if user 1 can decode its data successfully from y_1, then user 2 should be able to decode the data of user 1 from y_2. Then, user 2 can subtract the codeword of user 1 from y_2 to better decode its data. The superposition scheme can be simplified to the following one :

Random codebook generation : In a first step, the encoder has to randomly and independently generate 2^{NR_2} sequences $\mathbf{u}(m_2), m_2 \in \left[1 : 2^{NR_2}\right]$ each $\sim \Pi_{i=1}^{N} p_U(u_i)$. Then, $\forall m_2 \in \left[1 : 2^{NR_2}\right]$ it generates randomly and conditionally independently 2^{NR_1} sequences $\mathbf{x}(m_1, m_2), m_1 \in \left[1 : 2^{NR_1}\right]$, each $\sim \Pi_{i=1}^{N} p_{X|U}(x_i|u_i(m_2))$

Encoding : To send (m_1, m_2), the transmitter has to transmit $\mathbf{x}_1(m_1, m_2)$.

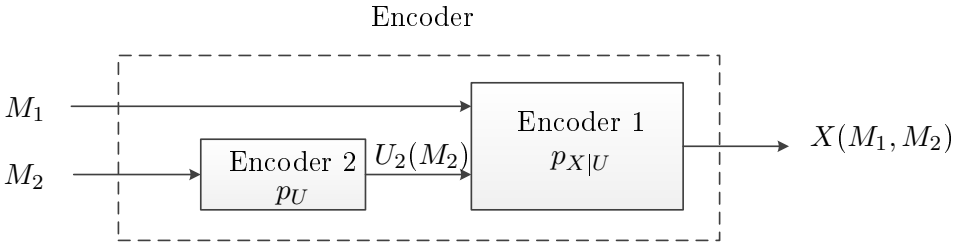

FIGURE 2.9 – Encoding procedure with superposition

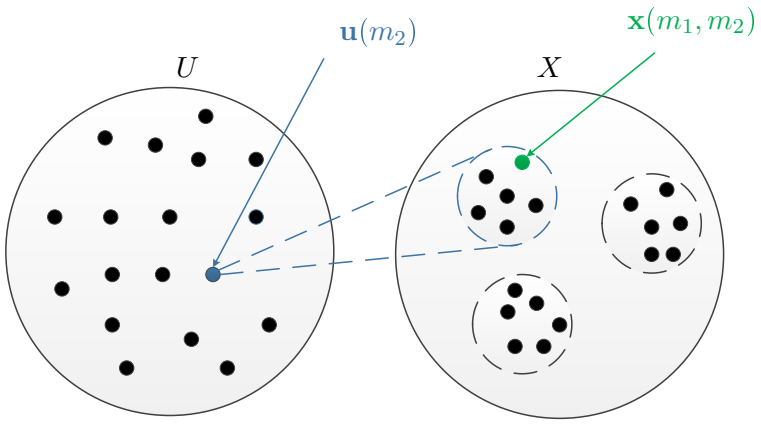

FIGURE 2.10 – SC scheme for a BC encoder

Decoding : Firstly, decoder 1 finds a unique $m_1 \in \left[1 : 2^{NR_1}\right]$ such that

$$(\mathbf{u}(m_1), \mathbf{y}_1) \in \mathcal{T}_\epsilon(U, Y_1)$$

Furthermore, decoder 1 decodes m_1 treating interference m_2 as noise. On the other hand, decoder 2 finds a unique $m_2 \in \left[1 : 2^{NR_2}\right]$ such that for some $\tilde{m}_1 \in \left[1 : 2^{NR_1}\right]$

$$(\mathbf{u}(\tilde{m}_1), \mathbf{x}(m_2, \tilde{m}_1), \mathbf{y}_2) \in \mathcal{T}_\epsilon(U, X, Y_2)$$

Moreover, decoder 2 decodes m_2 by recognizing the structure of U. However, since decoding m_1 correctly is not its goal, it can only find some $\tilde{m}_1$.

2.5.3 Gaussian interference channel

The outputs of a two-user real Gaussian Interference Channel (G-IFC) can be written in the standard form [43]

$$\begin{aligned} y_1 &= x_1 + \sqrt{a}x_2 + z_1 \\ y_2 &= \sqrt{b}x_1 + x_2 + z_2 \end{aligned} \tag{2.24}$$

where $\sqrt{a}$ and $\sqrt{b}$ are the crosstalk coefficients, x_i and y_i the inputs and outputs of the channel and z_i represents the noise at receiver $i = 1, 2$. It should be noted that in the standard form, the direct links have unit gains and the noise has unit variance. The capacity region of a G-IFC is defined at the closure of the set of rate pairs (R_1, R_2) for which both receivers can decode their own messages with arbitrarily small positive error probability. The capacity region of the standard G-IFC is known only for three cases :

— If $a = 0$, $b = 0$, i.e., if there is no interference at all, the capacity region is the set of rate pairs (R_1, R_2), such that

$$\begin{aligned} R_1 &\leqslant \frac{1}{2}\log_2(1 + P_1) \\ R_2 &\leqslant \frac{1}{2}\log_2(1 + P_2) \end{aligned}$$

— If $a \geqslant 1$, $b \geqslant 1$, i.e. if the interference is strong at the receivers, the capacity region is the set of rate pairs (R_1, R_2), such that

$$\begin{aligned} R_1 &\leqslant \frac{1}{2}\log_2(1 + P_1) \\ R_2 &\leqslant \frac{1}{2}\log_2(1 + P_2) \\ R_1 + R_2 &\leqslant \frac{1}{2}\min\left\{\log_2(1 + aP_2 + P_1), \log_2(1 + bP_1 + P_2)\right\} \end{aligned}$$

— If $a \geqslant 1 + P_1$, $b \geqslant 1 + P_2$, i.e. if the interference is very strong at the receivers, the capacity

region is the set of rate pairs (R_1, R_2), such that

$$R_1 \leqslant \frac{1}{2}\log_2(1+P_1)$$
$$R_2 \leqslant \frac{1}{2}\log_2(1+P_2)$$

which means that the presence of very strong interference is as good as having no interference at all.

While the capacity region of the general G-IFC remains unknown, many papers have investigated some special cases to study the capacity region [33, 44–48]. More specifically, Costa in [46] has considered the third case while the authors in [33, 44, 45] have studied the second case where $a \geqslant 1$ and $b \geqslant 1$. Besides, Han and Kobayashi have proposed the best inner bound in [33] by using SC and joint decoding. Furthermore, a simplified form of the Han-Kobayashi region was given by the authors in [49] and [50]. Motahari and Khandani established the capacity region of mixed interference where $a \leqslant 1$ and $b \geqslant 1$. A new outer-bound on the capacity region of G-IFC was developed in [48], that improves on the bounds of [51] and [52].

2.6 Wireless radio channel models

The wireless radio channel poses a severe challenge as a medium for reliable high-speed communication. In addition to noise, interference, and other channel obstructions, the radio channel is also susceptible to other unpredictable variations due to user movement. In wireless systems, the radio mobile channel is usually evaluated from statistical propagation models, where channel parameters are modeled as stochastic variables. This channel is affected by three mutually independent phenomena : multipath fading, path loss and shadowing. Figure 2.11 illustrates the ratio of the received-to-transmit power in dB versus log-distance for the combined effects of path loss, shadowing, and multipath.

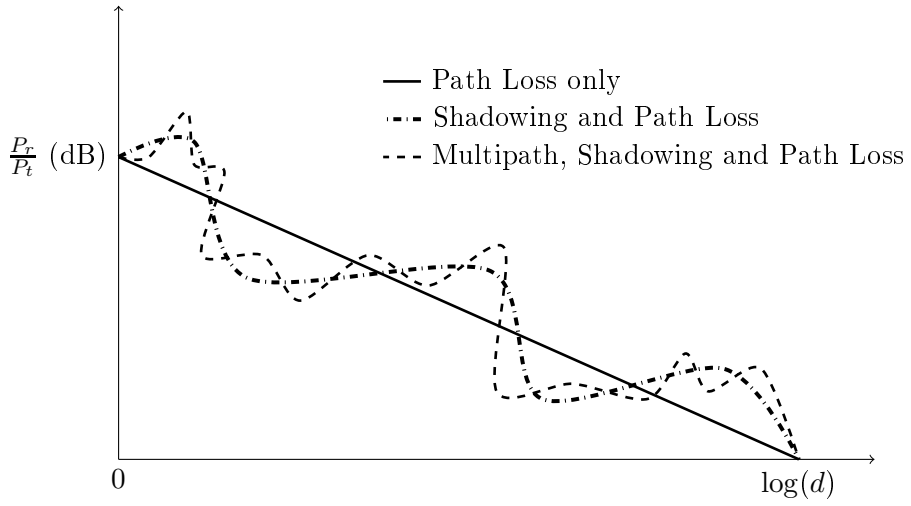

FIGURE 2.11 – Path Loss, Shadowing and Multipath versus distance

2.6.1 Rayleigh fading

Multipath propagation leads to rapid fluctuations of the phase and amplitude of the signal if the mobile moves over a distance in the order of a wave length or more. Variation due to multipath occurs over very short distances, on the order of the signal wavelength, so these variations are referred to as 'small-scale' propagation effects or multipath fading. One of the multipath fading models is Rayleigh, which is used in this thesis, and is considered as a reasonable model when there is a large number of reflections present between the transmitter and receiver. Rayleigh fading models assume that the magnitude of a signal that has passed through such a communication channel will vary randomly, or fade, according to a Rayleigh distribution, which is represented by the radial component of the sum of two uncorrelated Gaussian random variables.

2.6.2 Path loss

Path loss, or path attenuation, is the reduction in power density of an electromagnetic wave as it propagates through space. It is caused by dissipation of the power radiated by the transmitter as well as effects of the propagation channel. Variation due to path loss occurs over very large distances (100-1000 meters). For that, it is referred to as 'large-scale' propagation effects. These effects cause the received power to vary gradually due to signal attenuation determined by the geometry of the path profile in its entirety. This attenuation may be due to many effects, such as free-space loss, refraction, diffraction, reflection, aperture-medium coupling loss, and absorption. Path loss is also influenced by terrain contours, environment, propagation medium, the distance between the transmitter and the receiver, and the height and location of antennas.

In this thesis, we are interested in the COST231 model, which is an extension of the Hata model at 800 MHz in dense urban environment. COST231 model is formally expressed as [53]

$$L_{dB}(d) = 125.08 + 35.22 \times \log_{10}(d)$$

where d is the distance between transmitter and receiver.

2.6.3 Shadowing

Shadowing is caused by obstacles between the transmitter and receiver that absorb power. When the obstacle absorbs all the power, the signal is blocked. Shadowing is random since it depends on the random number and type of obstructions, and it introduces additional fluctuations on the signal level. Shadowing is referred to as 'large-scale' propagation effects, since it creates variation that occurs over distances proportional to the length of the obstructing object (10-100 meters in outdoor environments and less in indoor environments). In this thesis, we consider the log-normal shadowing model which can be given by

$$p(\psi) = \frac{\xi}{\sqrt{2\pi}\sigma_{\psi_{dB}}\psi} \exp\left[-\frac{(10\log_{10}\psi - \mu_{\psi_{dB}})^2}{2\sigma^2_{\psi_{dB}}}\right], \psi > 0$$

where $\xi = \frac{10}{\ln 10}$, $\mu_{\psi_{dB}}$ is the mean of $\psi_{dB} = 10 \log_{10} \psi$ in dB and $\sigma_{\psi_{dB}}$ is the standard deviation of ψ_{dB} also in dB.

2.6.4 Capacity of fading channel

The fundamental channel capacity defines the maximum data rate that can be supported on a channel. For that, the capacity of fading channels depends on the channel knowledge at both transmitter and receiver. This knowledge, called CSI can be available only at the receiver. In this case, the capacity with receiver CSI is defined as the average of AWGN capacity. On the other hand, the capacity with transmitter/receiver knowledge requires optimal adaptation based on current channel state. This capacity is almost the same capacity as with receiver knowledge only.

2.6.5 Outage probability

The slow fading channel can be defined by the following complex baseband representation

$$y[m] = h[m]x[m] + z[m] \tag{2.25}$$

where $\{h[m]\}$ is the fading process which can be considered roughly constant over the period of use, i.e., $\{h[m]\} = h$ for all m and $\{z[m]\}$ is i.i.d. $\mathcal{CN}(0, \frac{N_0}{2})$. In this case, the maximum rate of reliable communication supported by this channel is $\log_2 \left(1 + |h|^2 \text{SNR}\right)$ bits per complex dimension, which depends on the channel gain h. Consequently, the term of outage probability is introduced and it is calculated as

$$p_{out}(R) = P\left\{\log_2 \left(1 + |h|^2 \text{SNR}\right) < R\right\} \tag{2.26}$$

where R is the data rate in bits per complex dimension.

2.7 Relay-assisted channel

2.7.1 Introduction

Communication from a single source to a single destination without the help of any other communicating terminal is called direct, single-user or point-to point communication. Whenever there is at least one additional node ready to help in communication, user-cooperation becomes possible in several schemes such as the three-terminal relay channel. This channel was introduced by Van der Meulen in 1968 [54] and 1971 [55]. In his original work, Van der Meulen derived upper and lower bounds on the capacity of the relay channel, and made several observations that led to improvement of his results in later years. The capacity of the general relay channel is still unknown, but the bounds of Van der Meulen were significantly improved by Cover and El Gamal in 1979 [35].

The relay channel is the three-terminal communication channel shown in Fig. 2.12. The terminals are labeled the source (S), the relay (R), and the destination (D). All information

originates at S, and must travel to D, with the help of R. The signal being transmitted from the source is labeled X. The signal received by the relay is Y_r. The transmitted signal from the relay is X_r, and the received signal at the destination is Y.

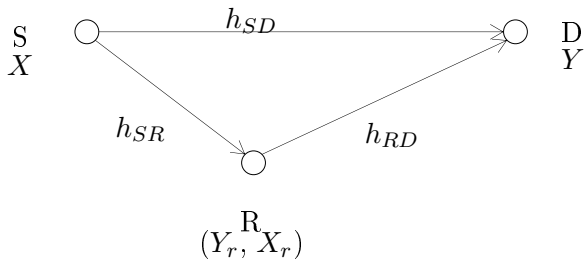

FIGURE 2.12 – Relay channel

2.7.2 Half-duplex and full-duplex relaying

A relay is said to be Half-Duplex (HD) when it cannot simultaneously transmit and receive in the same band. In other words, the transmission and reception channels must be orthogonal. Orthogonality between transmitted and received signals can be in time domain, in frequency domain, or using any set of signals that are orthogonal over the time-frequency plane. More specifically, the transmission in the HD mode is achieved in two time slots : In the first time slot, the source transmits the signal and the relay must wait for the transmitter to stop transmitting, before replying. In the second time slot, the source stops the transmission and the relay relays the message it receives during the previous time slot. On the other hand, if a relay transmits and receives simultaneously in the same band, it is said to be FD relay. In this case, the relay receives the signal on one frequency band, processes it and transmits it on the same frequency band with a small delay compared to the received frame duration. However, it continues to simultaneously receive from the source. This assumes that there is a good isolation between the receiver antennas and the transmit antennas of the relay. However, there is a minor rate loss caused by the delay. In addition, the transmitted signal interferes with the received signal. Although early literature on information theoretic relaying was based almost entirely on FD relaying ([35, 54, 55]), in recent years a lot of research, and especially research directed towards practical protocols, has been based on the premise of HD relaying ([56–60]). However, recent works investigate the practical aspect for the FD mode, by presenting some designs allowing simultaneous transmission and reception and removing the self-interference [61–63].

2.7.3 Relaying protocol strategies

Amplify-and-forward

In this scenario, the transmitted signal by the relay X_r is an amplified version of its own received signal Y_r, i.e. $X_r = \beta_{AF} Y_r$, where β_{AF} is the amplification factor defined in terms of

the source, relay and destination transmit powers, and the channel gains, such as

$$P_r = \mathbb{E}\left[|X_r|^2\right] \tag{2.27}$$

with P_r the transmit power of the relay. Consequently, the amplification factor is given by

$$\beta_{AF} = \sqrt{\frac{P_r}{P_S|h_{SD}|^2 + n_0}} \tag{2.28}$$

where P_S denotes the transmit power at the source and h_{SD} the channel complex gain between source and destination.

AF is a very simple and low-complexity protocol, however, it does not separate the useful source signal X from the noise signal at the relay. Hence, it also forwards an amplified version of the receiver noise.

Decode-and-Forward

By contrast to AF, DF and Compress-and-Forward (CF) apply non linear functions on the received signal at the relay. In the DF scenario, the relay decodes the source message X using its own received message Y_r. Based on the decoding source message, X_r is selected and transmitted to the destination and it does not necessarily have the same codebook size as the source message. The destination node then decodes first the relay message X_r, which helps to reduce the number of possible source messages X to the set of messages which is assigned to the decoded relay message. Afterwards, the destination may decode the source message X using this prior knowledge.

Compress-and-Forward

While DF provides transmit diversity, CF provides receive diversity. Instead of decoding the source message, the relay quantizes its received signal using $\hat{Y}_r$, which represents a digital version of the analog received signal Y_r. Using the relay message X_r, the quantized signal is communicated to the destination. At the destination, this quantized message $\hat{Y}_r$ is restored using the destination own receive signal Y as side information. Once $\hat{Y}_r$ is known at the destination, this latter can use both Y and $\hat{Y}_r$ to decode the source message.

2.7.4 Capacity region of a relay-assisted channel

The relay channel can be seen as a BC composed of both links 'source-relay' (S-R) and 'source-destination' (S-D), and a MAC formed at the receiver by the links between 'relay-destination' (R-D) and 'source-destination' (S-D). To find the capacity region of a relay channel, the properties of jointly typical sequences (detailed in Appendix A) are used, such as the messages are decoded at the receiver by checking which of the possible input messages is jointly typical with the received output. If there is one and only one such received signal, it will be considered as the message.

In this section, we detail the capacity calculation of the degraded relay channel shown in Fig. 2.12. For that, we consider L blocks, each of N symbols. A sequence of $L-1$ messages $m_i \in \left[1, 2^{NR}\right], i = 1, 2, \ldots, L-1$ will be sent over the channel in LB transmissions, where R denotes the rate. In each $N-$block $l = 1, 2, \ldots, L$, the same doubly indexed set of codewords is used

$$\begin{aligned} &\mathcal{C} = \{\mathbf{x}(m_l, s_l), \mathbf{x_r}(s_l)\}; \\ &m_l \in \left[1, 2^{NR}\right], s_l \in \left[1, 2^{NR_0}\right] \end{aligned} \tag{2.29}$$

Let $\mathcal{S} = \{\mathbf{s}_1, \mathbf{s}_2, \ldots, \mathbf{s}_{2^{NR_0}}\}$ be a partition of $\mathcal{M} = 1, 2, \ldots, 2^{NR}$ into 2^{NR_0} cells.

In block i, the transmitted signals are $\mathbf{x}(m_i, s_i)$ and $\mathbf{x}_r(s_i)$, while the received signals are $\mathbf{y}_r(i)$ and $\mathbf{y}(i)$. Then, at the end of block i, the relay calculates m_i from $\mathbf{y}_r(i)$. The unique jointly typical $\mathbf{x}_r(s_i)$ with the received $\mathbf{y}(i)$ is calculated. Thus s_i is known to the receiver. Afterward, the receiver calculates the set of all m_{i-1} such that $(\mathbf{x}(m_{i-1}|s_{i-1}), \mathbf{x}_r(s_{i-1}), \mathbf{y}(i-1))$ are jointly $\epsilon-$typical. The receiver then intersects this set and the cell $\mathbf{s}_i$ to find m_{i-1} which is the one and only one member of intersection. Thus, the receiver has correctly computed (m_{i-1}, s_i) from (m_{i-2}, s_{i-1}) and $(y(i-1), y(i))$.

Encoding and decoding procedures at the BC

Encoding : Let $m_i \in \left[1, 2^{NR}\right]$ be the index to be sent in block i, and assume that $m_{i-1} \in \mathbf{s}_i$. The encoder then sends $\mathbf{x}(m_i|s_i)$. The relay has an estimate $\hat{m}_{i-1}$ of the previous index m_{i-1}, where $\hat{m}_{i-1} \in \hat{\mathbf{s}}_{i_1}$. Then the relay encoder sends the codeword $\mathbf{x_r}(\hat{s}_i)$ in block i.

Decoding : At the end of block (i_1) the receiver knows $(m_1, m_2, \ldots, m_{i-2})$ and $(s_1, s_2, \ldots, s_{i-1})$ and the relay knows $(m_1, m_2, \ldots, m_{i-1})$ and consequently $(s_1, s_2, \ldots, s_i)$.

The decoding procedure at the end of block i in the broadcast phase is as follows : Knowing s_i, and receiving $\mathbf{y}_r(i)$, the relay receiver estimates the message of the transmitter $\hat{m}_i = m$ if and only if there exists a unique m such that $(\mathbf{x}(m|s_i), \mathbf{x}_r(s_i), \mathbf{y}_r(i))$ are jointly $\epsilon-$typical. Using (A.26), it can be shown that $\hat{m}_i = m_i$ with small probability of error if

$$R_{BC} < I\left(X; Y_r | X_r\right) \tag{2.30}$$

Achievable rate region for MAC

Links between (S-D) and (R-D) form a MAC at the receiver. From the (R-D) link, the receiver declares that $\hat{s}_i = s$ was sent if and only if there exists one and only one s such that $(\mathbf{x}_r(s), \mathbf{y}(i))$ are jointly $\epsilon-$typical. According to (A.16), $\hat{s}_i = s_i$ with arbitrary small probability of errors if

$$R_0 < I\left(X_r; Y\right) \tag{2.31}$$

if N is sufficiently large.

Assuming that s_i is decoded successfully at the receiver, it has now to decode m_i using the information is received from the (S-D) link. Then, $\hat{m}_{i-1} = m$ is declared to be the index sent in block $i-1$ if and only if there is a unique $m\mathcal{T}_\epsilon(\mathbf{s}_{s_i}, \mathbf{y}(i-1))$. Then, $\hat{m}_{i-1} = m_{i-1}$ if N is

sufficiently large and if

$$R_1 < I\left(X; Y|X_r\right) \tag{2.32}$$

Consequently, the rate has to be $R < R_0 + R_1$ which is given by

$$R_{MAC} < I\left(X, X_r; Y\right) \tag{2.33}$$

Then, the achievable rate region for a degraded DF relay channel is $R = \min\left\{R_{MAC}, R_{BC}\right\}$ which is written as

$$R = \min\left\{I\left(X, X_r; Y\right), I\left(X; Y_r|X_r\right)\right\} \tag{2.34}$$

2.8 Elements of convex optimization

In this section, we briefly review optimality conditions and dual method to solve a convex optimization problem. The definitions and concepts in this section are taken from [64, 65]. Let us define the general optimization problem of the form

$$\begin{aligned} &\min_{\mathbf{x}} f_0(\mathbf{x}) \\ &\text{s.t.}\, \mathbf{x} \in \mathbf{R}^n \\ &\text{s.t.}\, f_j(\mathbf{x}) \leqslant b_j, j = 1, \ldots, J \end{aligned} \tag{2.35}$$

where the vector $\mathbf{x} = (x_1, \ldots, x_n)$ is the optimization variable of the problem and the function $f_0 : \mathbf{R}^n \to \mathbf{R}$ is the objective function. The functions $f_j : \mathbf{R}^n \to \mathbf{R}$ with $j = 1, \ldots, J$ are the constraint functions, and the constants $b_1, \ldots, b_J$ are the limits, or bounds, for the constraints. Problem (2.35) is a convex optimization problem if the functions $f_0, \ldots, f_J : \mathbf{R}^n \to \mathbf{R}$ are convex, i.e., if they satisfy

$$f_j(\alpha\mathbf{x} + \beta\mathbf{y}) \leqslant \alpha f_j(\mathbf{x}) + \beta f_j(\mathbf{y}) \tag{2.36}$$

for all $\mathbf{x}, \mathbf{y} \in \mathbf{R}^n$ and all $\alpha, \beta \in \mathbf{R}$. Geometrically speaking, $f_j(x)$ is a convex function if the line segment between any two points $(x_1, f_j(x_1))$ and $(x_2, f_j(x_2))$ is always above the curve $(x, f_j(x))$ when x runs from x_1 to x_2, as illustrated in Fig. 2.13.

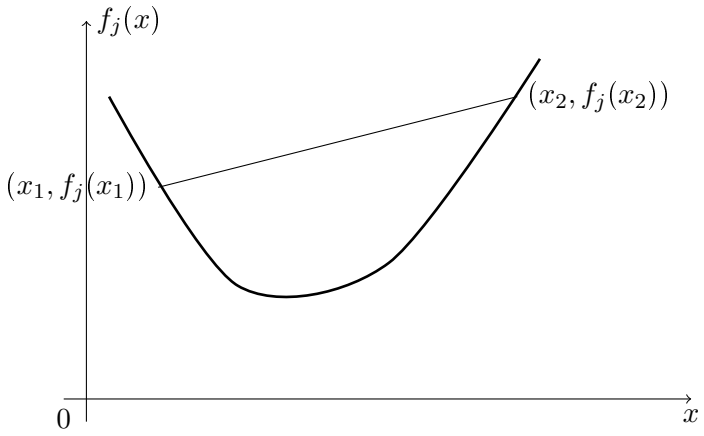

FIGURE 2.13 – Convex function

The Lagrangian of problem (2.35) is defined as

$$\mathbb{L}(\mu, \mathbf{x}) = f_0(\mathbf{x}) + \sum_{j=1}^{J} \mu_j f_j(\mathbf{x}) \tag{2.37}$$

where $\mu = (\mu_1, \ldots, \mu_J)^T \in \mathbf{R}_+^J$ with μ_j being the dual variable, also named as the Lagrange multiplier for the j^{th} constraint.

2.8.1 Dual decomposition

Many resource allocation problems result in a difficult combinatorial optimization problem. In recent years, the technique of dual decomposition, also called Lagrangian relaxation, has proven to be a powerful means of solving these problems by decomposing them into subproblems that are repeatedly solved independently and combined into a global solution. The dual decomposition method is applied on a separable or trivially parallelizable optimization problem, i.e. which can be solved separately (in parallel) for each constraint (or a couple of constraints) [66]. Let's denote a global optimum for problem (2.35) as $\mathbf{x}^*$. The Lagrangian relaxation problem of (2.35) is defined as the problem

$$\min_{\mathbf{x}} \mathbb{L}(\mu, \mathbf{x}) = f_0(\mathbf{x}) + \sum_{j=1}^{J} \mu_j f_j(\mathbf{x}) \tag{2.38}$$

The dual function $d(\mu)$ is defined as the optimum objective value of (2.38), i.e.,

$$d(\mu) = \min_{\mathbf{x}} \mathbb{L}(\mu, \mathbf{x}) = \mathbb{L}(\mu, \mathbf{x}_\mu) \tag{2.39}$$

where $\mathbf{x}_\mu$ represents a global optimum for (2.38) when μ is fixed. The dual problem is defined as

$$\max_{\mu} d(\mu) \tag{2.40}$$

$$\text{s.t. } \mu \succeq 0 \tag{2.41}$$

It can be easily seen that the dual problem is equivalent to a convex problem, since its feasible set is convex and $d(\mu)$ is convex in $\mu \in \mathbf{R}^J$.

2.8.2 Successive approximation based optimization method

In this section we present the successive convex optimization method to solve the general optimization problem (2.35). Initialized by a given feasible vector $\mathbf{x}^0$, this method solves convex approximations of (2.35) successively. To facilitate description, a superscript $(n+1)$ put to a variable indicates that the variable is produced at the end of the n^{th} iteration hereafter $(n \geqslant 0)$. At the n^{th} iteration, $\mathbf{y}^{n+1}$ is found as a global optimum for

$$\min_{\mathbf{x}} f_0^n(\mathbf{x}) \tag{2.42}$$

$$f_j^n(\mathbf{x}) \leqslant 0, j = 1, \ldots, J \tag{2.43}$$

where $\forall j, f_j^n(\mathbf{x})$ is a convex approximation of $f_j(\mathbf{x})$. The problem (2.43) is a convex approximation of (2.35) at the n^{th} iteration, thus it can be solved by any convex optimization method, e.g., the dual method. The idea behind SCA method is illustrated in Fig. 2.14.

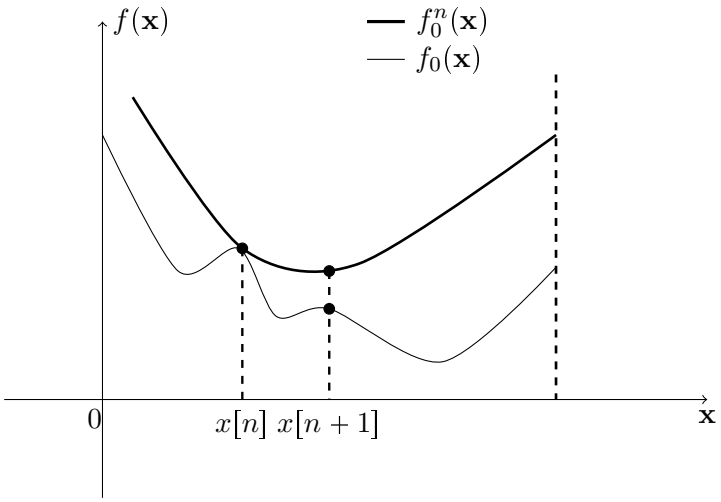

FIGURE 2.14 – Successive Convex Approximation

2.8.3 Waterfilling

Waterfilling is an optimization algorithm which is based on the consequence of Pascal's law on water : just as water finds its level even when filled in one part of a vessel with multiple openings,

the communication systems amplify each channel up to the required power level compensating for the channel impairments. To give a brief explanation of this technique, let us consider a practical optimization problem from information theory. It is about rate maximization for an OFDM-based communication system. This problem can be defined by

$$\max_{\mathbf{p}} \sum_{k=1}^{L} \log_2(p_k + \alpha_k) \tag{2.44}$$

$$\text{s.t.}\, \mathbf{p} \succeq 0 \tag{2.45}$$

$$\text{s.t.}\, \mathbf{1}^T\mathbf{p} = 1 \tag{2.46}$$

where $\mathbf{p} = (p_1, \ldots, p_L)$ and p_k denotes the transmitter power allocated to the k^{th} channel and $\log_2(p_k + \alpha_k)$ the capacity rate of the channel with $k = 1, \ldots, L$. To solve this problem, we determine the Lagrangian

$$\mathbb{L}(\mathbf{p}, \lambda, \nu) = -\sum_{k=1}^{L} \log_2(p_k + \alpha_k) + \lambda^T\mathbf{p} + \nu(\mathbf{1}^T\mathbf{p} - 1)$$

Then, we apply the Karush-Kuhn-Tucker (KKT) conditions to find the maximum.

$$\begin{aligned}
&\mathbf{p}^* \succeq 0 \\
&\mathbf{1}^T\mathbf{p}^* = 1 \\
&\lambda^* \succeq 0 \\
&\lambda_k^* p_k^* = 0\,(k = 1, \ldots, L) \\
&\nabla\mathbb{L}(\mathbf{p}^*, \lambda^*, \nu^*) = \frac{\partial\mathbb{L}}{\partial\mathbf{p}} = 0
\end{aligned}$$

From the KKT, we get

$$p_k^* = \left[\frac{1}{\nu^*} - \alpha_k\right]^+ \tag{2.47}$$

Waterfilling has been largely investigated in multiuser systems. In [67], a subcarrier allocation algorithm for a multiple access OFDM system was proposed, based on waterfilling algorithm. The same problem was investigated in [68], where the authors proposed an iterative waterfilling algorithm for both OFDM multiple access and broadcast channels. Besides, waterfilling is largely used in CR systems. However, the conventional waterfilling algorithm cannot be directly employed for power allocation in CR systems, due to the additional power constraints in the CR power allocation problem than in the classic waterfilling problems. For that, novel algorithms based on iterative waterfilling were proposed [69–71] to overcome such limitations.

Chapitre 3

Resource allocation with perfect CSI

3.1 Introduction

Throughout this thesis, the resource allocation problem for an uplink underlay cognitive system is investigated. In this chapter, we firstly evaluate the performance of the system by applying both SIC and SC at the SU and assuming perfect CSI at all nodes. In a second step, we investigate the same issue in the multiuser case. In this scenario, the secondary users are subject to two main constraints in the presence of the primary user : 1) their total power budget and 2) a maximum power level calculated according to the interference that they generate to the primary user. The objective is to maximize the sum rate of both primary and secondary systems, considering the interference threshold constraint and that the primary receiver always treats interference as noise.

In this chapter, we highlight the benefits of the proposed adaptive algorithm which encompasses two phases in the single-user case. The first step includes the adaptive selection of the decoding strategy at the secondary receiver which is either treating interference as noise or using SIC or SC. The second step describes the optimal distribution of the available power budget on the users with different methods. The problem is also treated for the multiuser case, where a subcarrier allocation procedure is added to the former algorithm. Simulation results show that our proposed scheme achieves higher secondary and sum rates compared with existing approaches.

The remaining of this chapter is organized as follows. We start by explaining the system model that will be used in both chapters 3 and 4. Then, we list the different decoding strategies at the SU in Section 3.4. In Section 3.5 and Section 3.6, we detail the concept and the conditions to apply SIC and SC, respectively, at the SU. The achievable rates at the primary and secondary users are studied in Section 3.7, while the power allocation problem is investigated in Section 3.8. In Section 3.9, we study the same issues when multiple secondary users exist in the secondary cell. Simulation results of the proposed algorithm are given in Section 3.10. Finally we provide

a summary of the contributions of the chapter in Section 3.11.

3.2 State of the art

An overview on CR networking and communications is given in [72], where cooperative sensing was proposed to solve the problem of collision in a spectrum sensing CR network. Several papers [14,15,73] have discussed the achievable rates of such a CR system from the view of information theory. More specifically, the achievable rates of a cognitive system where the SU has non-causal knowledge of the codeword of the PU are studied in [14]. Various encoding techniques are obtained for different cases in [14], such as rate splitting, dirty paper coding, and partial relaying by the secondary system in [15]. The same model is investigated in [73] to study the maximum achievable rate under the assumption that the secondary transmitter has side-information about the primary transmission. The authors supposed that the SU has to satisfy two conditions in order to be able to coexist with the PU : (i) no interference is accepted at the primary system and (ii) the primary receiver is unaware of the presence of the cognitive system. In [74], the authors investigate the problem of CR networks with energy limited CR nodes, minimizing the node power consumption to improve the energy efficiency. In [75], a new resource allocation scheme is proposed for a multi-carrier based underlay system. The co-channel interference is canceled opportunistically using multiuser detection and the transmit power is allocated optimally in order to maximize the achievable transmit rate. The authors in [76] propose an algorithm to maximize the secondary achievable rate using an opportunistic interference cancellation method at the secondary receiver. In [77], Wang et al. propose a power control scheme for to maximize the sum rate of multiple access network, under instantaneous interference power constraint at the primary network. In other works, multiple antennas are employed in order to perform the spectrum sharing without any degradation in the signal for the PU [78–81].

In [82,83], Asghari et al. investigated the resource allocation problem, in spectrum sharing CR broadcast channels, by utilizing spectrum sensing information about the primary's activity at the secondary base station. In [84], the authors studied how the secondary receiver could overcome interference from the primary transmitters, depending on the interference level received at the cognitive receiver. The authors in [85] reduced the self-interference in a generalized frequency division multiplexing based CR system, using SIC. SC was combined to binning in [86] to achieve capacity for the Gaussian cognitive interference channel, in cognitive overlay radio system. In [87] a new achievable rate region for an overlay CR network is derived using block Markov SC, conditional rate-splitting, conditional Gel'fand-Pinkser binning, and cooperative relaying. SC was applied in [88] to increase the system capacity of the forward link in a CDMA cellular system.

Adaptive resource allocation for the OFDM systems has been studied extensively during the past two decades. A comprehensive survey can be found in [89] and references therein. Moreover, resource allocation for OFDM-based CR networks has attracted much attention recently. An overview of the state-of-the-art research results can be found in [90]. This issue has been studied

for both single-user and multiuser cases. For single-user case, optimal and suboptimal power allocation schemes were proposed to maximize the sum capacity of the CR system under the interference constraints of the PUs in [6]. In [91], a low-complexity optimal power allocation algorithm was derived by exploiting the structure of the considered optimization problem. A greedy max-min algorithm was proposed to maximize the throughput of the CR system with a given power budget in [92]. In [93], the authors aimed to maximize the CR network throughput under interference limit and total power budget constraints. The optimal power allocation to achieve the ergodic capacity and the outage capacity in fading channel was derived in [94]. In [95] the authors maximized the secondary achievable rate under a new criterion referred to as rate loss constraint. The authors in [96] investigated the problem of random subcarrier allocation in OFDM-based CR networks without any spectrum sensing information at the SU. The SU's transmit power was adjusted in order to maintain the interference on the primary receiver under a predefined threshold. The downlink resource allocation problem in a spectrum sharing environment is studied in [97]. A time averaging is introduced to approximate the interference constraints for both short and long terms. In [98], a heuristic scheme is proposed where the secondary receiver either treats the interference as noise, or uses SIC or is switched off. The achievable rate is studied under the constraint that (i) an interference level is allowable on the PU and (ii) the primary encoder-decoder pair is oblivious to the presence of CR.

Resource allocation for multi-user OFDM-based CR system was investigated in [99–104]. The authors in [99] made use of subcarrier allocation to improve the performance of cognitive networks by exploiting the so-called multiuser interference diversity. They considered that the SU with the largest achievable receiver SNR is selected among all the SUs. In [100], a low complexity algorithm is developed to maximize the sum capacity of a CR system with proportional rate constraints. The proposed algorithm exhibits a tradeoff between capacity and fairness by jointly considering channel gain and the interference to the PUs. The multi-user diversity in an interweave scenario was studied in [101]. In [102], two fast resource allocation algorithms were derived for both real-time and non real-time services in multi-user OFDM-based CR networks. In [103], the sum capacity of a multiuser OFDM-based CR system was maximized while satisfying SUs' proportional rate requirements. The adaptive resource allocation problem in multiuser OFDM-based CR networks with imperfect spectrum sensing was investigated in [104]. The problem was addressed in two steps : subcarrier allocation and then power allocation.

3.3 System model

We consider a CR system model composed of one primary cell and one secondary cell which may contain several SUs. Transmission is performed in uplink and in OFDM in both cells. We assume that all transmissions are perfectly synchronous. This system model will be used in this chapter, as well as in Chapter 4 where only one SU is considered in the secondary cell. This system model can be seen as a cooperative underlay CR, due to the cooperation between the systems and the allowed interference threshold from the secondary transmitter on the primary receiver. The primary system occupies a licensed bandwidth B which is divided into L adjacent

and parallel subcarriers. The secondary Base Station (BS) is located at a distance d_{sec} from the primary BS. The considered scenario is basically the classic two-user interference channel [33] where the SUs need to adapt their decoding strategies to avoid disturbing the PU. Consequently, they have to transmit either when the primary system is off or under an interference constraint fixed by the PU. Thus, the secondary transmitters use channel interweave when the subbands are currently left vacant by the primary system, otherwise, they use channel underlay. Perfect CSI knowledge is considered throughout this chapter at each node. We also assume perfect sensing of primary activity. The cooperation between the primary and secondary systems can be provided by a band manager [105].

We start by defining the system model parameters for the single-user case. These parameters will be used throughout this thesis. However, some parameters related to the secondary mobile terminals will be modified for the multiuser case (section 3.9). In the single-user case, index p refers to the primary system, while index s refers to the secondary system. The received primary and secondary signals in each subcarrier $k \in \{1, \ldots, L\}$ can be written as (see Fig. 3.1)

$$\begin{aligned} y_p^k &= h_{pp}^k x_p^k + h_{ps}^k x_s^k + z_p^k \\ y_s^k &= h_{sp}^k x_p^k + h_{ss}^k x_s^k + z_s^k \end{aligned}$$

where y_i^k is the channel output and x_i^k is the channel input corresponding to data s_i^k with power P_i^k for subcarrier k and user i. $P_{i,\max}$ is the maximum transmit power of transmitter i. h_{ij}^k, a zero-mean complex circular Gaussian variable, denotes the channel gain between transmitter j and receiver i. The channel gains are assumed to be constant during a transmission time slot. z_i^k denotes the AWGN at receiver i. The noise variance $n_i^k = n_0$ is the same on each subcarrier k.

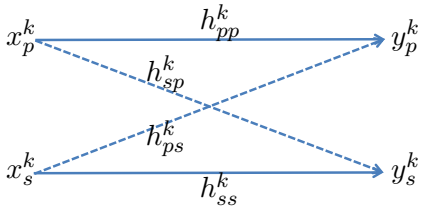

FIGURE 3.1 – Two user interference channel on subcarrier $k \in \{1, \ldots, L\}$

3.4 Decoding strategies at the SU

In the considered scenario, only the SU can adapt its decoding strategy. The limitation threshold of the interference created by the secondary transmitter is set according to the rate degradation that the PU can accept with respect to its maximum rate $R_{p,\max}^k = \frac{B}{L}\log_2\left(1 + \frac{|h_{pp}^k|^2 P_p^k}{n_0}\right)$. The allowed degradation, Δ, is defined as :

$$(1-\Delta)\, R_{p,\max}^k = \frac{B}{L}\log_2\left(1 + \frac{|h_{pp}^k|^2 P_p^k}{n_0 + I_{th}^k}\right)$$

where I_{th}^k is the interference threshold.

In this section, we will present a brief description of the different possible decoding strategies at the SU, that will be detailed later in this chapter. Three strategies are possible if the secondary is not switched off :

1. If the primary's power is equal to zero, i.e. $P_p^k = 0$, the secondary system uses channel interweave. It transmits on subcarrier k with no primary interference threshold.
2. Otherwise, i.e. if $P_p^k \neq 0$, the maximum transmit power of the secondary user is limited by the primary interference threshold, and there are two possible decoding scenarios at the secondary receiver :

   (a) If the interference is weak at the secondary receiver, i.e. if $|h_{sp}^k|^2 \leqslant |h_{ss}^k|^2$, the maximum capacity region is calculated by treating interference as noise at both receivers, i.e., sending only private information.

   (b) If the interference is strong at the secondary receiver, i.e. if $|h_{sp}^k|^2 > |h_{ss}^k|^2$, both messages are decoded. The channel seen at the secondary receiver is a MAC, whose rate constraints, referring to [41], are :

$$R_p^k \leqslant \frac{B}{L} \log_2 \left(1 + \frac{|h_{sp}^k|^2 P_p^k}{n_0} \right) \tag{3.1}$$

$$R_s^k \leqslant \frac{B}{L} \log_2 \left(1 + \frac{|h_{ss}^k|^2 P_s^k}{n_0} \right) \tag{3.2}$$

$$R_p^k + R_s^k \leqslant \frac{B}{L} \log_2 \left(1 + \frac{|h_{sp}^k|^2 P_p^k + |h_{ss}^k|^2 P_s^k}{n_0} \right) \tag{3.3}$$

   To decode its own message, the secondary receiver may use :

   i. Complete SIC, decoding first x_p^k and then x_s^k if the primary user's data rate at the secondary receiver is higher than the primary user's data rate at the primary receiver. In this case, the secondary receiver removes all interference from the PU.

   ii. If SIC cannot be applied, the secondary receiver may use SC strategy. The conditions under which SC can be applied will be detailed in the next section.

   iii. Otherwise, the secondary transmitter is switched off.

3.5 Successive Interference Cancellation

As we said in Section 3.4, SIC can be applied at the SU, by decoding first the primary's signal and then removing it in order to decode the secondary's signal interference-free. This interference cancellation method can be applied at the secondary receiver if the primary user's data rate at the secondary receiver (R_{p,y_s}^k) is higher than the PU's data rate at the primary

receiver (R^k_{p,y_p}) [106]. Besides,

$$R^k_{p,y_p} = \frac{B}{L}\log_2\left(1+\frac{|h^k_{pp}|^2P^k_p}{|h^k_{ps}|^2P^k_s+n_0}\right) \tag{3.4}$$

and

$$R^k_{p,y_s} = \frac{B}{L}\log_2\left(1+\frac{|h^k_{sp}|^2P^k_p}{|h^k_{ss}|^2P^k_s+n_0}\right) \tag{3.5}$$

Consequently, SIC is only applied if

$$\frac{|h^k_{pp}|^2P^k_p}{|h^k_{ps}|^2P^k_s+n_0} \leqslant \frac{|h^k_{sp}|^2P^k_p}{|h^k_{ss}|^2P^k_s+n_0} \tag{3.6}$$

i.e., if

$$a^kP^k_s \geqslant c^k \tag{3.7}$$

where

$$\begin{aligned} a^k &= |h^k_{sp}|^2|h^k_{ps}|^2 - |h^k_{pp}|^2|h^k_{ss}|^2 \\ c^k &= n_0\left(|h^k_{pp}|^2 - |h^k_{sp}|^2\right) \end{aligned}$$

3.6 Superposition Coding

3.6.1 Concept of the SC method

In theory, multiuser techniques such as SC are known to improve throughput in wireless networks. We aim to introduce and apply such a technique in a CR context, in order to achieve full capacity when several conditions are valid.

The secondary transmitter has then to transmit $x^k_s = \sqrt{(1-\alpha^k)}x^{k,(1)}_s + \sqrt{\alpha^k}x^{k,(2)}_s$, where $0 \leqslant \alpha^k \leqslant 1$, such that the secondary receiver receives $y^k_s = h^k_{sp}x^k_p + h^k_{ss}(\sqrt{(1-\alpha^k)}x^{k,(1)}_s + \sqrt{\alpha^k}x^{k,(2)}_s) + z^k_s$. The secondary receiver performs the decoding in three steps as illustrated in Fig. 3.2.

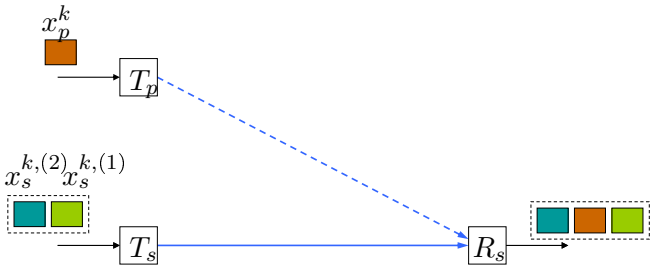

FIGURE 3.2 – Superposition Coding Concept

— **Step 1 :** $x_s^{k,(1)}$ is decoded from y_s^k by treating $\sqrt{\alpha^k}h_{ss}^k x_s^{k,(2)} + h_{sp}^k x_p^k$ as noise, then $y^{k'} = y^k - h_{ss}^k\sqrt{(1-\alpha^k)}x_s^{k,(1)}$ is obtained. The achievable rate is equal to :

$$R_s^{k,(1)} = \frac{B}{L}\log_2\left(1 + \frac{(1-\alpha^k)|h_{ss}^k|^2 P_s^k}{\alpha^k|h_{ss}^k|^2 P_s^k + |h_{sp}^k|^2 P_p^k + n_0}\right) \tag{3.8}$$

— **Step 2 :** x_p^k is decoded from $y^{k'}$ by treating $\sqrt{\alpha^k}h_{ss}^k x_s^{k,(2)}$ as noise, then $y^{k''} = y^{k'} - h_{sp}^k x_p^k$ is obtained. Thus, we have

$$R_p^k = \frac{B}{L}\log_2\left(1 + \frac{|h_{sp}^k|^2 P_p^k}{\alpha^k|h_{ss}^k|^2 P_s^k + n_0}\right) \tag{3.9}$$

— **Step 3 :** $x_s^{k,(2)}$ is decoded from $y^{k''}$. Consequently

$$R_s^{k,(2)} = \frac{B}{L}\log_2\left(1 + \frac{\alpha^k|h_{ss}^k|^2 P_s^k}{n_0}\right) \tag{3.10}$$

We can verify that

$$R_p^k + R_s^{k,(1)} + R_s^{k,(2)} = \frac{B}{L}\log_2\left(1 + \frac{|h_{sp}^k|^2 P_p^k + |h_{ss}^k|^2 P_s^k}{n_0}\right) \tag{3.11}$$

which corresponds to the sum rate expression of a MAC system, at the secondary receiver.

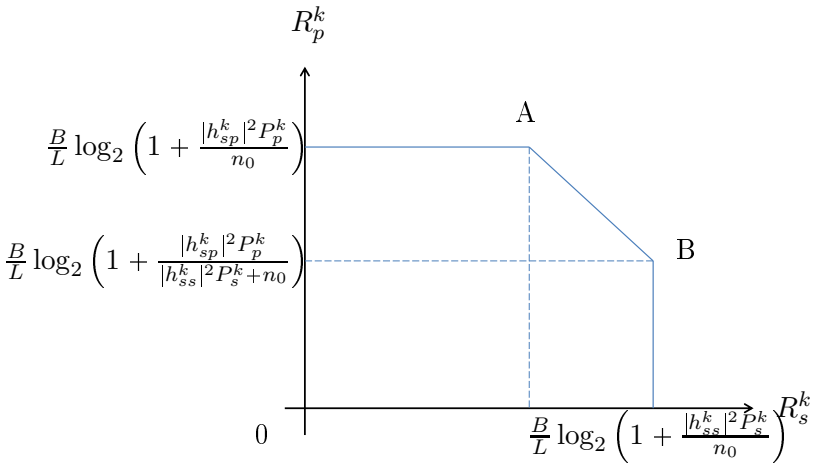

FIGURE 3.3 – Capacity Region

SC strategy will be used when SIC is not applicable, in order to achieve the capacity region's borders by reaching the tilted segment AB in Fig. 3.3. We study the two extreme values of α^k, and we will detail the conditions on α^k in the next paragraph :

— If $\alpha^k = 0$,

$$\begin{cases} R_p^k = \frac{B}{L}\log_2\left(1+\frac{|h_{sp}^k|^2P_p^k}{n_0}\right) \\ R_s^{k,(1)} = \frac{B}{L}\log_2\left(1+\frac{|h_{ss}^k|^2P_s^k}{|h_{sp}^k|^2P_p^k+n_0}\right) \\ R_s^{k,(2)} = 0 \end{cases} \tag{3.12}$$

This case matches with the point A on the capacity region, where the secondary receiver treats interference as noise.

— If $\alpha^k = 1$,

$$\begin{cases} R_p^k = \frac{B}{L}\log_2\left(1+\frac{|h_{sp}^k|^2P_p^k}{|h_{ss}^k|^2P_s^k+n_0}\right) \\ R_s^{k,(1)} = 0 \\ R_s^{k,(2)} = \frac{B}{L}\log_2\left(1+\frac{|h_{ss}^k|^2P_s^k}{n_0}\right) \end{cases} \tag{3.13}$$

In this case, we attain the point B on the capacity region, where the secondary is applying SIC.

It is worth noting that SC is chosen here because we work on the instantaneous channel. If we considered the ergodic channel, segment AB could also be reached by using time sharing strategy [14].

3.6.2 Conditions on α^k

The PU's rate seen by the primary's receiver (R_{p,y_p}^k) (3.4) is equal to the PU's rate seen by the secondary receiver (R_{p,y_s}^k) (3.9) :

$$\frac{|h_{pp}^k|^2P_p^k}{|h_{ps}^k|^2P_s^k+n_0} = \frac{|h_{sp}^k|^2P_p^k}{\alpha^k|h_{ss}^k|^2P_s^k+n_0} \tag{3.14}$$

From this equality we get

$$\alpha^k = \frac{(|h_{sp}^k|^2-|h_{pp}^k|^2)n_0+|h_{ps}^k|^2|h_{sp}^k|^2P_s^k}{|h_{pp}^k|^2|h_{ss}^k|^2P_s^k}. \tag{3.15}$$

α^k must be between 0 and 1, so

$$\begin{aligned} 0 &< \left(|h_{sp}^k|^2-|h_{pp}^k|^2\right)n_0+|h_{ps}^k|^2|h_{sp}^k|^2P_s^k \\ &< |h_{ss}^k|^2|h_{pp}^k|^2P_s^k \end{aligned} \tag{3.16}$$

which is equivalent to

$$\begin{aligned} \frac{\left(|h_{pp}^k|^2-|h_{sp}^k|^2\right)}{|h_{ps}^k|^2|h_{sp}^k|^2} &< \frac{P_s^k}{n_0} \\ &< \frac{|h_{pp}^k|^2|h_{ss}^k|^2}{|h_{ps}^k|^2|h_{sp}^k|^2}\frac{P_s^k}{n_0}+\frac{\left(|h_{pp}^k|^2-|h_{sp}^k|^2\right)}{|h_{ps}^k|^2|h_{sp}^k|^2} \end{aligned} \tag{3.17}$$

Two conditions are finally obtained :

$$\begin{cases} \frac{\left(|h_{pp}^k|^2 - |h_{sp}^k|^2\right)}{|h_{ps}^k|^2 |h_{sp}^k|^2} < \frac{P_s^k}{n_0} \\ \frac{P_s^k}{n_0}\left(|h_{ps}^k|^2 |h_{sp}^k|^2 - |h_{ss}^k|^2 |h_{pp}^k|^2\right) < \left(|h_{pp}^k|^2 - |h_{sp}^k|^2\right) \end{cases} \tag{3.18}$$

These conditions can be rewritten as :

$$\begin{cases} \frac{\left(|h_{pp}^k|^2 - |h_{sp}^k|^2\right)}{|h_{ps}^k|^2 |h_{sp}^k|^2} < \frac{P_s^k}{n_0} \\ P_s^k a^k < c^k \end{cases} \tag{3.19}$$

The first inequality is always true if $|h_{pp}^k|^2 - |h_{sp}^k|^2 < 0$. In the opposite case, it becomes a constraint to ensure $0 < \alpha^k < 1$.

For the second inequality, we have four possibilities :

— If $c^k > 0$ and $a^k > 0$, then :

$$P_s^k < \frac{c^k}{a^k} \tag{3.20}$$

— If $c^k > 0$ and $a^k < 0$, then :

$$P_s^k > \frac{c^k}{a^k} \tag{3.21}$$

which is always true because the second term is negative.

— If $c^k < 0$ and $a^k > 0$, then :

$$P_s^k < \frac{c^k}{a^k} \tag{3.22}$$

which is always impossible.

— If $c^k < 0$ and $a^k < 0$, then :

$$P_s^k > \frac{c^k}{a^k} \tag{3.23}$$

In brief, we can apply our algorithm once conditions (3.19), given in table 3.1, are valid.

		c^k	
		Positive	Negative
a^k	Positive	$\frac{P_s^k}{n_0} > \frac{\lvert h_{pp}^k\rvert^2 - \lvert h_{sp}^k\rvert^2}{\lvert h_{ps}^k\rvert^2 \lvert h_{sp}^k\rvert^2}$ $P_s^k < \frac{c^k}{a^k}$	Impossible
	Negative	$\frac{P_s^k}{n_0} > \frac{\lvert h_{pp}^k\rvert^2 - \lvert h_{sp}^k\rvert^2}{\lvert h_{ps}^k\rvert^2 \lvert h_{sp}^k\rvert^2}$	$P_s^k > \frac{c^k}{a^k}$

TABLE 3.1 – Superposition Coding Conditions

3.7 Achievable rate region for primary and secondary systems

The proposed algorithm to determine the best decoding strategy that should be used at the SU and then to calculate the achievable rate is iterative. Before describing the algorithm, we first detail the achievable primary and secondary rates. In the sequel, we denote by n the iteration at which the expressions are described.

3.7.1 Primary user

As stated before, the primary receiver always considers interference as noise and thus cannot adapt its decoding strategy as it does in the interference channel. The rate of the primary system at iteration n is given by :

$$R_{p,n}^k = \frac{B}{L} \log_2 \left(1 + \frac{\mid h_{pp}^k \mid^2 P_{p,n}^k}{n_0 + \mid h_{ps}^k \mid^2 P_{s,n}^k} \right) \tag{3.24}$$

3.7.2 Secondary user

The achievable secondary rate depends on the chosen decoding strategy at the SU. If $P_{p,(n-1)}^k \neq 0$, different decoding strategies for the SU are identified based on the interference level. The decoding strategy on each subcarrier k at the n^{th} iteration is defined according to both primary and secondary powers in the previous iteration. These power levels are optimized using waterfilling and Lagrangian methods for PU and SU respectively, as it will be detailed in Section 3.8.2. The different decoding strategies that can be applied at the SU under certain conditions are :

1. **Strategy 1 :** If $P_{p,(n-1)}^k = 0$, the secondary receiver decodes its message interference-free and the secondary rate is defined by

$$R_{s,n}^k = \frac{B}{L} \log_2 \left(1 + \frac{\lvert h_{ss}^k \rvert^2 P_{s,n}^k}{n_0} \right) \tag{3.25}$$

In the sequel, this strategy is called 'interweave'.

2. **Strategy 2 :** If $P_{p,(n-1)} \neq 0$ and $|h_{sp}^k|^2 < |h_{ss}^k|^2$, the interference to the SU is weak and is treated as noise. In this case, the achievable secondary rate is given by

$$R_{s,n}^k = \frac{B}{L}\log_2\left(1 + \frac{|h_{ss}^k|^2 P_{s,n}^k}{|h_{sp}^k|^2 P_{p,n-1}^k + n_0}\right) \tag{3.26}$$

3. **Strategy 3 :** If $P_{p,(n-1)} \neq 0$ and $|h_{sp}^k|^2 \geqslant |h_{ss}^k|^2$, the interference on the SU is strong. Therefore, if $a^k P_{s,n}^k \geqslant c^k$ is verified, SIC can be applied [106]. In this case, the achievable secondary rate is

$$R_{s,n}^k = \frac{B}{L}\log_2\left(1 + \frac{|h_{ss}^k|^2 P_{s,n}^k}{n_0}\right) \tag{3.27}$$

This rate will be referred as $R_{s,SIC}^k$ in the rest of the thesis.

4. **Strategy 4 :** If $P_{p,(n-1)} \neq 0$ and $|h_{sp}^k|^2 \geqslant |h_{ss}^k|^2$ but (3.7) is not verified, the ability to apply SC at the SU is tested subject to the validation of the set of inequalities in (3.19)

$$\frac{\left(|h_{pp}^k|^2 - |h_{sp}^k|^2\right)}{|h_{ps}^k|^2|h_{sp}^k|^2} < \frac{P_{s,n}^k}{n_0} \tag{3.28}$$

$$P_{s,n}^k a^k < c^k \tag{3.29}$$

If (3.28) and (3.29) are valid, the secondary achievable rate is given by

$$R_{s,n}^k = \frac{B}{L}\log_2\left(1 + \frac{\alpha^k |h_{ss}^k|^2 P_{s,n}^k}{n_0}\right) + \frac{B}{L}\log_2\left(1 + \frac{(1-\alpha^k)|h_{ss}^k|^2 P_{s,n}^k}{\alpha^k |h_{ss}^k|^2 P_{s,n}^k + |h_{sp}^k|^2 P_{p,n-1}^k + n_0}\right) \tag{3.30}$$

with

$$\alpha^k = \frac{(|h_{sp}^k|^2 - |h_{pp}^k|^2)n_0 + |h_{ps}^k|^2|h_{sp}^k|^2 P_{s,n}^k}{|h_{pp}^k|^2|h_{ss}^k|^2 P_{s,n}^k} \tag{3.31}$$

5. **Strategy 5 :** If $P_{p,(n-1)} \neq 0$ and $|h_{sp}^k|^2 \geqslant |h_{ss}^k|^2$ but neither SIC nor SC can be applied, the secondary transmitter is turned off.

These different decoding strategies lead to four different expressions for the secondary rate defined in different domains and described in (3.32) to (3.35). $R_{s,n}^{k,int}$ is the achievable rate when the interference is treated as noise. $R_{s,n}^{k,SIC}$ represents both SIC and interweave cases and $R_{s,n}^{k,SC}$ the achievable rate when SC is applied. $R_{s,n}^{k,off}$ denotes the null rate when the secondary transmitter is turned off.

$$R_{s,n}^{k,int} = \frac{B}{L}\log_2\left(1+\frac{|h_{ss}^k|^2 P_{s,n}^k}{|h_{sp}^k|^2 P_{p,n-1}^k + n_0}\right), k \in \mathcal{S}_2 \tag{3.32}$$

$$R_{s,n}^{k,SIC} = \frac{B}{L}\log_2\left(1+\frac{|h_{ss}^k|^2 P_{s,n}^k}{n_0}\right), k \in \mathcal{S}_1 \text{ and } \mathcal{S}_3 \tag{3.33}$$

$$R_{s,n}^{k,SC} = R_{s,n,1}^{k,SC} + R_{s,n,2}^{k,SC}, k \in \mathcal{S}_4 \tag{3.34}$$

$$R_{s,n}^{k,off} = 0, k \in \mathcal{S}_5 \tag{3.35}$$

where

$$R_{s,n,1}^{k,SC} = \frac{B}{L}\log_2\left(1+\frac{\frac{|h_{ps}^k|^2|h_{sp}^k|^2}{|h_{pp}^k|^2}P_{s,n}^k + \frac{(|h_{sp}^k|^2-|h_{pp}^k|^2)n_0}{|h_{pp}^k|^2}}{n_0}\right)$$

and

$$R_{s,n,2}^{k,SC} = \frac{B}{L}\log_2\left(1+\frac{\left(|h_{ss}^k|^2 - \frac{|h_{ps}^k|^2|h_{sp}^k|^2}{|h_{pp}^k|^2}\right)P_{s,n}^k - \frac{(|h_{sp}^k|^2-|h_{pp}^k|^2)n_0}{|h_{pp}^k|^2}}{\frac{|h_{ps}^k|^2|h_{sp}^k|^2}{|h_{pp}^k|^2}P_{s,n}^k + \frac{(|h_{sp}^k|^2-|h_{pp}^k|^2)n_0}{|h_{pp}^k|^2} + |h_{sp}^k|^2 P_{p,n}^k + n_0}\right)$$

$$\begin{cases} \mathcal{S}_1 = \{k \in \{1,\dots,L\} \text{ for 'Interweave'}\} \\ \mathcal{S}_2 = \{k \in \{1,\dots,L\} \text{ when interference is treated as a noise}\} \\ \mathcal{S}_3 = \{k \in \{1,\dots,L\} \text{ for 'SIC'}\} \\ \mathcal{S}_4 = \{k \in \{1,\dots,L\} \text{ for 'SC'}\} \\ \mathcal{S}_5 = \{k \in \{1,\dots,L\} \text{ when the secondary transmitter is turned off}\} \end{cases}$$

We summarize the algorithm used to select the decoding strategy at the secondary receiver in the chart on Fig. 3.4, when $P_{p,n-1}^k \neq 0$.

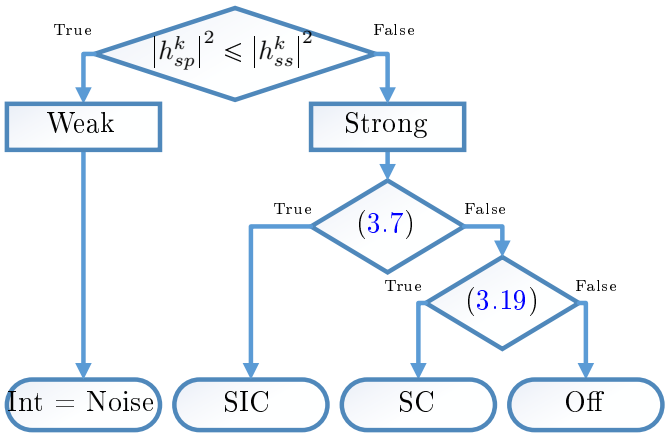

FIGURE 3.4 – Decoding strategies for the secondary user on subcarrier k

3.7.3 Influence of the interference constraint on the achievable rate

In this section, we point out the influence of the interference constraint on the secondary achievable rate. For that, we define $P_{s,n}^{k,I} = \frac{I_{th}^k}{|h_{ps}^k|^2}$ as the maximum allowable power within the SU's subcarriers, which corresponds to the maximum tolerated interference level generated to the PU. We denote by $R_{s,n}^{k,I}$ the rate achieved when $P_{s,n}^k = P_{s,n}^{k,I}$. Let $R_{p,n}^{k,SIC}$ be the maximum rate of the primary transmitter as seen by the secondary receiver. It is given by the first equation in (3.12). Several scenarios are possible :

— If $|h_{sp}^k|^2 \leqslant |h_{ss}^k|^2$, we treat the weak interference case, where interference is always considered as noise.

— If $|h_{sp}^k|^2 > |h_{ss}^k|^2$ (strong interference case), we have two cases :

1. If $R_{s,n}^{k,I} > R_{s,n}^{k,SIC}$, three different cases are studied (Fig. 3.5) :

   (a) If $R_{p,y_p,n}^k \leqslant R_{p,y_s,n}^k$, the abscissa of point B in the capacity region is reachable and SIC is applied. This corresponds to the hatched region in Fig. 3.5.

   (b) If $R_{p,y_p,n}^k > R_{p,y_s,n}^k$ but $R_{p,y_p,n}^k$ is below the point A, i.e. $R_{p,y_p,n}^k < R_{p,n}^{k,SIC}$, the point B is no more reachable and we have to verify if the conditions (3.19) are valid to apply SC and to reach the segment AB.

   (c) Otherwise, i.e. if $R_{p,y_p,n}^k > R_{p,n}^{k,SIC}$ we switch off the secondary transmitter.

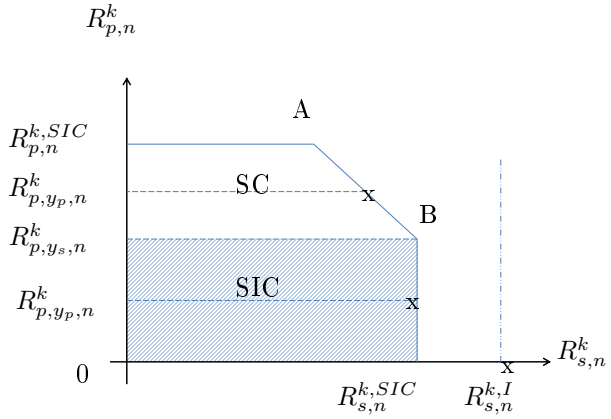

FIGURE 3.5 – Application of SIC and SC when $R_{s,n}^{k,I} > R_{s,n}^{k,SIC}$

2. Otherwise, if $R_{s,n}^{k,I} < R_{s,n}^{k,SIC}$, the achievable secondary rate is now limited by $R_{s,n}^{k,I}$, and we study the same cases as above, but we are no longer able to reach the border of the capacity region (Fig. 3.6) :

   (a) If $R_{p,y_p,n}^k \leqslant R_{p,y_s,n}^k$, we are inside the hatched slab in Fig. 3.6 and SIC is applied. The maximum reachable reate is always $R_{s,n}^{k,I}$.

   (b) If $R_{p,y_p,n}^k > R_{p,y_s,n}^k$ but $R_{p,y_p,n}^k < R_{p,n}^{k,SIC}$, we verify if the conditions (3.19) are valid and we apply SC to ensure a secondary rate equal to $R_{s,n}^{k,I}$.

   (c) Otherwise, i.e. if $R_{p,y_p,n}^k > R_{p,n}^{k,SIC}$ we switch off the secondary transmitter.

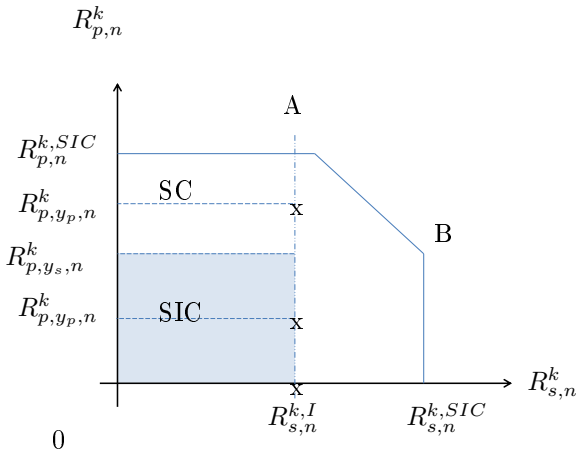

FIGURE 3.6 – Application of SIC and SC when $R^{k,I}_{s,n} < R^{k,SIC}_{s,n}$

3.8 Power Control

3.8.1 Equal power allocation

The primary user's power is always optimized using waterfilling. For the secondary user, performance with Equal Power Allocation (EPA) and optimization is compared. First of all, EPA is applied by taking into account $P^{k,I}_{s,n}$. The power allocated to each subcarrier of the secondary user is then equal to the minimum between $P^{k,EPA}_{s,n}$ and $P^{k,I}_{s,n}$, where

$$\begin{cases} P^{k,I}_{s,n} = \frac{I^k_{th}}{|h^k_{ps}|^2}, \\ P^{k,EPA}_{s,n} = \frac{P_{s,max}}{L}. \end{cases} \tag{3.36}$$

3.8.2 Power allocation optimization

In a second step, an iterative optimization algorithm is proposed in order to optimally allocate the available power. Firstly, the type of interference created by the PU on the secondary receiver in each subcarrier k is obtained based on the channel gain and the initial power equally allocated per subcarrier for both PU and SU. Then, according to this interference, the appropriate decoding strategy per subcarrier is identified and the secondary rate is calculated at each subcarrier. Once the decoding strategies are specified for each subcarrier, the power allocation procedure is performed in order to maximize the secondary rate. The power allocation procedure is summarized in Fig. 3.7.

At the n^{th} iteration, a test is done in order to define the decoding strategy used at the secondary receiver. The achievable rate per subcarrier is calculated according to the aforementioned cases and is used in the power optimization algorithm on the SU. Once $R^k_{s,n}$ is determined for all subcarriers, the PU can update its power $\mathbf{p}_{p,n}$ using waterfilling and based on the measured interference from the previous iteration, $\mathbf{p}_{s,n-1}$. Similarly, the secondary system updates its power $\mathbf{p}_{s,n}$ using gradient descent process, based on $\mathbf{p}_{p,n-1}$. Our algorithm is summarized in Algorithm 1, where at the n^{th} iteration, $\mathbf{p}_{i,n} = (P^1_{i,n}, \ldots, P^L_{i,n})^T$, with $i = \{p, s\}$ and $\mathbf{p}_n = \{\mathbf{p}_{p,n}, \mathbf{p}_{s,n}\}$. This

process is repeated until the stopping criterion is met. Note that the convergence of the power optimization algorithm is guaranteed even if the primary power control is not synchronized with the secondary power control, as proven in [107].

Algorithm 1 Proposed Resource Allocation Algorithm

1: **Input** channel gains ;
2: Initialize $\mathbf{p}_{p,0}$, $\mathbf{p}_{s,0}$ and set $n = 0$;
3: Determine the decoding strategy applied at the secondary receiver on each subcarrier k ;
4: **Repeat**
5: $n = n + 1$;
6: Compute $\mathbf{p}_{s,n}$ based on $\mathbf{p}_{p,n-1}$ and the decoding strategy ;
7: Compute $\mathbf{p}_{p,n}$ based on $\mathbf{p}_{s,n-1}$ and the decoding strategy ;
8: **Until** stopping criterion is reached ;
9: **Output** the optimized vectors $\mathbf{p}_{p,n}$ and $\mathbf{p}_{s,n}$.

Now, we investigate the power allocation strategy for the SU. The objective is to optimally choose the power vector $\mathbf{p}_{s,n}$ in order to maximize the secondary rate, while keeping the interference and the power constraints satisfied. If the interference constraint is not met, the subcarrier is switched off. At the n^{th} iteration, the power optimization problem is written as

$$\max_{\mathbf{p}_{s,n}} R_{s,n} \tag{3.37a}$$

$$\text{s.t.} \sum_{k=1}^{L} P_{s,n}^{k} \leqslant P_{s,max} \tag{3.37b}$$

$$\text{s.t.} \; P_{s,n}^{k} \geqslant 0 \, \forall \, k \in \{1, \ldots, L\} \tag{3.37c}$$

$$\text{s.t.} \; |h_{ps}^{k}|^2 P_{s,n}^{k} \leqslant I_{th}^{k} \, \forall \, k \notin \mathcal{S}_1 \tag{3.37d}$$

$$\text{s.t.} \; (3.7), \forall \, k \in \mathcal{S}_3 \tag{3.37e}$$

$$\text{s.t.} \; (3.19), \forall \, k \in \mathcal{S}_4 \tag{3.37f}$$

where $R_{s,n} = \sum_{k \in \mathcal{S}_2} R_{s,n}^{k,int} + \sum_{k \in \mathcal{S}_1 \cap \mathcal{S}_3} R_{s,n}^{k,SIC} + \sum_{k \in \mathcal{S}_4} R_{s,n}^{k,SC}$

Since the optimization problem is separable, it can be efficiently solved using the Lagrange dual decomposition method by decomposing the original problem into three subproblems, depending on the decoding strategies applied at the SU.

The Lagrangian of problem (3.37) taking into account constraints (3.37b) and (3.37c) can be written as

$$\mathbb{L}\left(P_{s,n}^{k}, \lambda\right) = -R_{s,n} + \lambda \left(\sum_{k=1}^{L} P_{s,n}^{k} - P_{s,\max} \right) - \sum_{k=1}^{L} \nu^{k} P_{s,n}^{k} \tag{3.38}$$

with $\lambda, \nu^{k} \geqslant 0$ being Lagrange multipliers. Note that ν^{k} is a slack variable and thus it can be eliminated [64]. Let D be the set specified by the remaining constraints in (3.37d), (3.37e) and (3.37f). Consequently, problem (3.37) can be given by subproblems C_{int}, C_{SIC} and C_{SC} defined

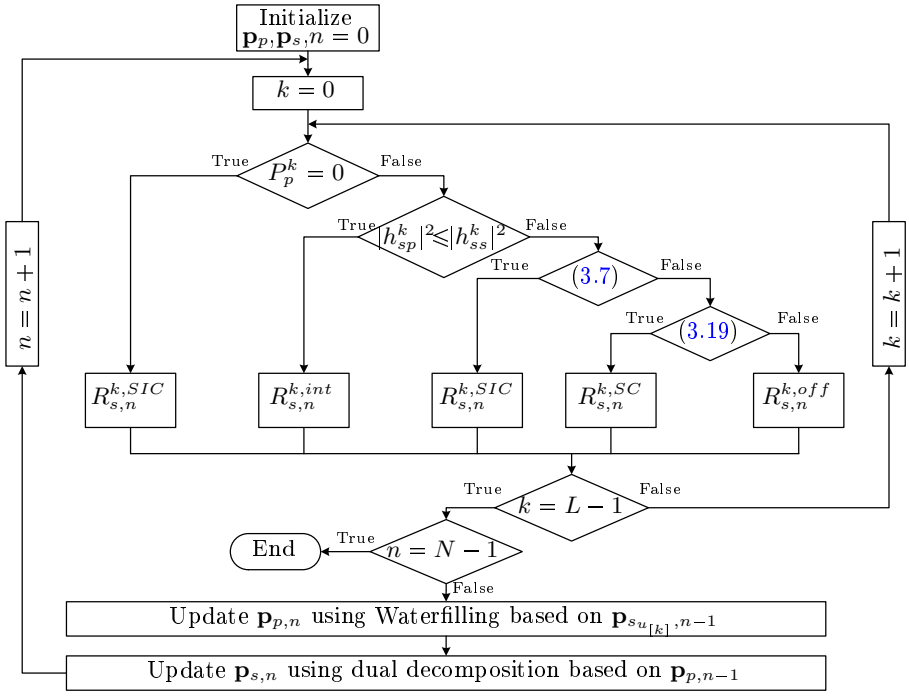

FIGURE 3.7 – Power Allocation Procedure

over $\mathcal{S}_2$, $\mathcal{S}_3$ and $\mathcal{S}_4$ respectively as

$$C_{int}: \max_{\{P_{s,n}^k\}_{k\in\mathcal{S}_2}} \sum_{k\in\mathcal{S}_2} R_{s,n}^{int} - \mu_{s,n} \sum_{k\in\mathcal{S}_2} P_{s,n}^k \tag{3.39a}$$

$$|h_{ps}^k|^2 P_{s,n}^k \leqslant I_{th}^k, \forall k \in \mathcal{S}_2$$

$$C_{SIC}: \max_{\{P_{s,n}^k\}_{k\in\mathcal{S}_3}} \sum_{k\in\mathcal{S}_3} R_{s,n}^{SIC} - \mu_{s,n} \sum_{k\in\mathcal{S}_3} P_{s,n}^k \tag{3.39b}$$

$$|h_{ps}^k|^2 P_{s,n}^k \leqslant I_{th}^k, \forall k \in \mathcal{S}_3$$

$$a^k P_{s,n}^k \geqslant c^k, \forall k \in \mathcal{S}_3$$

$$C_{SC}: \max_{\{P_{s,n}^k\}_{k\in\mathcal{S}_4}} \sum_{k\in\mathcal{S}_4} R_{s,n}^{SC} - \mu_{s,n} \sum_{k\in\mathcal{S}_4} P_{s,n}^k \tag{3.39c}$$

$$|h_{ps}^k|^2 P_{s,n}^k \leqslant I_{th}^k, \forall k \in \mathcal{S}_4$$

$$\frac{\left(|h_{pp}^k|^2 - |h_{sp}^k|^2\right)}{|h_{ps}^k|^2 |h_{sp}^k|^2} < \frac{P_{s,n}^k}{n_0}, \forall k \in \mathcal{S}_4$$

$$a^k P_{s,n}^k < c^k \, \forall k \in \mathcal{S}_4$$

where the subtracted term in the objective function represents the total power constraint which is common to all subproblems. Therefore the Lagrange dual function associated with (3.39) can be defined as

$$g(\lambda) = \max_{\mathbf{p}_{s,n}} \mathbb{L}\left(P_{s,n}^k, \lambda\right) - \lambda\left(\sum_{k=1}^{L} P_{s,n}^k - P_{s,\max}\right) \tag{3.40}$$

where $p_{s,n}$ is constant. It can be verified that problem C_{int} and problem C_{SIC} are convex. On the other hand, $R_{s,n}^{k,SC}$, and especially $R_{s,n,2}^{k,SC}$ is not convex in $P_{s,n}^{k}$. It can then be approximated using the first order Taylor approximation at a feasible point $\overline{P_{s,n}^{k}}$, in order to turn it into a convex optimization problem. The approximated function of this term can be given by

$$R_{s,n,2}^{SC} \simeq R_{s,n,2}^{k,SC}(\overline{P_{s,n}^{k}}) + B_{n}^{k}(\overline{P_{s,n}^{k}}) \left(P_{s,n}^{k} - \overline{P_{s,n}^{k}}\right)$$

with

$$B_{n}^{k} = \frac{\partial R_{s,n,2}^{k,SC}}{\partial P_{s,n}^{k}}$$

Besides, we demonstrate that the objective function is strictly increasing in $\mathbf{p}_{s,n}$. Then, the problem can be transformed into an equality-constrained problem, and the stopping condition becomes

$$\sum_{k=1}^{L} P_{s,n}^{k} = P_{s,max} \tag{3.41}$$

Thus, an analytical solution of all subproblems can be obtained with the Karush-Kuhn-Tucker conditions [64]. In the following, we only detail the solution of subproblem C_{SC}. For that, let us define the unconstrained subproblem

$$\hat{C}_{SC} : \max_{\{P_{s,n}^{k}\}_{k\in\mathcal{S}_4}} \sum_{k\in\mathcal{S}_4} R_{s,n}^{k,SC} - \mu_{s,n} \sum_{k\in\mathcal{S}_4} P_{s,n}^{k}$$

with Lagrangian

$$\hat{\mathbb{L}}\left(P_{s,n}^{k}, \mu_{s,n}\right) = -\sum_{k\in\mathcal{S}_4} R_{s,n}^{k,SC} + \mu_{s,n} \sum_{k\in\mathcal{S}_4} P_{s,n}^{k}$$

Let $\hat{f}$ be the partial derivative of $\hat{\mathbb{L}}$ with respect to $P_{s,n}^{k}$.

$$\hat{f}\left(P_{s,n}^{k}, \mu_{s,n}\right) = -\frac{|h_{ps}^{k}|^2}{|h_{ps}^{k}|^2 P_{s,n}^{k} + n_0} - B_{n}^{k}\left(\overline{P_{s,n}^{k}}\right) + \mu_{s,n} = 0$$

Thus, the solution of subproblem $\hat{C}_{SC}$ can be given by

$$\hat{P}_{s,n}^{k} = \frac{1}{\mu_{s,n} - B_{n}^{k}\left(\overline{P_{s,n}^{k}}\right)} - \frac{n_0}{|h_{ps}^{k}|^2}$$

which can be expressed by

$$\hat{P}_{s,n}^{k} = \frac{1}{\hat{\mu}_{s,n}} - \frac{n_0}{|h_{ps}^{k}|^2}$$

where

$$\hat{\mu}_{s,n} = \left(\mu_{s,n} - B_n^k\left(\overline{P_{s,n}^k}\right)\right)$$

Taking into consideration the constraints of subproblem C_{SC}, its general solution $P_{s,n}^{k,SC}$ has to be positive and

$$n_0 \frac{\left(|h_{pp}^k|^2 - |h_{sp}^k|^2\right)}{|h_{ps}^k|^2 |h_{sp}^k|^2} < P_{s,n}^{k,SC} < \min\left\{\frac{c^k}{a^k}, \frac{I_{\text{th}}^k}{|h_{ps}^k|^2}\right\}$$

which depends on the sign of a^k and c^k. (See Table 3.1).

The solution of problem (3.39) is directly provided by waterfilling for both subproblems C_{int} and C_{SIC} and by modified waterfilling for subproblem C_{SC}. It is given in Table 3.2, provided that the values of $\overline{P_{s,n}^{k,SC}}$ are updated using the sequential algorithm 2. So far we have got $\mathbb{L}(\lambda)$ for a given λ. Then, we can get the dual problem which aims to minimize $\mathbb{L}(\lambda)$

$$\begin{aligned} &\min_{\lambda} g(\lambda) \\ &\text{s.t.} \lambda \geqslant 0 \end{aligned} \tag{3.42}$$

This problem can be solved by using sub-gradient method [108].

The presented solution can be a general solution for the power optimization problem in an uplink underlay CR system, studied in [106] and [109]. The problem coefficients are presented in Table 3.3.

Algorithm 2 Sequential Convex Approximation Algorithm to solve C_{SC}

1: **Input** A solution accuracy $\omega > 0$, $m = 0$ and a feasible point $\overline{\mathbf{p}_{s,0}}$ for problem C_{SC} ;
2: **Repeat**
3: $m = m + 1$
4: Compute $\frac{\partial R_{s,m}^{k,SC}}{\partial P_{s,m}^k}(\overline{P_{s,m}^k})$;
5: Calculate $P_{s,m}^k \, \forall k \in \mathcal{S}_4$ using table I ;
6: **Until** Stopping criterion is reached ;
7: **Output** $\mathbf{p}_{s,m}$.

TABLE 3.2 – Optimized values of $P_{s,n}^k$

Conditions	Decoding strategies	$P_{s,n}^k$
$P_{p,(n-1)}^k = 0$ any value for a^k and c^k	Interweave	$\left[\frac{1}{\mu_{s,n}} - \frac{1}{b_{s,(n-1)}^k}\right]^+$
$P_{p,(n-1)}^k \neq 0$ $\left\{a^k = 0; c^k = 0\right\}$	Int = Noise	$\min\left\{\left[\frac{1}{\mu_{s,n}} - \frac{1}{b_{s,(n-1)}^k}\right]^+ ; \frac{I_{\text{th}}^k}{\left\|h_{ps}^k\right\|^2}\right\}$
$P_{p,(n-1)}^k \neq 0$ $\left\{a^k < 0; c^k > 0\right\}$	SIC	0
	SC	$\min\left\{\max\left\{\left[\frac{1}{\hat{\mu_{s,n}}} - \frac{1}{b_{s,(n-1)}^k}\right]^+ ; \frac{n_0(\left\|h_{pp}^k\right\|^2 - \left\|h_{sp}^k\right\|^2)}{\left\|h_{sp}^k\right\|^2 \left\|h_{ps}^k\right\|^2}\right\} ; \frac{I_{\text{th}}^k}{\left\|h_{ps}^k\right\|^2}\right\}$
$P_{p,(n-1)}^k \neq 0$ $\left\{a^k > 0; c^k < 0\right\}$	SIC	$\min\left\{\left[\frac{1}{\mu_{s,n}} - \frac{1}{b_{s,(n-1)}^k}\right]^+ ; \frac{I_{\text{th}}^k}{\left\|h_{ps}^k\right\|^2}\right\}$
	SC	0
$P_{p,(n-1)}^k \neq 0$ $\left\{a^k < 0; c^k < 0\right\}$	SIC	$\min\left\{\frac{c^k}{a^k}; \left[\frac{1}{\mu_{s,n}} - \frac{1}{b_{s,(n-1)}^k}\right]^+ ; \frac{I_{\text{th}}^k}{\left\|h_{ps}^k\right\|^2}\right\}$
	SC	$\min\left\{\max\left\{\left[\frac{1}{\hat{\mu_{s,n}}} - \frac{1}{b_{s,(n-1)}^k}\right]^+ ; \frac{n_0(\left\|h_{pp}^k\right\|^2 - \left\|h_{sp}^k\right\|^2)}{\left\|h_{sp}^k\right\|^2 \left\|h_{ps}^k\right\|^2}; \frac{c^k}{a^k}\right\} ; \frac{I_{\text{th}}^k}{\left\|h_{ps}^k\right\|^2}\right\}$
$P_{p,(n-1)}^k \neq 0$ $\left\{a^k > 0; c^k > 0\right\}$	SIC if $\frac{c^k}{a^k} \leqslant \frac{I_{\text{th}}^k}{\left\|h_{ps}^k\right\|^2}$	$\min\left\{\max\left\{\left[\frac{1}{\mu_{s,n}} - \frac{1}{b_{s,(n-1)}^k}\right]^+ ; \frac{c^k}{a^k}\right\} ; \frac{I_{\text{th}}^k}{\left\|h_{ps}^k\right\|^2}\right\}$
	SIC otherwise	0
	SC	$\min\left\{\max\left\{\left[\frac{1}{\hat{\mu_{s,n}}} - \frac{1}{b_{s,(n-1)}^k}\right]^+ ; \frac{n_0(\left\|h_{pp}^k\right\|^2 - \left\|h_{sp}^k\right\|^2)}{\left\|h_{sp}^k\right\|^2 \left\|h_{ps}^k\right\|^2}\right\} ; \frac{c^k}{a^k}; \frac{I_{\text{th}}^k}{\left\|h_{ps}^k\right\|^2}\right\}$

TABLE 3.3 – Optimization coefficients for problem (3.39)

Cases	$b^k_{s,(n-1)}$
$P^k_{p,(n-1)} \neq 0$ and $\left\|h^k_{sp}\right\|^2 \leqslant \left\|h^k_{ss}\right\|^2$	$\frac{\left\|h^k_{ss}\right\|^2}{n_0+\left\|h^k_{sp}\right\|^2 P^k_{p,(n-1)}}$
$P^k_{p,(n-1)} \neq 0$ and $\left\|h^k_{sp}\right\|^2 > \left\|h^k_{ss}\right\|^2$	$\frac{\left\|h^k_{ss}\right\|^2}{n_0}$
$P^k_{p,(n-1)} = 0$	$\frac{\left\|h^k_{ss}\right\|^2}{n_0}$

Cases	a^k
$P^k_{p,(n-1)} \neq 0$ and $\left\|h^k_{sp}\right\|^2 \geqslant \left\|h^k_{ss}\right\|^2$	$\left\|h^k_{sp}\right\|^2 \left\|h^k_{ps}\right\|^2 - \left\|h^k_{pp}\right\|^2 \left\|h^k_{ss}\right\|^2$
all other cases	0

Cases	c^k
$P^k_{p,(n-1)} \neq 0$ and $\left\|h^k_{sp}\right\|^2 \geqslant \left\|h^k_{ss}\right\|^2$	$n_0\left(\left\|h^k_{pp}\right\|^2 - \left\|h^k_{sp}\right\|^2\right)$
all other cases	0

3.9 Multiuser case

In this section, we suppose that N_u SUs exist in the secondary cell. The algorithm proposed for the single-user case is now adapted to the multiuser case. Before investing the power allocation problem, we consider the subcarrier allocation algorithm. The resource allocation problem is then composed of two steps. First, the SU with the maximum achievable rate is activated within subcarrier k, and then the power allocation problem is faced. In the following, let $s_{u_{[k]}}$ denotes the SU activated at subcarrier k, $P_{s_{u_{[k]}}}$ its power and $R_{s_{u_{[k]}}}$ its achievable rate. The channel model is then described by

$$\begin{aligned} y^k_p &= h^k_{pp}x^k_p + h^k_{ps_{u_{[k]}}}x^k_{s_{u_{[k]}}} + z^k_p \\ y^k_s &= h^k_{sp}x^k_p + h^k_{ss_{u_{[k]}}}x^k_{s_{u_{[k]}}} + z^k_s \end{aligned}$$

3.9.1 Description of the algorithm

At the n^{th} iteration, a test is done in order to define the decoding strategy used at the secondary receiver. The achievable rate per subcarrier is calculated according to the aforementioned cases and is used to select one of the SUs within subcarrier k and then to optimize the power allocation for the active SU. Once $R^k_{s_{u_{[k]}},n}$ is determined for all subcarriers, the PU can update its power $\mathbf{P}_{p,n}$ using waterfilling and based on the measured interference from the previous iteration, $\mathbf{p}_{s_{u_{[k]}},n-1}$. Similarly, the secondary system updates its power $\mathbf{p}_{s_{u_{[k]}},n}$ using dual decomposition process, based on $\mathbf{p}_{p,n-1}$. This alternative process is repeated until the stopping

criterion is reached.

Our proposed algorithm is executed alternatingly between the primary and the secondary systems. More specifically, given a starting power allocation $\mathbf{p}_{p,0}$ and $\mathbf{p}_{s,0}$, the SUs apply a per subcarrier decoding strategy which depends on the primary and SUs power allocation obtained from the iteration $n-1$. Based on the applied decoding strategy, an achievable rate is computed for each SU on each subcarrier. Finally, the SU with the highest rate is activated within subcarrier k and the SU power optimization problem is solved.

A summary of our proposed scheme is given in Algorithm 3, where at the n^{th} iteration, $\mathbf{p}_{i,n} = (P_{i,n}^1, \ldots, P_{i,n}^L)^T$, with $i = \{p, s_{u_{[k]}}\}$ and $\mathbf{p}_n \in \{\mathbf{p}_{p,n}, \mathbf{p}_{s_{u_{[k]}},n}\}$.

Algorithm 3 Proposed Resource Allocation Algorithm for Multiuser Case

1: **Input** channel gains ;
2: Initialize $\mathbf{p}_{p,0}$, $\mathbf{p}_{s,0}$ and set $n = 0$;
3: Determine the decoding strategy applied at the secondary receiver on each subcarrier k ;
4: Compute the estimated achievable rate for all the users on each subcarrier k ;
5: Activate the SU $u_{[k]}$ with the highest estimated rate at subcarrier k ;
6: **Repeat**
7: $n = n + 1$;
8: Compute $\mathbf{p}_{s_{u_{[k]}},n}$ based on $\mathbf{p}_{p,n-1}$ and the decoding strategy ;
9: Compute $\mathbf{p}_{p,n}$ based on $\mathbf{p}_{s_{u_{[k]}},n-1}$ and the decoding strategy ;
10: **Until** stopping criterion is reached ;
11: **Output** the optimized vectors $\mathbf{p}_{p,n}$ and $\mathbf{p}_{s_{u_{[k]}},n}$.

3.9.2 Subcarrier Allocation

We evaluate within each subcarrier the data rate that can be achieved in all the links between SUs and the secondary BS by assuming EPA and by redistributing the powers of inactive subcarriers. The data rate $\hat{R}_{u_{[k]}}^k$ is obtained depending on the decoding strategy applied in the subcarrier and by taking into account the power limitation due to the interference threshold. This estimated rate is defined in equations (3.32) to (3.35), where equal power allocation is also set in each subcarrier of the PU.

The average secondary rate per subcarrier and based on the decoding strategy for different distances d_{sec} between primary and secondary BSs is given in Fig. 3.8 when only one user is considered. The x-axis represents the different decoding strategies for the SU : '1' represents the interweave case and '5' the case when the secondary transmitter is switched off while the other indexes represent the underlay case, with '2', '3' and '4' indicate treating interference as noise, SIC and SC strategies respectively. Fig. 3.8 shows that in underlay cases, the highest average data rate is obtained with SC, while the lowest is achieved when the interference is treated as noise.

We propose the following subcarrier allocation algorithm. To initialize, the power per subcarrier on each secondary link is set as the minimum between $P_{u_{[k]},\max}/l_{u_{[k]}}$ and $I_{th}^k/|h_{ps_{u_{[k]}}}^k|^2$,

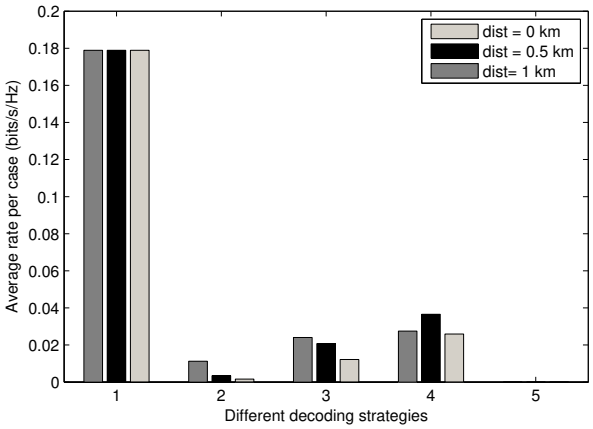

FIGURE 3.8 – Average secondary rate per subcarrier based on the decoding strategy

where $l_{u_{[k]}}$ is the estimated number of subcarriers allocated to user $u_{[k]}$, and it is set to L/N_u. At each subcarrier, the users with a SC decoding strategy are firstly searched, and then among them, the one with the highest estimated rate is selected. Afterward, the method is repeated in a similar manner for the SIC case, then for the strategy where the interference is treated as noise. The algorithm is repeated for all subcarriers and users and is represented in Fig. 3.9.

3.9.3 Power allocation optimization

On each subcarrier, only one of the SUs is active. Once subcarriers have been allocated, the decoding algorithm proposed for the single-secondary user case can be extended to the multiuser case replacing the index s for the secondary terminals by $s_{u_{[k]}}$. The power allocation algorithm for the PU remains unchanged. The decoding strategy and power allocation are run for each SU independently.

The optimization problem for each user $u_{[k]}$ at the n^{th} iteration can be expressed by :

$$\max_{\{\mathbf{p}_{u_{[k]},n}\}} R_{s,n} \tag{3.43a}$$

$$\text{s.t.} \sum_{k\in\mathcal{S}_{u_{[k]}}} P^k_{s_{u_{[k]}},n} \leqslant P_{s_{u_{[k]}},\max} \tag{3.43b}$$

$$\text{s.t. } P^k_{s_{u_{[k]}},n} \geqslant 0, \forall k \in \mathcal{S}_{u_{[k]}} \tag{3.43c}$$

$$\text{s.t. } |h^k_{ps_{u_{[k]}}}|^2 P^k_{s_{u_{[k]}},n} \leqslant I^k_{th}, \forall k \notin \mathcal{S}_1 \tag{3.43d}$$

$$\text{s.t. } a^k P^k_{s_{u_{[k]}}} \geqslant c^k, \forall k \in \mathcal{S}_{u_{[k]}} \text{ in SIC case} \tag{3.43e}$$

$$\text{s.t. } \frac{\left(|h^k_{pp}|^2 - |h^k_{sp}|^2\right)}{|h^k_{ps_{u_{[k]}}}|^2 |h^k_{sp}|^2} < \frac{P^k_{s_{u_{[k]}}}}{n_0}, \forall\, k \in \mathcal{S}_{u_{[k]}} \text{ in SC case} \tag{3.43f}$$

$$\text{s.t. } P^k_{s_{u_{[k]}}} a^k < c^k, \forall\, k \in \mathcal{S}_{u_{[k]}} \text{ in SC case} \tag{3.43g}$$

where $R_{s,n} = \sum_{k\in\mathcal{S}_2} R^{k,int}_{s,n} + \sum_{k\in\mathcal{S}_1\cap\mathcal{S}_3} R^{k,SIC}_{s,n} + \sum_{k\in\mathcal{S}_4} R^{k,SC}_{s,n}$ and $\mathcal{S}_{u_{[k]}}$ is the set of subcarriers

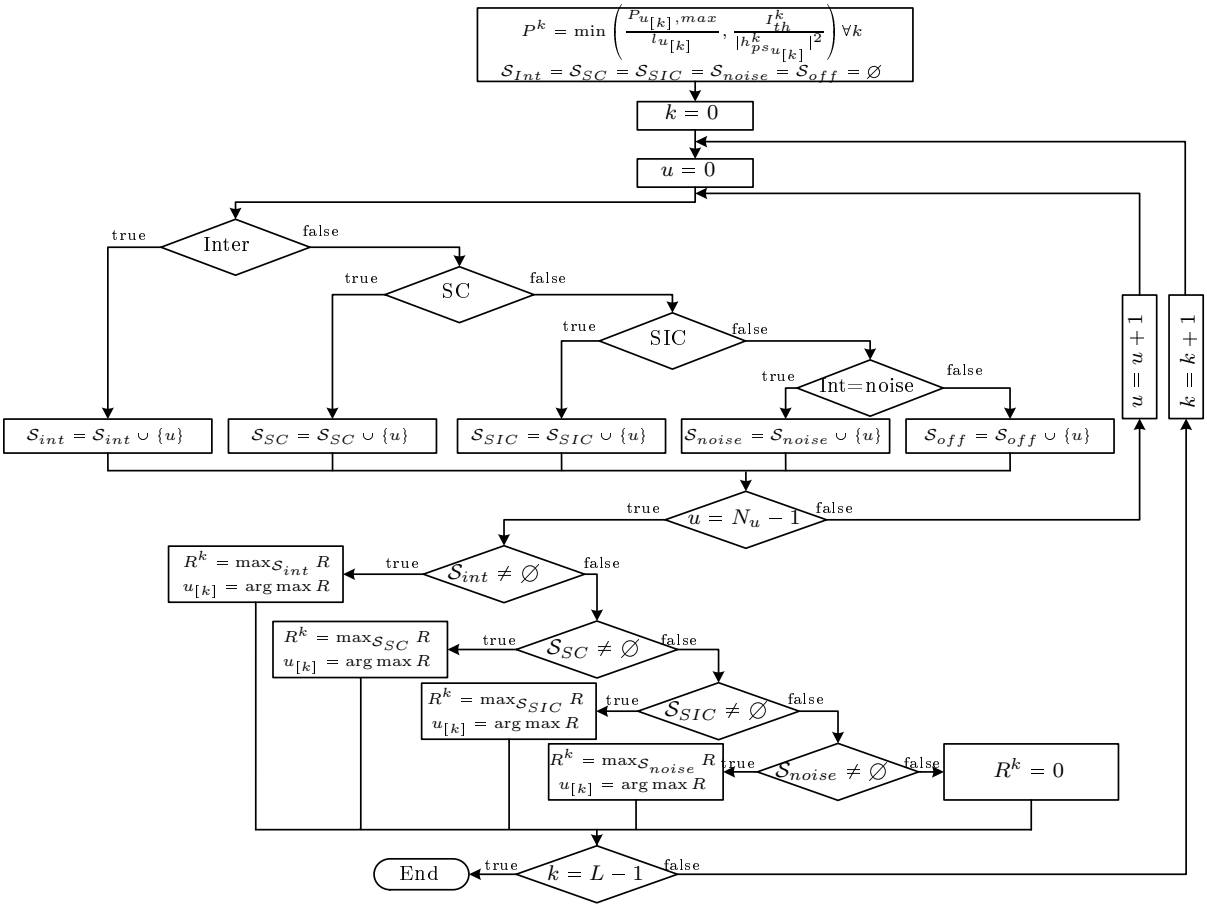

FIGURE 3.9 – Subcarrier Allocation Algorithm

allocated to user $u_{[k]}$.

The solution of this problem is given in Tables 3.2 and 3.3, by adapting the indexes to the multiuser case.

3.10 Simulation results

3.10.1 Performance evaluation for the single-user case

With perfect CSI, the complex channel gains h_{ij}^k take into account path loss, log-normal shadowing and Rayleigh fading. We suppose here that all subcarriers are subject to independent Rayleigh fading. The path loss model is COST 231 extension to Hata model at 800 MHz in dense urban environment, $L_{dB}(d) = 125.08 + 35.22 \times \log_{10}(d)$, and the shadowing standard deviation is equal to 6 dB. Both primary and secondary cells have omnidirectional antennas with the same radius $d_p = d_s = 1$ km. The allowed data rate decrease due to interference on the primary system is $\Delta = 0.1$, which means that 90% of the interference-free rate is guaranteed. The stopping criterion of Algorithm 1 is either $\frac{|R_{s,n} - R_{s,n-1}|}{|R_{s,n-1}|} < 10^{-4}$ or n = 10 iterations and for Algorithm 2 is either $\frac{|\sum_k R_{s,m}^{k,SC}| - |\sum_k R_{s,m-1}^{k,SC}|}{|\sum_k R_{s,m-1}^{k,SC}|} < 10^{-4}$ or $m = 10$. It is important to note that for the power allocation algorithm, a convergence at 2% on the secondary rate is reached after 6 iterations.

Performance evaluation for one secondary user

Statistics

In order to get an insight on the distribution of the different studied cases in terms of users positions, we consider three different scenarios. In the first and second scenarios, the primary BS is considered as the center of reference for the users coordinates with $x_{BS_p} = y_{BS_p} = 0$ km, and the secondary BS is fixed at (1 km, 0 km).

In the first scenario, the position of the primary transmitter is fixed with $x_p = 0.6$ km and $y_p = 0$ km and the secondary transmitter is allowed to move along its own cell. The statistics of the possible decoding strategies given in terms of the percentage of applying each of them are represented in Fig. 3.10.

The weak interference case, where the interference is treated as noise, depends exclusively on $|h_{sp}^k|^2$ and $|h_{ss}^k|^2$. With a large number of runs, represented by subfigure 'Int', this case is only affected by the path loss, and consequently by the distance between the SU and its BS. On the other hand, subfigures 'SC' and 'SIC' prove that these two methods are complementary and that the application of SC in the algorithm will improve the system rates. The SU is switched off when neither SIC nor SC can be applied and also whenever the interference constraints are not satisfied. This case is inversely proportional to $|h_{ps}^k|^2$ as shown in subfigure 'OFF'.

In the second scenario, the position of the secondary transmitter is fixed at $x_s = 1.4$ km and $y_s = 0$ km and the primary transmitter is allowed to move along its own cell. The statistics of all cases are represented in Fig. 3.11. We can see that the interference is treated as noise

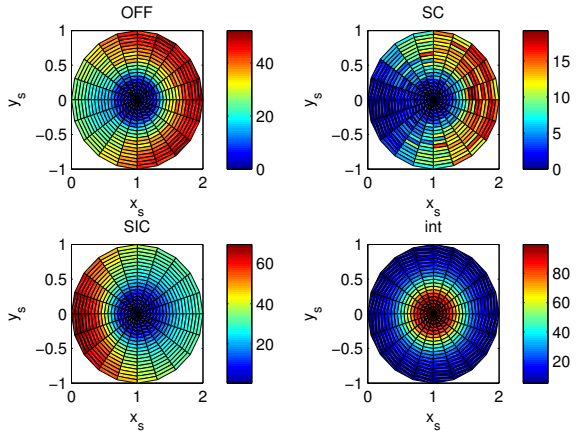

FIGURE 3.10 – Statistics of the decoding strategies for $x_p = 0.6$ km and $y_p = 0$ km

when it is weak, i.e., whenever the distance between the PU and the secondary BS is greater than the distance between the secondary mobile and its BS, which is equal to 0.4 km in our case. Otherwise, the strong interference case is activated and several methods can be applied depending on the conditions studied previously. Since $|h_{ss}^k|^2$ is fixed, all cases depend on $|h_{sp}^k|^2$.

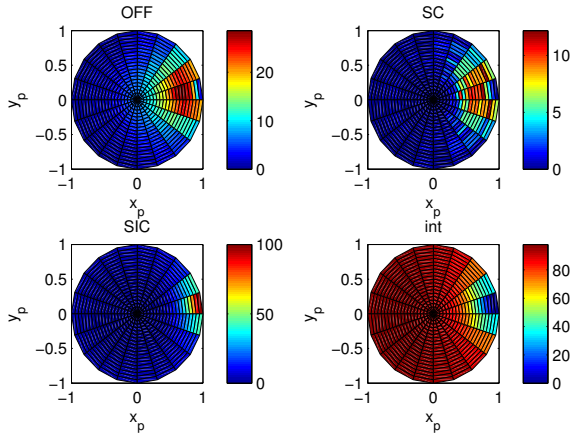

FIGURE 3.11 – Statistics of the decoding strategies for $x_s = 1.4$ km and $y_s = 0$ km

In the last scenario, the influence of both primary and secondary locations are evaluated. Both primary and secondary users are allowed to move along the x-axis. Both users are chosen to move between the two BSs. Statistics are given in terms of d_p and d_s, the distance between each BS and its mobile. (See Fig. 3.12).

When $d_p < d_s$, the interference is weak and is treated as noise at the secondary receiver. In the opposite side, SIC or SC can be used. The SU is turned off whenever these methods cannot be applied or the interference threshold is not satisfied.

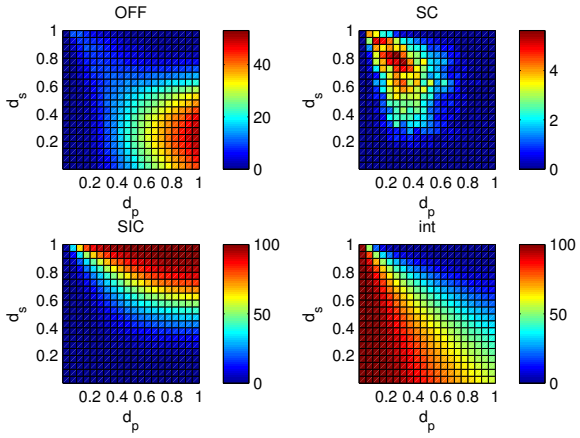

FIGURE 3.12 – Statistics of the decoding strategies for mobiles moving on X-axis between the BSs

Rates improvement and comparison with several methods

The impact of the proposed algorithm on both sum, primary and secondary rates is shown in Fig. 3.13 and Fig. 3.14. By comparing the proposed method with the algorithm in [106] for the single user scenario where only SIC is applied in the strong interference case, denoted by 'SIC', the proposed method shows an improvement due to the application of SC. Applying only the SC method (results referred to as 'SIC & SC'), an improvement that lies between 0.7 and 1.2% is obtained on the sum rate of the system, while the secondary rate increases between 5 and 17.3%. On the other hand, the sum rate increases between 1.6 and 2.1% while the secondary rate increases between 11.5 and 25.4% when only power control is added to 'SIC'. These results are marked by 'SIC and power control' in the legend of both figures.

The improvement provided by the power optimization in presence of SC strategy is highlighted. When both SC and dual decomposition are applied, the proposed algorithm denoted by 'SIC & SC & power control', the sum and secondary rates are compared with 'SIC'. The improvement is then between 2.3 and 3% on the sum rate, while it is between 16.9 and 43.5% on the secondary rate. In all these cases, there is a negligible degradation on the PU rate which never exceeds 0.7%. This degradation is due to the increased power level allocated to the SU with our algorithm.

The proposed algorithm is also compared with three other schemes :

— The case where the secondary system is always switched off (denoted by 'RP' for 'Reference on Primary'). In this case, waterfilling is applied on the primary user and the complexity is calculated as $O(L \log_2 L)$ [110].

— The classical power allocation scheme where the secondary system can transmit on the whole bandwidth of a cognitive underlay/interweave system by considering the primary system's interference as noise in all subcarriers. This algorithm is denoted by 'FB' for 'Full Band' and its complexity is $2 \cdot N \cdot O(L \log_2 L)$, with N is the number of iterations.

— An algorithm where the secondary system can only transmit in the subcarriers with weak

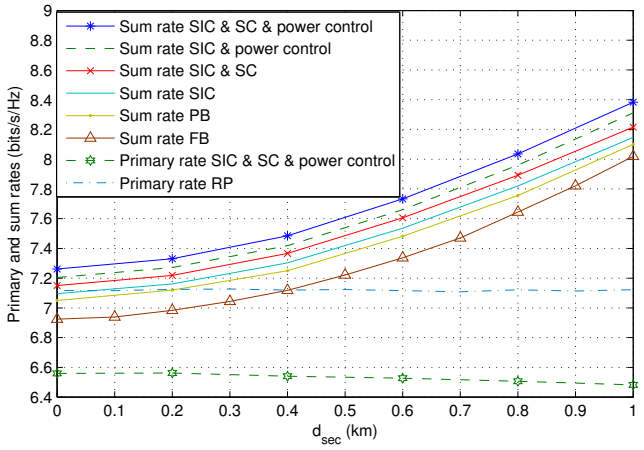

FIGURE 3.13 – Sum rate and primary rate compared with various methods

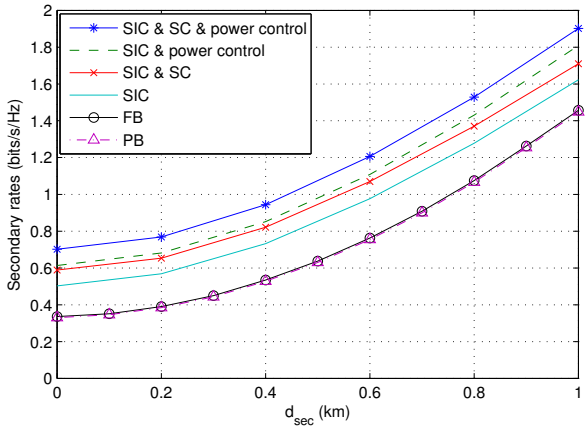

FIGURE 3.14 – Secondary rate compared with different methods

interference ($|h_{sp}^k|^2 \leqslant |h_{ss}^k|^2$) by considering the primary system's interference as noise in these subcarriers. This algorithm is denoted by 'PB' for 'Partial Band' and its complexity is $3/2 \cdot N \cdot O(L \log_2 L)$.

Both sum and primary rates are shown in Fig. 3.13. The adaptive decoding strategy with the proposed power control scheme achieves the highest sum rate. Compared with 'RP', the achievable sum rate gain increases with d_{sec} from 0.9 to 14.27%. Moreover, the data rate gain obtained by comparing the proposed method with 'FB' and 'PB' is respectively 4.3 - 5.02% and 1.22 - 3.38%.

The proposed method presents the lowest primary rate but the degradation comparing to 'FB' does not exceed 0.8%, where this gain reaches 4% when comparing with 'PB', while the achieved gain on the secondary rate is about 40%, as shown in Fig. 3.14.

Performance evaluation with several secondary users

In this section, the performance of the proposed algorithm is evaluated with various numbers of users in the secondary cell. We note that the stopping criterion for Algorithm 3 is either $\frac{|R_{s_{u_{[k]},n}} - R_{s_{u_{[k]},n-1}}|}{|R_{s_{u_{[k]},n-1}}|} < 10^{-4}$ or $n = 10$ iterations. This alternative process is repeated N times. In a first scenario, we suppose that only two SUs are present in the secondary cell. The influence of this multiuser diversity is presented in Fig. 3.15. The obtained gain for the sum rate, thanks to the multiuser aspect, has increased from 5.5 - 12% in a scenario which does not apply SC, to 9.4 - 14% in our contribution.

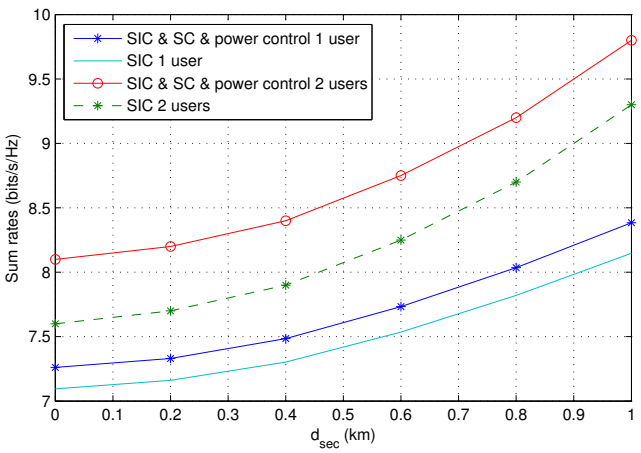

FIGURE 3.15 – Sum rates with two secondary users

The evolution of the secondary rates with respect to the number of users in the secondary cell by considering the different scenarios (with and without SC, with and without power control) is drawn in Fig. 3.16, with d_{sec}= 0.6 km. The simulations show that the growth of the secondary rate increases from 9 - 14% when only SIC is applied, to 21 - 31% when SIC, SC and power control are applied.

Finally, the proposed algorithm is compared with exhaustive search, where the SU with the maximum estimated rate is allocated to each subcarrier, without selecting the users based

on their decoding strategies. The achievable rates with the proposed algorithm are 4% less than those of the exhaustive search which represents an upper bound for the secondary rates. Consequently, we can conclude that our heuristic subcarrier allocation algorithm which is less complex than the exhaustive search, still quite effective.

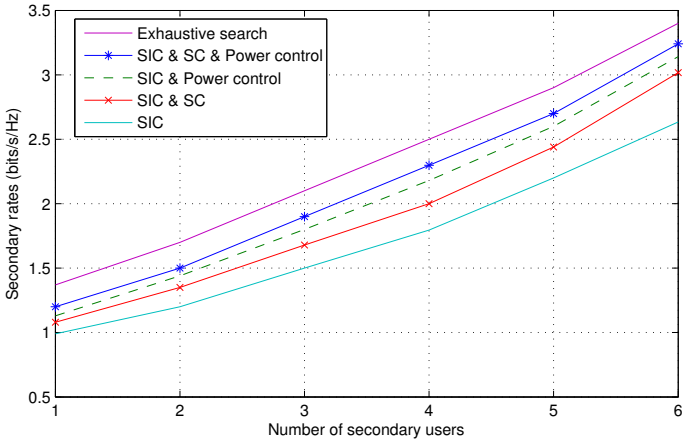

FIGURE 3.16 – Secondary rates depending on the number of users, for d_{sec}= 0.6 km

3.11 Conclusion

In this chapter, we proposed a resource allocation algorithm for a cognitive radio system in both single-user and multiuser scenarios. For the former scenario, an adaptive decoding algorithm based on both successive interference cancellation and superposition coding strategy is proposed in order to maximize the secondary achievable rate. The power allocation problem is then investigated in order to optimally allocate the power over the different subcarriers, taking into account the interference limit constraint and the power budget for each user. A general solution is proposed using waterfilling and dual decomposition methods. For the latter scenario, the proposed algorithm involves two steps. Firstly, a multiuser decoding algorithm is proposed based on the single-user case, in order to compute the achievable rates of different users. After an orthogonal subcarrier allocation, where the user with the maximum achievable rate is activated within each subcarrier, the secondary rate maximization problem is formulated as a nonlinear problem and an iterative algorithm similar to the single-user case is proposed. A general solution for the power optimization problem in an uplink underlay cognitive system is proposed. Both theoretical analysis and simulation results have shown that the proposed algorithm achieves higher sum rate than classical algorithms, for both single-user and multiuser cases, providing high-enough data rates for the secondary system at the expense of a very low degradation of the primary system's rate. In the next chapter, the same problem for the studied system model is investigated under the assumption that only statistical channel state information about the primary's channels is available at the secondary user.

Chapitre 4

Resource allocation algorithm with statistical CSI

4.1 Introduction

In the previous chapter, we investigated the resource allocation problem for both single-user and multiuser OFDM-based CR system, assuming that perfect channel knowledge is available at all system nodes with the help of a band manager. However, obtaining full knowledge about the channel gains at the SU is very difficult to implement in practice. In this chapter, we investigate the dynamic resource allocation problem in a single-user underlay CR system with the assumption that only statistical CSI on both primary links is available at the SU.

The remaining of this chapter is organized as follows. The studied system model is described in Section 4.3. In Section 4.4, the outage probabilities of each constraint in the power allocation problem are detailed and the new optimization problem is presented. The first order Taylor approximation is applied on non-convex constraints and non-concave objective functions in Section 4.5. The said problem with approximated constraints and objective functions is solved by using dual decomposition and bisection methods in Sections 4.6 and 4.7, respectively. In Section 4.8, the SCA algorithm is described in order to give the general solution of the investigated problem. Finally, simulation results are given in Section 4.9 and a conclusion of the chapter is provided in Section 4.10.

4.2 State of the art

In practice, perfect channel knowledge is difficult to obtain. The impact of imperfect CSI on capacity region was investigated in [111–116] with uncertainty, quantization or estimation errors. In [111], the authors considered a cognitive underlay scenario assuming that the secondary

receiver has only partial information of the link between its transmitter and the primary receiver. This paper studied different capacity regions considering average or peak interference constraints at the primary receiver and introduced the concept of interference-outage allowed by the primary receiver. The same problem was considered in [112] with average received power constraint at the primary receiver in a discrete-time block-fading channel with imperfect CSI. In [113], Suraweera et al., investigated the impact of imperfect CSI of the SU-PU link on the SU mean capacity, considering the effect of CSI quantization with a finite number of quantization levels. The ergodic capacity maximization problem with quantized information about CSI available at the SU through a limited feedback link was studied in [114], while optimum power strategy and ergodic capacity were derived under outage constraints in [115]. The impact of noisy CSI on spectral efficiency of multiuser multi-carrier CRs was considered in [116], where novel interference management schemes were derived based on different average-case and worst-case models of channel estimation error. In all previously cited works, imperfect CSI was considered only on the cross-link between the secondary transmitter and the primary receiver. Furthermore, other works considered the effect of statistical CSI rather than instantaneous channel estimation errors [117,118]. In [117], Smith et al. study the impact of limited channel knowledge on the CR system capacity by comparing the effect of a statistical CSI and an erroneous instantaneous CSI of the primary channel gains. In [118], the authors investigated the effect of statistical CSI on all the channels for the primary and secondary links on the SU capacity without addressing the power allocation problem.

4.3 Channel Model

In this chapter, the same system model as in Chapter 3 is studied, assuming that only statistical knowledge on the primary channels is available at the SU. Without loss of generality, only one SU with index s is considered in the secondary cell. We recall that the received primary and secondary signals in each subcarrier $k \in \{1, \dots, L\}$ can be written as

$$y_p^k = h_{pp}^k x_p^k + h_{ps}^k x_s^k + z_p^k \tag{4.1}$$

$$y_s^k = h_{sp}^k x_p^k + h_{ss}^k x_s^k + z_s^k \tag{4.2}$$

Since $h_{ij}^k \sim \mathcal{CN}(0, \lambda_{ij}^k)$ with $(i,j) \in \{p,s\}^2$, $|h_{ij}^k|^2$ is exponentially distributed and its probability density function is expressed by $\frac{1}{\lambda_{ij}^k} \exp^{-\frac{x}{\lambda_{ij}^k}}$. We now assume that only λ_{pp}^k and λ_{ps}^k are known at the secondary receiver. Under this assumption, the convexity of the power optimization problem is studied in the following section. Different outage terms are investigated. The first one, which is called "interference outage probability" is related to the interference constraint defined in eq. (3.37d). The second outage probability results from the SIC constraint presented by inequality (3.14). Finally, three outage probabilities result from the application of SC at the SU : Two outage probabilities related to SC constraints in (3.19) and one outage rate probability on the secondary rate when SC is applied since it depends on $|h_{pp}^k|^2$ and $|h_{ps}^k|^2$. Most of these outage probability constraints are not convex, consequently, the optimization problem is a non-convex

problem. In Section 4.6, a sequential approximation algorithm is proposed to solve the problem.

4.4 Determination of the outage probabilities

In the previous chapter, we investigated the power optimization problem presented in (4.3) assuming that perfect channel knowledge is available at the different nodes of the system. In this chapter, we investigate the same problem for the single-user case with statistical CSI. For that, we first detail the outage probability that results from each of the problem constraints and then we proceed to the dual decomposition and convex approximation methods to solve the problem. For simplicity, we drop the iteration index n in this section and we reintroduce it in the next section where the optimization problem is investigated.

$$\max_{\mathbf{p}_s} R_s \tag{4.3a}$$

$$\text{s.t. } \sum_{k=1}^{L} P_s^k \leqslant P_{s,max} \tag{4.3b}$$

$$\text{s.t. } P_s^k \geqslant 0 \,\forall\, k \in \{1,\ldots,L\} \tag{4.3c}$$

$$\text{s.t. } |h_{ps}^k|^2 P_s^k \leqslant I_{th}^k \,\forall\, k \notin \mathcal{S}_1 \tag{4.3d}$$

$$\text{s.t. } a^k P_s^k \geqslant c^k, \forall\, k \in \mathcal{S}_3 \tag{4.3e}$$

$$\text{s.t. } \frac{\left(|h_{pp}^k|^2 - |h_{sp}^k|^2\right)}{|h_{ps}^k|^2 |h_{sp}^k|^2} < \frac{P_s^k}{n_0}, \forall\, k \in \mathcal{S}_4 \tag{4.3f}$$

$$\text{s.t. } P_s^k a^k < c^k, \forall\, k \in \mathcal{S}_4 \tag{4.3g}$$

where $R_s = \sum_{k\in\mathcal{S}_2} R_s^{k,int} + \sum_{k\in\mathcal{S}_1\cap\mathcal{S}_3} R_s^{k,SIC} + \sum_{k\in\mathcal{S}_4} R_s^{k,SC}$

4.4.1 Interference constraint with statistical CSI

The outage probability on constraint (4.3d) is

$$\mathbb{P}_r\left\{|h_{ps}^k|^2 P_s^k > I_{th}^k\right\} \leqslant \theta^k \tag{4.4}$$

where θ^k is the authorized interference outage. Since $|h_{ps}^k|^2$ is exponentially distributed, with variance λ_{ps}^k, this probability can be calculated by

$$\int_{\frac{I_{th}^k}{P_s^k}}^{\infty} \frac{1}{\lambda_{ps}^k} \exp^{-\frac{x}{\lambda_{ps}^k}} dx \leqslant \theta^k$$

Therefore, the interference outage constraint can be written as

$$\exp^{-\frac{I_{th}^k}{P_s^k \lambda_{ps}^k}} \leqslant \theta^k \tag{4.5}$$

which is equivalent to

$$P_s^k \leqslant \frac{I_{th}^k}{\lambda_{ps}^k \log\left(\frac{1}{\theta^k}\right)} \tag{4.6}$$

4.4.2 SIC constraint with statistical CSI

The SIC constraint in (4.3e) was first obtained from the inequality

$$\frac{|h_{pp}^k|^2 P_p^k}{|h_{ps}^k|^2 P_s^k + n_0} \leqslant \frac{|h_{sp}^k|^2 P_p^k}{|h_{ss}^k|^2 P_s^k + n_0} \tag{4.7}$$

Then, the outage probability on constraint (4.3e) can be calculated as

$$\mathbb{P}_r \left\{ \frac{|h_{pp}^k|^2}{n_0 + |h_{ps}^k|^2 P_s^k} > \frac{|h_{sp}^k|^2}{n_0 + |h_{ss}^k|^2 P_s^k} \right\} \leqslant \epsilon^k \tag{4.8}$$

Since $|h_{pp}^k|^2$ is exponentially distributed, with variance λ_{pp}^k, this probability can be calculated by

$$\mathbb{E}\left\{ \int_{\frac{|h_{sp}^k|^2\left(n_0+|h_{ps}^k|^2 P_s^k\right)}{n_0+|h_{ss}^k|^2 P_s^k}}^{\infty} \frac{1}{\lambda_{pp}^k} \exp^{-\frac{x}{\lambda_{pp}^k}} dx \right\} \leqslant \epsilon^k$$

which is equivalent to

$$\mathbb{E}\left\{ \exp^{-\frac{|h_{sp}^k|^2\left(n_0+|h_{ps}^k|^2 P_s^k\right)}{\lambda_{pp}^k\left(n_0+|h_{ss}^k|^2 P_s^k\right)}} \right\} \leqslant \epsilon^k$$

Since $|h_{ps}^k|^2$ is exponentially distributed, with variance λ_{ps}^k, the outage probability on (4.3e) can be calculated by

$$\exp^{-\frac{|h_{sp}^k|^2 n_0}{\lambda_{pp}^k\left(n_0+|h_{ss}^k|^2 P_s^k\right)}} \int_0^{\infty} \frac{1}{\lambda_{ps}^k} \exp^{-\left(\frac{|h_{sp}^k|^2 P_s^k}{\lambda_{pp}^k\left(n_0+|h_{ss}^k|^2 P_s^k\right)} + \frac{1}{\lambda_{ps}^k}\right) y} dy \leqslant \epsilon^k$$

which is given by

$$\exp^{-\frac{|h_{sp}^k|^2 n_0}{\lambda_{pp}^k\left(n_0+|h_{ss}^k|^2 P_s^k\right)}} \frac{1}{1 + \frac{\lambda_{ps}^k |h_{sp}^k|^2 P_s^k}{\lambda_{pp}^k (n_0 + |h_{ss}^k|^2 P_s^k)}} \leqslant \epsilon^k$$

Consequently, the outage probability on constraint (4.3e) can be given by

$$\exp^{-\frac{\nu^k n_0}{\lambda_{pp}^k}} \frac{1}{1 + \frac{\lambda_{ps}^k}{\lambda_{pp}^k} \nu^k P_s^k} \leqslant \epsilon^k \tag{4.9}$$

where

$$\nu^k = \frac{|h_{sp}^k|^2}{n_0 + |h_{ss}^k|^2 P_s^k} \tag{4.10}$$

4.4.3 SC constraints with statistical CSI

If only statistical CSI about $|h_{pp}^k|^2$ and $|h_{ps}^k|^2$ is available at the SU, outage can occur on either secondary rate or SC constraints. Thus, three outage probabilities can be calculated :

1. Rate outage on $R_s^{k,SC}$ and more specifically the outage probability on α^k which is the only factor in $R_{s,n}^{k,SC}$ depending on $|h_{pp}^k|^2$ and $|h_{ps}^k|^2$.
2. Outage probability on constraint (4.3f).
3. Outage probability on constraint (4.3g).

Outage probability on α^k

To avoid the difficulty resulting by calculating the outage rate probability on the SU rate when SC is applied, and since only α^k depends on $|h_{pp}^k|^2$ and $|h_{ps}^k|^2$, we aim to calculate the outage probability on α^k and not on the secondary rate. We recall the equation used to calculate α^k with perfect CSI (3.14)

$$\frac{|h_{pp}^k|^2}{|h_{ps}^k|^2 P_s^k + n_0} = \frac{|h_{sp}^k|^2}{\alpha^k |h_{ss}^k|^2 P_s^k + n_0} \tag{4.11}$$

which can be equivalently written as

$$\frac{|h_{pp}^k|^2}{|h_{sp}^k|^2} = \frac{|h_{ps}^k|^2 P_s^k + n_0}{\alpha^k |h_{ss}^k|^2 P_s^k + n_0}$$

With statistical CSI, constraint (4.11) becomes

$$\Pr\left\{ \frac{|h_{pp}^k|^2}{|h_{sp}^k|^2} = \frac{|h_{ps}^k|^2 P_s^k + n_0}{\alpha^k |h_{ss}^k|^2 P_s^k + n_0} \right\} = 1 \tag{4.12}$$

which is equivalent to $\Pr\{X = Y\} = 1$ where

$$\begin{aligned} X &\triangleq \frac{|h_{pp}^k|^2}{|h_{sp}^k|^2} \\ Y &\triangleq \frac{|h_{ps}^k|^2 P_s^k + n_0}{\alpha^k |h_{ss}^k|^2 P_s^k + n_0} \end{aligned}$$

Basically for two random variables

$$\Pr\{X = Y\} = \int_{t \in \mathcal{S}} f_{X,Y}(X = t, Y = t)\, dt \tag{4.13}$$

where $f_{X,Y}\left(X=t, Y=t\right)$ is the joint probability distribution function of X and Y. By independence, and since X and Y are both exponentially distributed, it follows that the joint probability density function of X and Y is

$$f_{X,Y}\left(X=t, Y=t\right) = \frac{1}{\lambda_X \lambda_Y} e^{-\left(\frac{1}{\lambda_X}+\frac{1}{\lambda_X}\right)t} \tag{4.14}$$

hence

$$\begin{aligned} \Pr\left\{X=Y\right\} &= \int_0^\infty \frac{1}{\lambda_X \lambda_Y} e^{-\left(\frac{1}{\lambda_X}+\frac{1}{\lambda_X}\right)t} dt & (4.15)\\ &= \frac{1}{\lambda_X + \lambda_Y} & (4.16) \end{aligned}$$

with

$$\lambda_X = \mathbb{E}\left\{\frac{|h_{pp}^k|^2}{|h_{sp}^k|^2}\right\} = \frac{\lambda_{pp}^k}{|h_{sp}^k|^2}$$

and

$$\lambda_Y = \mathbb{E}\left\{\frac{|h_{ps}^k|^2 P_s^k + n_0}{\alpha^k |h_{ss}^k|^2 P_s^k + n_0}\right\} = \frac{\lambda_{ps}^k P_s^k + n_0}{\alpha^k |h_{ss}^k|^2 P_s^k + n_0}$$

Consequently, constraint (4.12) can be written as

$$\frac{\lambda_{pp}^k}{|h_{sp}^k|^2} + \frac{\lambda_{ps}^k P_s^k + n_0}{\alpha^k |h_{ss}^k|^2 P_s^k + n_0} = 1 \tag{4.17}$$

which is equivalent to

$$\alpha^k = \frac{|h_{sp}^k|^2 \lambda_{ps}^k P_s^k + \lambda_{pp}^k n_0}{|h_{ss}^k|^2 P_s^k \left(|h_{sp}^k|^2 - \lambda_{pp}^k\right)} \tag{4.18}$$

Outage probability on equation (4.3f)

The outage probability on (4.3f) is calculated as

$$\mathbb{P}_r\left\{\frac{\left(|h_{pp}^k|^2 - |h_{sp}^k|^2\right)}{|h_{ps}^k|^2 |h_{sp}^k|^2} \geqslant \frac{P_s^k}{n_0}\right\} \leqslant \delta^k \tag{4.19}$$

which is equivalent to

$$\mathbb{P}_r\left\{|h_{pp}^k|^2 \geqslant \frac{|h_{ps}^k|^2 |h_{sp}^k|^2 P_s^k}{n_0} + |h_{sp}^k|^2\right\} \leqslant \delta^k$$

Since $|h_{pp}^k|^2$ is exponentially distributed, with variance λ_{pp}^k, this probability can be calculated

by

$$\mathbb{E}\left[\int_{\frac{|h_{ps}^k|^2|h_{sp}^k|^2P_s^k}{n_0}+|h_{sp}^k|^2}^{\infty}\frac{1}{\lambda_{pp}^k}\exp^{-\frac{1}{\lambda_{pp}^k}x}dx\right]\leqslant\delta^k$$

which is given by

$$\mathbb{E}\left[\exp^{-\frac{1}{\lambda_{pp}^k}\left(\frac{|h_{ps}^k|^2|h_{sp}^k|^2P_s^k}{n_0}+|h_{sp}^k|^2\right)}\right]\leqslant\delta^k \tag{4.20}$$

Since $|h_{ps}^k|^2$ is exponentially distributed, with variance λ_{ps}^k, the outage probability on (4.20) becomes

$$\exp^{-\frac{|h_{sp}^k|^2}{\lambda_{pp}^k}}\int_0^{\infty}\frac{1}{\lambda_{ps}^k}\exp^{-\left(\frac{|h_{sp}^k|^2P_s^k}{\lambda_{pp}^kn_0}+\frac{1}{\lambda_{ps}^k}\right)y}dy\leqslant\delta^k$$

The outage probability on (4.3f) is then given by

$$\exp^{-\frac{|h_{sp}^k|^2}{\lambda_{pp}^k}}\frac{1}{1+\frac{|h_{sp}^k|^2P_s^k\lambda_{ps}^k}{\lambda_{pp}^kn_0}}\leqslant\delta^k \tag{4.21}$$

Outage probability on equation (4.3g)

The outage probability on constraint (4.3g) is calculated as

$$\mathbb{P}_r\left\{\frac{|h_{pp}^k|^2P_p^k}{n_0+|h_{ps}^k|^2P_s^k}\leqslant\frac{|h_{sp}^k|^2P_p^k}{n_0+|h_{ss}^k|^2P_s^k}\right\}\leqslant\gamma^k \tag{4.22}$$

which can be equivalently formulated as

$$1-\mathbb{P}_r\left\{\frac{|h_{pp}^k|^2P_p^k}{n_0+|h_{ps}^k|^2P_s^k}>\frac{|h_{sp}^k|^2P_p^k}{n_0+|h_{ss}^k|^2P_s^k}\right\}\leqslant\gamma^k \tag{4.23}$$

The outage probability on (4.3g) can be then deduced from (4.9) and it is equal to

$$\exp^{-\frac{\nu^kn_0}{\lambda_{pp}^k}}\frac{1}{1+\frac{\lambda_{ps}^k}{\lambda_{pp}^k}\nu^kP_s^k}\geqslant1-\gamma^k \tag{4.24}$$

4.4.4 Synthesis

Consequently, the power allocation problem given in (4.3) with statistical CSI and outage limits ϵ^k, θ^k, δ^k and γ^k can be formulated as

$$\max_{\mathbf{p}_s} R_s \tag{4.25a}$$

$$\text{s.t.} \sum_{k=1}^{L} P_s^k \leqslant P_{s,\max} \tag{4.25b}$$

$$\text{s.t. } P_s^k \geqslant 0, \forall k \in \{1,\dots,L\} \tag{4.25c}$$

$$\text{s.t. } \exp^{-\frac{I_{th}^k}{P_s^k \lambda_{ps}^k}} \leqslant \theta^k, \forall k \notin \mathcal{S}_1 \tag{4.25d}$$

$$\text{s.t. } \exp^{-\frac{\nu^k n_0}{\lambda_{pp}^k}} \frac{1}{1+\frac{\lambda_{ps}^k}{\lambda_{pp}^k}\nu^k P_s^k} \leqslant \epsilon^k, \forall k \in \mathcal{S}_3 \tag{4.25e}$$

$$\text{s.t. } \exp^{-\frac{|h_{sp}^k|^2}{\lambda_{pp}^k}} \frac{1}{1+\frac{|h_{sp}^k|^2 P_s^k \lambda_{ps}^k}{\lambda_{pp}^k n_0}} \leqslant \delta^k, \forall k \in \mathcal{S}_4 \tag{4.25f}$$

$$\text{s.t. } \exp^{-\frac{\nu^k n_0}{\lambda_{pp}^k}} \frac{1}{1+\frac{\lambda_{ps}^k}{\lambda_{pp}^k}\nu^k P_s^k} \geqslant 1-\gamma^k, \forall k \in \mathcal{S}_4 \tag{4.25g}$$

where

$$\nu^k = \frac{|h_{sp}^k|^2}{n_0 + |h_{ss}^k|^2 P_s^k} \tag{4.26}$$

and $R_s = \sum_{k\in\mathcal{S}_2} R_s^{k,int} + \sum_{k\in\mathcal{S}_1\cap\mathcal{S}_3} R_s^{k,SIC} + \sum_{k\in\mathcal{S}_4} R_s^{k,SC}$.

It can be seen that constraints (4.25e), (4.25f) and (4.25g) are not convex. In addition, the rate $R_s^{k,SC}$ is not concave in P_s^k. This results in nonconvex optimization problem. So, in order to obtain a convex optimization problem, the first order Taylor approximation can be applied on these functions at a feasible point $\overline{P_s^k}$.

4.5 First Taylor approximation

In this section, the first order Taylor approximation is applied on non-convex constraints as well as on non-concave objective functions in problem (4.25). In the next two sections, both dual decomposition and bisection methods are adapted to solve the optimization problem.

4.5.1 Applying Taylor approximation on (4.25e)

The outage probability on the SIC constraint (4.25e) is equivalent to

$$\frac{n_0|h_{sp}^k|^2}{\lambda_{pp}^k(n_0+|h_{ss}^k|^2P_s^k)} + \log\left(1+\frac{\lambda_{ps}^k|h_{sp}^k|^2P_s^k}{\lambda_{pp}^k(n_0+|h_{ss}^k|^2P_s^k)}\right) \geqslant \log(\frac{1}{\epsilon^k}) \tag{4.27}$$

The first ratio in (4.27) can be written as follows

$$\frac{n_0|h_{sp}^k|^2}{\lambda_{pp}^k(n_0+|h_{ss}^k|^2P_s^k)}=\frac{|h_{sp}^k|^2}{\lambda_{pp}^k}\frac{1}{1+\frac{|h_{ss}^k|^2P_s^k}{n_0}}$$

Using Taylor approximation at feasible point $\overline{P_s^k}$, this term can be expressed by

$$\frac{|h_{sp}^k|^2}{\lambda_{pp}^k}\frac{1}{1+\frac{|h_{ss}^k|^2P_s^k}{n_0}}\approx\frac{|h_{sp}^k|^2}{\lambda_{pp}^k}\left(\frac{1}{1+\frac{|h_{ss}^k|^2}{n_0}\overline{P_s^k}}-\frac{|h_{ss}^k|^2}{n_0\left(1+\frac{|h_{ss}^k|^2}{n_0}\overline{P_s^k}\right)^2}(P_s^k-\overline{P_s^k})\right)$$

The second part of (4.27) can be approximated with first order Taylor approximation at feasible point $\overline{P_s^k}$ as

$$\begin{aligned}\log\left(1+\frac{\lambda_{ps}^k|h_{sp}^k|^2P_s^k}{\lambda_{pp}^k(n_0+|h_{ss}^k|^2P_s^k)}\right)&\approx\log\left(1+\frac{\lambda_{ps}^k|h_{sp}^k|^2\overline{P_s^k}}{\lambda_{pp}^k(n_0+|h_{ss}^k|^2\overline{P_s^k})}\right)\\&+\frac{\lambda_{pp}^k\lambda_{ps}^k|h_{sp}^k|^2n_0}{\left(\lambda_{pp}^k(n_0+|h_{ss}^k|^2\overline{P_s^k})\right)\left(\lambda_{pp}^k(n_0+|h_{ss}^k|^2\overline{P_s^k})+\lambda_{ps}^k|h_{sp}^k|^2\overline{P_s^k}\right)}\left(P_s^k-\overline{P_s^k}\right)\end{aligned}$$

The SIC outage probability is then formulated as

$$\begin{aligned}&\frac{|h_{sp}^k|^2}{\lambda_{pp}^k}\left(\frac{1}{1+\frac{|h_{ss}^k|^2}{n_0}\overline{P_s^k}}-\frac{|h_{ss}^k|^2}{n_0\left(1+\frac{|h_{ss}^k|^2}{n_0}\overline{P_s^k}\right)^2}(P_{s,n}^k-\overline{P_s^k})\right)+\log\left(1+\frac{\lambda_{ps}^k|h_{sp}^k|^2\overline{P_s^k}}{\lambda_{pp}^k(n_0+|h_{ss}^k|^2\overline{P_s^k})}\right)\\&+\frac{\lambda_{pp}^k\lambda_{ps}^k|h_{sp}^k|^2n_0}{\left(\lambda_{pp}^k(n_0+|h_{ss}^k|^2\overline{P_s^k})\right)\left(\lambda_{pp}^k(n_0+|h_{ss}^k|^2\overline{P_s^k})+\lambda_{ps}^k|h_{sp}^k|^2\overline{P_s^k}\right)}\left(P_s^k-\overline{P_s^k}\right)\geqslant\log(\frac{1}{\epsilon^k})\end{aligned}\tag{4.28}$$

which can be written as

$$E^kP_s^k\geqslant F^k\tag{4.29}$$

where

$$E^k=\frac{\lambda_{pp}^k\lambda_{ps}^k|h_{sp}^k|^2n_0}{\left(\lambda_{pp}^k(n_0+|h_{ss}^k|^2\overline{P_s^k})\right)\left(\lambda_{pp}^k(n_0+|h_{ss}^k|^2\overline{P_s^k})+\lambda_{ps}^k|h_{sp}^k|^2\overline{P_s^k}\right)}-\frac{|h_{sp}^k|^2}{\lambda_{pp}^k}\frac{|h_{ss}^k|^2}{n_0\left(1+\frac{|h_{ss}^k|^2}{n_0}\overline{P_s^k}\right)^2}\tag{4.30}$$

and

$$F^k = \log(\frac{1}{\epsilon^k}) - \frac{|h_{sp}^k|^2}{\lambda_{pp}^k}\left(\frac{1}{1+\frac{|h_{ss}^k|^2}{n_0}\overline{P_s^k}} + \frac{|h_{ss}^k|^2\overline{P_s^k}}{n_0\left(1+\frac{|h_{ss}^k|^2}{n_0}\overline{P_s^k}\right)^2}\right) - \log\left(1+\frac{\lambda_{ps}^k|h_{sp}^k|^2\overline{P_s^k}}{\lambda_{pp}^k(n_0+|h_{ss}^k|^2\overline{P_s^k})}\right) \tag{4.31}$$

$$+ \frac{\lambda_{pp}^k\lambda_{ps}^k|h_{sp}^k|^2 n_0\overline{P_s^k}}{\left(\lambda_{pp}^k(n_0+|h_{ss}^k|^2\overline{P_s^k})\right)\left(\lambda_{pp}^k(n_0+|h_{ss}^k|^2\overline{P_s^k})+\lambda_{ps}^k|h_{sp}^k|^2\overline{P_s^k}\right)} \tag{4.32}$$

4.5.2 Applying Taylor approximation on (4.25g)

The outage probability on the SC constraint in (4.25g) is equivalent to

$$\frac{n_0|h_{sp}^k|^2}{\lambda_{pp}^k(n_0+|h_{ss}^k|^2P_s^k)} + \log\left(1+\frac{\lambda_{ps}^k|h_{sp}^k|^2P_s^k}{\lambda_{pp}^k(n_0+|h_{ss}^k|^2P_s^k)}\right) \leqslant \log(\frac{1}{1-\gamma^k}) \tag{4.33}$$

By similarity with (4.29), constraint (4.25g) can be written as

$$E^kP_s^k \leqslant J^k \tag{4.34}$$

where

$$J^k = \log(\frac{1}{1-\gamma^k}) - \frac{|h_{sp}^k|^2}{\lambda_{pp}^k}\left(\frac{1}{1+\frac{|h_{ss}^k|^2}{n_0}\overline{P_s^k}} + \frac{|h_{ss}^k|^2\overline{P_s^k}}{n_0\left(1+\frac{|h_{ss}^k|^2}{n_0}\overline{P_s^k}\right)^2}\right) - \log\left(1+\frac{\lambda_{ps}^k|h_{sp}^k|^2\overline{P_s^k}}{\lambda_{pp}^k(n_0+|h_{ss}^k|^2\overline{P_s^k})}\right) \tag{4.35}$$

$$+ \frac{\lambda_{pp}^k\lambda_{ps}^k|h_{sp}^k|^2 n_0\overline{P_s^k}}{\left(\lambda_{pp}^k(n_0+|h_{ss}^k|^2\overline{P_s^k})\right)\left(\lambda_{pp}^k(n_0+|h_{ss}^k|^2\overline{P_s^k})+\lambda_{ps}^k|h_{sp}^k|^2\overline{P_s^k}\right)} \tag{4.36}$$

4.5.3 Applying Taylor approximation on (4.25f)

The outage probability on the SC constraint in (4.25f) is equivalent to

$$\log\left(1+\frac{|h_{sp}^k|^2\lambda_{ps}^kP_s^k}{\lambda_{pp}^kn_0}\right) > \log\left(\frac{1}{\delta^k}\right) - \frac{|h_{sp}^k|^2}{\lambda_{pp}^k} \tag{4.37}$$

Applying first order Taylor approximation on $\log\left(1+\frac{|h_{sp}^k|^2\lambda_{ps}^kP_s^k}{n_0}\right)$, we obtain

$$\log\left(1+\frac{|h_{sp}^k|^2\lambda_{ps}^kP_s^k}{\lambda_{pp}^kn_0}\right) \approx \log\left(1+\frac{|h_{sp}^k|^2\lambda_{ps}^k\overline{P_s^k}}{\lambda_{pp}^kn_0}\right) + \frac{|h_{sp}^k|^2\lambda_{ps}^k}{|h_{sp}^k|^2\lambda_{ps}^k\overline{P_s^k}+\lambda_{pp}^kn_0}\left(P_s^k-\overline{P_s^k}\right)$$

Consequently, (4.25f) is equivalent to

$$G^kP_s^k > H^k \tag{4.38}$$

where

$$G^k = \frac{|h_{sp}^k|^2 \lambda_{ps}^k}{|h_{sp}^k|^2 \lambda_{ps}^k \overline{P_s^k} + \lambda_{pp}^k n_0}$$

and

$$H^k = \log\left(\frac{1}{\rho^k}\right) + \frac{|h_{sp}^k|^2}{\lambda_{pp}^k} + \frac{|h_{sp}^k|^2 \lambda_{ps}^k \overline{P_s^k}}{|h_{sp}^k|^2 \lambda_{ps}^k \overline{P_s^k} + \lambda_{pp}^k n_0} - \log\left(1 + \frac{|h_{sp}^k|^2 \lambda_{ps}^k \overline{P_s^k}}{\lambda_{pp}^k n_0}\right)$$

4.5.4 Applying Taylor approximation on $R_s^{k,SC}$

We recall the expression of the secondary achievable rate when SC is applied, which was given in eq. (3.30)

$$R_s^{k,SC} = R_{s,1}^{k,SC} + R_{s,2}^{k,SC} \tag{4.39}$$

where

$$R_{s,1}^{k,SC} = \frac{B}{L}\log_2\left(1 + \frac{|h_{sp}^k|^2 \lambda_{ps}^k P_s^k + \lambda_{pp}^k n_0}{n_0\left(|h_{sp}^k|^2 - \lambda_{pp}^k\right)}\right) \tag{4.40}$$

and

$$R_{s,2}^{k,SC} = \frac{B}{L}\log_2\left(1 + \frac{\left(\left(|h_{sp}^k|^2 - \lambda_{pp}^k\right)|h_{ss}^k|^2 - |h_{sp}^k|^2 \lambda_{ps}^k\right) P_s^k - \lambda_{pp}^k n_0}{|h_{sp}^k|^2 \lambda_{ps}^k P_s^k + \lambda_{pp}^k n_0 + \left(|h_{sp}^k|^2 - \lambda_{pp}^k\right)\left(|h_{sp}^k|^2 P_p^k + n_0\right)}\right) \tag{4.41}$$

We can verify that $R_{s,1}^{k,SC}$ is concave in P_s^k while $R_{s,2}^{k,SC}$ is not. Thus, it can then be approximated using the first order Taylor approximation at a feasible point $\overline{P_s^k}$. The approximated function of (4.41) can be given by

$$R_{s,2}^{k,SC} \simeq R_{s,2}^{k,SC}(\overline{P_s^k}) + B^k(\overline{P_s^k})\left(P_s^k - \overline{P_s^k}\right)$$

with

$$B^k = \frac{\partial R_{s,2}^{k,SC}}{\partial P_s^k}$$

4.6 Solving the optimization problem by decomposition

As we have proceeded in Section 3.8 of the previous chapter, the investigated optimization problem can be efficiently solved using the Lagrange dual decomposition method, since it is separable, by decomposing the original problem into three subproblems depending on the decoding strategies applied at the SU. In this section, we firstly present the decomposed optimization problem and then we calculate the first order Taylor approximation of each non-convex constraint. Finally, we propose a general solution of the investigated problem using dual decomposition. As

mentioned in the previous section, our algorithm is iterative and index n is reintroduced in this section to denote the iteration.

First of all, we write the Lagrangian of problem (4.25) taking into account constraints (4.25b) and (4.25c) as

$$\mathbb{L}\left(P_{s,n}^{k},\lambda\right)=-R_{s,n}+\lambda\left(\sum_{k=1}^{L}P_{s,n}^{k}-P_{s,\max}\right)-\sum_{k=1}^{L}\mu^{k}P_{s,n}^{k} \tag{4.42}$$

with $\lambda,\mu^{k}\geqslant 0$ being Lagrange multipliers. μ^{k} can be dropped since it is a slack variable. Let D be the set specified by the remaining constraints in (4.25d), (4.25e), (4.25f) and (4.25g). Consequently, problem (4.25) can be given by three subproblems C_{int}, C_{SIC} and C_{SC} defined over $\mathcal{S}_2$, $\mathcal{S}_3$ and $\mathcal{S}_4$ respectively as

$$C_{int}:\max_{\{P_{s,n}^{k}\}_{k\in\mathcal{S}_2}}\sum_{k\in\mathcal{S}_2}R_{s,n}^{k,int}-\mu_{s,n}\sum_{k\in\mathcal{S}_2}P_{s,n}^{k} \tag{4.43a}$$

$$P_{s,n}^{k}\leqslant\frac{I_{th}^{k}}{\lambda_{ps}^{k}\log(\frac{1}{\theta^{k}})},\forall k\in\mathcal{S}_2$$

$$C_{SIC}:\max_{\{P_{s,n}^{k}\}_{k\in\mathcal{S}_3}}\sum_{k\in\mathcal{S}_3}R_{s,n}^{k,SIC}-\mu_{s,n}\sum_{k\in\mathcal{S}_3}P_{s,n}^{k} \tag{4.43b}$$

$$P_{s,n}^{k}\leqslant\frac{I_{th}^{k}}{\lambda_{ps}^{k}\log(\frac{1}{\theta^{k}})},\forall k\in\mathcal{S}_3$$

$$E^{k}P_{s,n}^{k}\geqslant F^{k},\forall k\in\mathcal{S}_3$$

$$C_{SC}:\max_{\{P_{s,n}^{k}\}_{k\in\mathcal{S}_4}}\sum_{k\in\mathcal{S}_4}R_{s,n}^{k,SC}-\mu_{s,n}\sum_{k\in\mathcal{S}_4}P_{s,n}^{k} \tag{4.43c}$$

$$P_{s,n}^{k}\leqslant\frac{I_{th}^{k}}{\lambda_{ps}^{k}\log(\frac{1}{\theta^{k}})},\forall k\in\mathcal{S}_4$$

$$G^{k}P_{s,n}^{k}>H^{k},\forall k\in\mathcal{S}_4$$

$$E^{k}P_{s,n}^{k}\leqslant J^{k},\forall k\in\mathcal{S}_4$$

where the subtracted term in the objective function represents the total power constraint which is common to all subproblems. Problem (4.43) reformulates the aforementioned problem introducing the results obtained in the previous section. In this section we proceed to the resolution of three subproblems in order to find a general solution for problem (4.43). Note that the Lagrange dual function associated with (4.43) can be defined as

$$g(\lambda)=\max_{\mathbf{p}_{s,n}}\mathbb{L}\left(P_{s,n}^{k},\lambda\right)-\lambda\left(\sum_{k=1}^{L}P_{s,n}^{k}-P_{s,\max}\right) \tag{4.44}$$

where $p_{s,n}$ is constant.

The subproblem when interference is treated as noise can be formulated as C_{int} :

$$\begin{aligned} &\max_{\{P_{s,n}^k\}_{k\in\mathcal{S}_2}} \sum_{k\in\mathcal{S}_2} R_{s,n}^{k,int} - \mu_{s,n} \sum_{k\in\mathcal{S}_2} P_{s,n}^k \\ &P_{s,n}^k \leqslant \frac{I_{th}^k}{\lambda_{ps}^k \log(\frac{1}{\theta^k})}, \forall k \in \mathcal{S}_2 \\ &P_{s,n}^k \geqslant 0, \forall k \in \mathcal{S}_2 \end{aligned} \tag{4.45}$$

To solve subproblem C_{int}, let us define the unconstrained subproblem

$$\hat{C}_{int} : \max_{\{P_{s,n}^k\}_{k\in\mathcal{S}_2}} \sum_{k\in\mathcal{S}_2} R_{s,n}^{k,int} - \mu_{s,n} \sum_{k\in\mathcal{S}_2} P_{s,n}^k$$

with Lagrangian

$$\hat{\mathbb{L}}_{int}\left(P_{s,n}^k, \mu_{s,n}\right) = -\sum_{k\in\mathcal{S}_2} R_{s,n}^{k,int} + \mu_{s,n} \sum_{k\in\mathcal{S}_2} P_{s,n}^k$$

Let $\hat{f}_{int}$ be the partial derivative of $\hat{\mathbb{L}}_{int}$ with respect to $P_{s,n}^k$.

$$\hat{f}\left(P_{s,n}^k, \mu_{s,n}\right) = -\frac{|h_{ss}^k|^2}{|h_{sp}^k|^2 P_{p,n-1}^k + n_0} + \mu_{s,n} = 0$$

Thus, the solution of subproblem $\hat{C}_{int}$ can be given by

$$\hat{P}_{s,n}^{k,int} = \left[\frac{1}{\mu_{s,n}} - \frac{|h_{sp}^k|^2 P_{p,n-1}^k + n_0}{|h_{ss}^k|^2}\right]^+$$

Taking into consideration the constraint of subproblem C_{int}, its general solution $P_{s,n}^{k,int}$ has to be

$$P_{s,n}^{k,int} = \min\left\{\hat{P}_{s,n}^{k,int}, \frac{I_{th}^k}{\lambda_{ps}^k \log(\frac{1}{\theta^k})}\right\}$$

When SIC is applied, the optimization subproblem is formulated as C_{SIC} :

$$\begin{aligned} &\max_{\{P_{s,n}^k\}_{k\in\mathcal{S}_3}} \sum_{k\in\mathcal{S}_3} R_{s,n}^{k,SIC} - \mu_{s,n} \sum_{k\in\mathcal{S}_3} P_{s,n}^k \\ &P_{s,n}^k \leqslant \frac{I_{th}^k}{\lambda_{ps}^k \log(\frac{1}{\theta^k})}, \forall k \in \mathcal{S}_3 \\ &E^k P_{s,n}^k \geqslant F^k, \forall k \in \mathcal{S}_3 \\ &P_{s,n}^k \geqslant 0 \end{aligned} \tag{4.46}$$

To solve subproblem C_{SIC}, let us define the unconstrained subproblem

$$\hat{C}_{SIC}: \max_{\{P_{s,n}^k\}_{k\in\mathcal{S}_3}} \sum_{k\in\mathcal{S}_3} R_{s,n}^{k,SIC} - \mu_{s,n} \sum_{k\in\mathcal{S}_3} P_{s,n}^k$$

with Lagrangian

$$\hat{\mathbb{L}}_{SIC}\left(P_{s,n}^k, \mu_{s,n}\right) = -\sum_{k\in\mathcal{S}_3} R_{s,n}^{k,SIC} + \mu_{s,n} \sum_{k\in\mathcal{S}_3} P_{s,n}^k$$

Let $\hat{f}_{SIC}$ be the partial derivative of $\hat{\mathbb{L}}_{SIC}$ with respect to $P_{s,n}^k$.

$$\hat{f}_{SIC}\left(P_{s,n}^k, \mu_{s,n}\right) = -\frac{|h_{ss}^k|^2}{|h_{ss}^k|^2 P_{s,n}^k + n_0} + \mu_{s,n} = 0$$

Thus, the solution of subproblem $\hat{C}_{SIC}$ can be given by

$$\hat{P}_{s,n}^{k,SIC} = \left[\frac{1}{\mu_{s,n}} - \frac{n_0}{|h_{ss}^k|^2}\right]^+$$

Taking into consideration the constraint of subproblem C_{SIC}, its general solution $P_{s,n}^{k,SIC}$ has to meet the conditions in Table 4.1

		E^k	
		Positive	Negative
F^k	Positive	$P_{s,n}^{k,SIC} > \frac{E^k}{F^k}$	Impossible
	Negative	No constraint	$P_{s,n}^{k,SIC} < \frac{E^k}{F^k}$

TABLE 4.1 – SIC Conditions

When SC is applied, the optimization subproblem is C_{SC} :

$$\begin{aligned}
&\max_{\{P_{s,n}^k\}_{k\in\mathcal{S}_4}} \sum_{k\in\mathcal{S}_4} R_{s,n}^{k,SC} - \mu_{s,n} \sum_{k\in\mathcal{S}_4} P_{s,n}^k \qquad (4.47)\\
&P_{s,n}^k \leqslant \frac{I_{th}^k}{\lambda_{ps}^k \log(\frac{1}{\theta^k})}, \forall k \in \mathcal{S}_4\\
&G^k P_{s,n}^k > H^k, \forall k \in \mathcal{S}_4\\
&E^k P_{s,n}^k \leqslant J^k, \forall k \in \mathcal{S}_4\\
&P_{s,n}^k \geqslant 0
\end{aligned}$$

To solve subproblem C_{SC}, let us define the unconstrained subproblem

$$\hat{C}_{SC}: \max_{\{P_{s,n}^k\}_{k\in\mathcal{S}_4}} \sum_{k\in\mathcal{S}_4} R_{s,n}^{k,SC} - \mu_{s,n} \sum_{k\in\mathcal{S}_4} P_{s,n}^k$$

with Lagrangian

$$\hat{\mathbb{L}}_{SC}\left(P_{s,n}^k, \mu_{s,n}\right) = -\sum_{k\in\mathcal{S}_4} R_{s,n}^{k,SC} + \mu_{s,n} \sum_{k\in\mathcal{S}_4} P_{s,n}^k$$

Let $\hat{f}_{SC}$ be the partial derivative of $\hat{\mathbb{L}}_{SC}$ with respect to $P_{s,n}^k$.

$$\hat{f}_{SC}\left(P_{s,n}^k, \mu_{s,n}\right) = -\frac{\lambda_{ps}^k}{\lambda_{ps}^k P_{s,n}^k + n_0} + B_n^k\left(\overline{P_{s,n}^k}\right) + \mu_{s,n} = 0$$

Thus, the solution of subproblem $\hat{C}_{SC}$ can be given by

$$\hat{P}_{s,n}^{k,SC} = \frac{1}{\mu_{s,n} + B_n^k\left(\overline{P_{s,n}^k}\right)} - \frac{n_0}{\lambda_{ps}^k}$$

which can be written as

$$\hat{P}_{s,n}^{k,SC} = \frac{1}{\hat{\mu}_{s,n}} - \frac{n_0}{\lambda_{ps}^k}$$

with

$$\hat{\mu}_{s,n} = \mu_{s,n} + B_n^k\left(\overline{P_{s,n}^k}\right)$$

Taking into consideration the constraint of subproblem C_{SC}, its general solution $P_{s,n}^{k,SC}$ has to meet the conditions in Tables 4.2 and 4.3

		E^k	
		Positive	Negative
J^k	Positive	$P_{s,n}^{k,SC} \leqslant \frac{J^k}{E^k}$	No constraint
	Negative	Impossible	$P_{s,n}^{k,SC} \geqslant \frac{J^k}{E^k}$

TABLE 4.2 – Conditions from constraint (4.25f)

Consequently, the general solution of problem (4.25) can be given by Table 4.4

		G^k	
		Positive	Negative
H^k	Positive	$P_{s,n}^{k,SC} > \frac{H^k}{G^k}$	Impossible
	Negative	No constraint	$P_{s,n}^{k,SC} < \frac{H^k}{G^k}$

TABLE 4.3 – Conditions from constraint (4.25g)

TABLE 4.4 – Optimized values of $P_{s,n}^k$

Conditions	Decoding strategies	$P_{s,n}^k$
$P_{p,(n-1)}^k = 0$	Interweave	$\left[\frac{1}{\mu_{s,n}} - \frac{1}{b_{s,(n-1)}^k}\right]^+$
$P_{p,(n-1)}^k \neq 0$	Int = Noise	$\min\left\{\left[\frac{1}{\mu_{s,n}} - \frac{1}{b_{s,(n-1)}^k}\right]^+ ; \frac{I_{th}^k}{\lambda_{ps}^k \log(\frac{1}{\theta^k})}\right\}$
$P_{p,(n-1)}^k \neq 0$ $\{E^k < 0; F^k > 0\}$	SIC	0
$P_{p,(n-1)}^k \neq 0$ $\{E^k > 0; F^k < 0\}$	SIC	$\min\left\{\left[\frac{1}{\mu_{s,n}} - \frac{1}{b_{s,(n-1)}^k}\right]^+ ; \frac{I_{th}^k}{\lambda_{ps}^k \log(\frac{1}{\theta^k})}\right\}$
$P_{p,(n-1)}^k \neq 0$ $\{E^k < 0; F^k < 0\}$	SIC	$\min\left\{\left[\frac{1}{\mu_{s,n}} - \frac{1}{b_{s,(n-1)}^k}\right]^+ ; \frac{I_{th}^k}{\lambda_{ps}^k \log(\frac{1}{\theta^k})}; \frac{F^k}{E^k}\right\}$
$P_{p,(n-1)}^k \neq 0$ $\{E^k > 0; F^k > 0\}$	SIC if $\frac{F^k}{E^k} \leqslant \frac{I_{th}^k}{\lambda_{ps}^k \log(\frac{1}{\theta^k})}$ otherwise	$\max\left\{\min\left\{\left[\frac{1}{\mu_{s,n}} - \frac{1}{b_{s,(n-1)}^k}\right]^+ ; \frac{I_{th}^k}{\lambda_{ps}^k \log(\frac{1}{\theta^k})}\right\} ; \frac{E^k}{F^k}\right\}$ 0
$P_{p,(n-1)}^k \neq 0$ $\{G^k < 0; H^k > 0\}$ or $\{E^k > 0; J^k < 0\}$	SC	0
$P_{p,(n-1)}^k \neq 0$ $\{G^k > 0; H^k > 0\}$ and $\{E^k > 0; J^k > 0\}$	SC	$\max\left\{\min\left\{\left[\frac{1}{\hat{\mu}_{s,n}} - \frac{1}{b_{s,(n-1)}^k}\right]^+ ; \frac{I_{th}^k}{\lambda_{ps}^k \log(\frac{1}{\theta^k})}; \frac{J^k}{E^k}\right\} ; \frac{H^k}{G^k}\right\}$
$P_{p,(n-1)}^k \neq 0$ $\{G^k > 0; H^k > 0\}$ and $\{E^k < 0; J^k > 0\}$	SC	$\max\left\{\min\left\{\left[\frac{1}{\hat{\mu}_{s,n}} - \frac{1}{b_{s,(n-1)}^k}\right]^+ ; \frac{I_{th}^k}{\lambda_{ps}^k \log(\frac{1}{\theta^k})}\right\} ; \frac{H^k}{G^k}\right\}$

$P^k_{p,(n-1)} \neq 0$ $\{G^k > 0; H^k > 0\}$ and $\{E^k < 0; J^k < 0\}$	SC	$\max\left\{\min\left\{\left[\frac{1}{\hat{\mu}_{s,n}} - \frac{1}{b^k_{s,(n-1)}}\right]^+; \frac{I^k_{th}}{\lambda^k_{ps}\log(\frac{1}{\theta^k})}\right\}; \frac{H^k}{G^k}; \frac{J^k}{E^k}\right\}$
$P^k_{p,(n-1)} \neq 0$ $\{G^k > 0; H^k < 0\}$ and $\{E^k > 0; J^k > 0\}$	SC	$\min\left\{\left[\frac{1}{\hat{\mu}_{s,n}} - \frac{1}{b^k_{s,(n-1)}}\right]^+; \frac{I^k_{th}}{\lambda^k_{ps}\log(\frac{1}{\theta^k})}; \frac{J^k}{E^k}\right\}$
$P^k_{p,(n-1)} \neq 0$ $\{G^k > 0; H^k < 0\}$ and $\{E^k < 0; J^k > 0\}$	SC	$\min\left\{\left[\frac{1}{\hat{\mu}_{s,n}} - \frac{1}{b^k_{s,(n-1)}}\right]^+; \frac{I^k_{th}}{\lambda^k_{ps}\log(\frac{1}{\theta^k})}\right\}$
$P^k_{p,(n-1)} \neq 0$ $\{G^k > 0; H^k < 0\}$ and $\{E^k < 0; J^k < 0\}$	SC	$\max\left\{\min\left\{\left[\frac{1}{\hat{\mu}_{s,n}} - \frac{1}{b^k_{s,(n-1)}}\right]^+; \frac{I^k_{th}}{\lambda^k_{ps}\log(\frac{1}{\theta^k})}\right\}; \frac{J^k}{E^k}\right\}$
$P^k_{p,(n-1)} \neq 0$ $\{G^k < 0; H^k < 0\}$ and $\{E^k > 0; J^k > 0\}$	SC	$\min\left\{\left[\frac{1}{\hat{\mu}_{s,n}} - \frac{1}{b^k_{s,(n-1)}}\right]^+; \frac{I^k_{th}}{\lambda^k_{ps}\log(\frac{1}{\theta^k})}; \frac{J^k}{E^k}; \frac{H^k}{G^k}\right\}$
$P^k_{p,(n-1)} \neq 0$ $\{G^k < 0; H^k < 0\}$ and $\{E^k > 0; J^k > 0\}$	SC	$\min\left\{\left[\frac{1}{\hat{\mu}_{s,n}} - \frac{1}{b^k_{s,(n-1)}}\right]^+; \frac{I^k_{th}}{\lambda^k_{ps}\log(\frac{1}{\theta^k})}; \frac{H^k}{G^k}\right\}$
$P^k_{p,(n-1)} \neq 0$ $\{G^k < 0; H^k < 0\}$ and $\{E^k < 0; J^k < 0\}$	SC	$\max\left\{\min\left\{\left[\frac{1}{\hat{\mu}_{s,n}} - \frac{1}{b^k_{s,(n-1)}}\right]^+; \frac{I^k_{th}}{\lambda^k_{ps}\log(\frac{1}{\theta^k})}; \frac{H^k}{G^k}\right\}; \frac{J^k}{E^k}\right\}$

TABLE 4.5 – Values of coefficient $b^k_{s,(n-1)}$ in Table 4.4

Cases	$b^k_{s,(n-1)}$
$P^k_{p,(n-1)} = 0$	$\frac{\left\|h^k_{ss}\right\|^2}{n_0}$
$P^k_{p,(n-1)} \neq 0$ and $\left\|h^k_{sp}\right\|^2 \leqslant \left\|h^k_{ss}\right\|^2$	$\frac{\left\|h^k_{ss}\right\|^2}{\left\|h^k_{sp}\right\|^2 P^k_{p,(n-1)} + n_0}$
$P^k_{p,(n-1)} \neq 0$ and $\left\|h^k_{sp}\right\|^2 > \left\|h^k_{ss}\right\|^2$ (SIC)	$\frac{\left\|h^k_{ss}\right\|^2}{n_0}$
$P^k_{p,(n-1)} \neq 0$ and $\left\|h^k_{sp}\right\|^2 > \left\|h^k_{ss}\right\|^2$ (SC)	$\frac{\lambda^k_{ps}}{n_0}$

Consequently, we have got $g(\lambda)$ for a given λ. Then, we can solve the dual problem which

aims to minimize $g(\lambda)$

$$\min_{\lambda} g(\lambda) \qquad (4.48)$$
$$\text{s.t.} \lambda \geqslant 0$$

4.7 Solving the optimization problem by bisection

Another method to solve problem (4.25) is to use the bisection method. The Lagrangian of problem (4.25) is

$$\mathbb{L}(P_{s,n}^k, \eta^k, \vartheta^k, \kappa^k, \xi^k, \Delta) = -\tilde{R}_{s,n} + \sum_{k=1}^{L} \eta^k \left[P_s^k - \frac{I_{th}^k}{\lambda_{ps}^k \log(\frac{1}{\theta^k})} \right] + \Delta \left[\sum_{k=1}^{L} P_s^k - P_{s,\max} \right]$$
$$+ \sum_{k=1}^{L} \rho^k \vartheta^k \left[F^k - F^k P_{s,n}^k \right] + \sum_{k=1}^{L} \iota^k \kappa^k \left[P_{s,n}^k \left(E^k - G^k \right) + H^k - J^k \right] \qquad (4.49)$$

where η^k, ϑ^k, κ^k, ξ^k, and Δ are the Lagrange multipliers, $\rho^k = 1$ if $k \in \mathcal{S}_3$ and zero otherwise, and $\iota^k = 1$ if $k \in \mathcal{S}_4$ and zero otherwise. $\tilde{R}_{s,n}$ denotes the secondary achievable rate at iteration n, calculated with the new value of α^k given in eq.

Let f be the partial derivative of $\mathbb{L}$ with respect to P_s^k.

$$f(P_{s,n}^k, \eta^k, \vartheta^k, \kappa^k, \xi^k, \pi^k, \Delta) = -\frac{B}{L} \frac{q_{s,n}^k}{1 + q_{s,n}^k P_{s,n}^k} + \eta^k + \Delta$$
$$+ \rho^k \vartheta^k \left(\frac{|h_{sp}^k|^2 |h_{ss}^k|^2}{\lambda_{pp}^k n_0 \left(1 + \frac{|h_{ss}^k|^2}{n_0} \overline{P_{s,n}^k} \right)^2} - \frac{\lambda_{pp}^k \lambda_{ps}^k |h_{sp}^k|^2 n_0}{(\lambda_{pp}^k)^2 (n_0 + |h_{ss}^k|^2 P_{s,n}^k)^2} \right)$$
$$- \iota^k \kappa^k \left(\frac{n_0 \lambda_{pp}^k |h_{sp}^k|^2 |h_{ss}^k|^2}{{\lambda_{pp}^k}^2 \left(n_0 + |h_{ss}^k|^2 P_{s,n}^k \right)^2} + \frac{\lambda_{pp}^k |h_{ss}^k|^2}{\lambda_{pp}^k \left(|h_{ss}^k|^2 P_{s,n}^k + n_0 \right)} + \frac{\lambda_{ps}^k |h_{sp}^k|^2 + \lambda_{pp}^k |h_{ss}^k|^2}{\left(\lambda_{ps}^k |h_{sp}^k|^2 + \lambda_{pp}^k |h_{ss}^k|^2 \right) \overline{P_{s,n}^k} + \lambda_{pp}^k n_0} \right)$$
$$- \iota^k \xi^k \frac{|h_{sp}^k|^2 \lambda_{ps}^k}{|h_{sp}^k|^2 \lambda_{ps}^k P_{s,n}^k + n_0} \qquad (4.50)$$

with

$$q_{s,n}^k = \begin{cases} \frac{|h_{ss}^k|^2}{n_0} & \text{if } k \in \mathcal{S}_1 \cup \mathcal{S}_3 \\ \frac{|h_{ss}^k|^2}{|h_{sp}^k|^2 P_{p,n-1}^k + n_0} & \text{if } k \in \mathcal{S}_2 \\ 0 & \text{otherwise} \end{cases} \qquad (4.51)$$

We can prove that $\frac{\partial f}{\partial P_{s,n}^k} > 0$. The function f is then strictly varying in $P_{s,n}^k$ and we can find the solution of $f(P_{s,n}^k)$ using the bisection approach [64].

4.8 Sequential convex approximation algorithm

Previously, we proposed an approximation method to transform the optimization problem in (4.25) into a convex problem. To improve the restrictive approximation, we propose a sequential algorithm where the optimization problem (4.25) is approximated using the optimal solution obtained at the previous iteration using either dual decomposition or bisection method. The proposed algorithm is summarized in Algorithm 4, where at the m^{th} iteration, $\mathbf{p}_{s,m} = (P^1_{s,m}, \ldots, P^L_{s,m})^T$.

Algorithm 4 Sequential Convex Approximation Algorithm

1: **Input** θ^k, ϵ^k, δ^k, $\gamma^k > 0$, $m = 0$, and a feasible point $\overline{\mathbf{p}_{s,0}}$ for problem (4.25) ;
2: **Repeat**
3: $m = m + 1$
4: Solve (4.25) using bisection method to obtain $\mathbf{p}_{s,m}$;
5: Set $\overline{\mathbf{p}_{s,m}} = \mathbf{p}_{s,m}$;
6: **Until** $\frac{|\sum_k R^k_{s,m}| - |\sum_k R^k_{s,m-1}|}{|\sum_k R^k_{s,m-1}|} < \sigma$;
7: **Output** $\mathbf{p}_{s,m}$.

Once $\mathbf{p}_s$ is computed for a given $\mathbf{p}_p$ using bisection method, an iterative process is applied to switch between the primary and secondary users in order to optimally allocate both of them taking into account the total power constraint of each user and the interference limit allowed on the primary receiver. Let N be the maximum number of iterations needed by the sequential algorithm to converge and M the maximum number of iterations for the bisection method with complexity $\mathcal{O}(M)$. Thus, the complexity of Algorithm 4 is $\mathcal{O}(NLM)$. On the other hand, the complexity of waterfilling which is applied on the primary user is calculated as $\mathcal{O}(L \log_2 L)$.

4.9 Simulation results with statistical CSI

The performance of the proposed algorithm with statistical CSI is assessed using Monte-Carlo simulations, where the mobiles positions follow a uniform distribution. We use the same parameters as in chapter 3. All outage limits θ^k, ϵ^k, δ^k and γ^k are equal to 0.01.

First of all, we evaluate the performance of our proposed algorithm by comparing it with the classical power allocation scheme where the secondary system can transmit on the whole bandwidth of a cognitive underlay system by considering the primary system's interference as noise in all subcarriers. In this case, only interference outage is considered. This algorithm is denoted by 'FB' for 'Full Band'. Simulation results in figures 4.1 and 4.2 demonstrate that our algorithm outperforms 'FB' for small distances between the BSs.

In figure 4.1, we also compare the secondary achievable rate using statistical CSI with the achievable rate when full CSI is available at the secondary transmitter. While in figure 4.2, sum rates are compared in both full and statistical CSI scenarios. Due to the lack of perfect CSI on the primary channels, rigorous outage limits are imposed on the outage probabilities which

leads to strict constraints and thus results in a degradation of the secondary rate and thus in the sum rate.

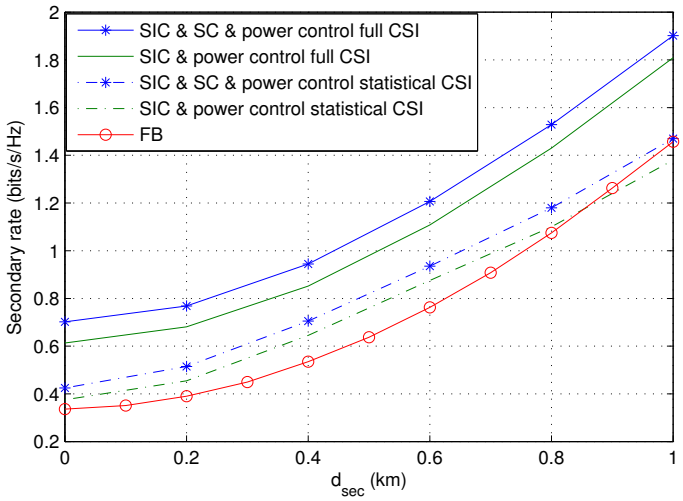

FIGURE 4.1 – Secondary rates with statistical CSI

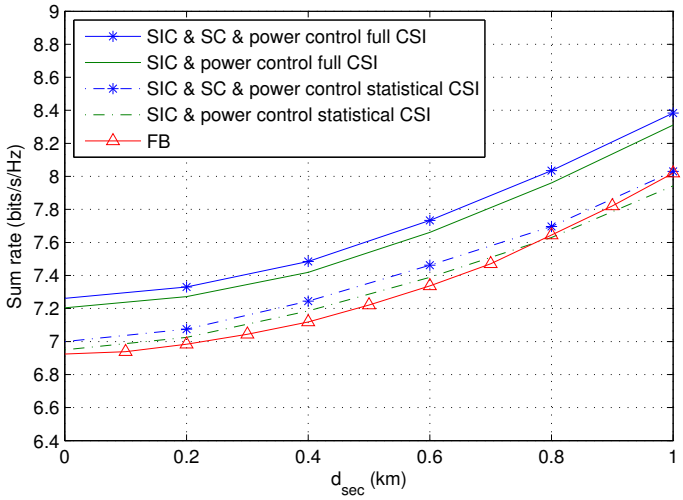

FIGURE 4.2 – Sum rates with statistical CSI

To study the influence of outage limits on the secondary achievable rate, we present in Figure 4.3 the performance in terms of achievable rate versus ϵ^k and θ^k for a fixed d_{sec}= 0.4 km. The dashed line represents the secondary achievable rate at this distance with full CSI. The first curve labeled as ϵ^k is obtained for a fixed θ^k=1% while varying ϵ^k. The second curve represents the variation of the secondary rate versus θ^k for ϵ^k fixed at 1%. Figure 4.3 establishes that the secondary achievable rate with statistical CSI approaches from the secondary achievable rate with full CSI when ϵ^k and θ^k increase. We can also observe that the SIC outage limit has a greater effect on the secondary rate degradation than the interference outage limit.

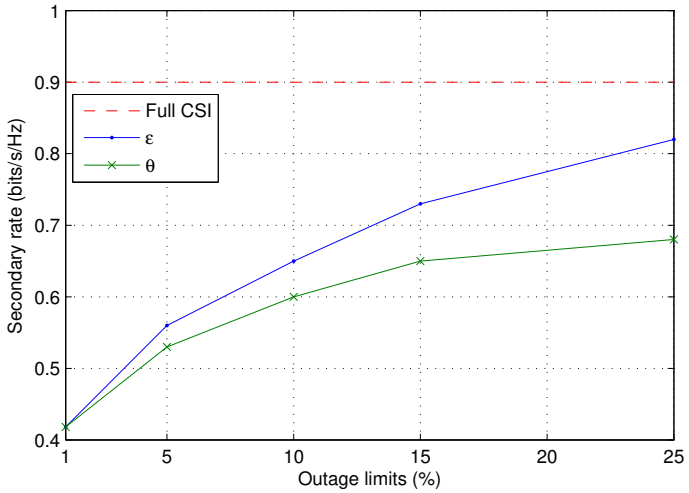

FIGURE 4.3 – Achievable secondary rate depending on the outage limits at $d_{sec} = 0.4$ km

4.10 Conclusion

In this chapter, we proposed a resource allocation algorithm for a single-user CR system where only statistical CSI about primary links is available at the SU. In a first step, the outage probabilities for different optimization problem constraints are calculated. A non-convex optimization problem is obtained. Then, the first Taylor approximation is applied on non convex constraints and non concave objective functions in order to turn the optimization problem into a convex problem. The approximated problem is the investigated using both dual decomposition and SCA methods. Simulation results showed that the proposed algorithm is efficient and robust. In the next chapter, the studied system model will be extended to a CR relay network, where the secondary BS can serve as a relay node in order to maximize the primary's rate.

Chapitre 5

CR system with Relay at the secondary BS

5.1 Introduction

In the previous two chapters, we proposed an adaptive decoding algorithm at the SU aiming at maximizing the secondary achievable rate. However, this latter represents a small portion of the total system rate. Consequently, we propose a new relay-assisted CR system model where the secondary BS serves as a Full-Duplex (FD) relay node in order to boost the primary transmission and thus to maximize the primary rate. In this chapter, we firstly give an overview of different possible relay schemes and protocols. Then, we focus on FD relay scheme and detail the achievable rate expressions in single-carrier for both Amplify-and-Forward (AF) and Decode-and-Forward (DF) relaying protocols. Finally, we investigate the multi-carrier case for the FD DF relay node.

The remaining of this chapter is organized as follows. In Section 5.2, we depict the scenarios and solutions proposed in the literature for relay-assisted systems. Moreover, in Section 5.3, we describe the possible system model with AF and DF. In Section 5.4 we determine the achievable rates at both primary and secondary users when AF protocol is considered at the relay node. The same approach is presented in Section 5.5 for DF relaying protocol. In Section 5.6, we describe the power optimization problem at both primary and secondary users in the multi-carrier case. Finally, in order to draw a clear baseline reference for the performance of the simulation model, we conduct some basic simulations and show the results in Section 5.7.

5.2 State of the art

There are many scenarios for the interference channel with relay, with or without cognitive nodes. In [119], the authors investigate an interference relay channel, where the relay is viewed as a cognitive transmitter helping two independent source-destination pairs. The obtained results are mainly applicable when the underlying interference channel has weak interference for which only private information should be transmitted. The authors assume that the sources do not cooperate, then it is not possible to remove all the interference at the destinations. For that, the results of this paper point out the benefits of beamforming, interference cancellation and generalized dirty paper coding at the relay to improve the achievable rates pairs. The same scenario was studied in [120], where each transmitter has access to only its respective message. The authors present a new achievable region for the G-IFC with a cognitive relay, which is a generalization of the region given in [119], assuming that there is a cognitive relay node which has non-causal access to the messages of both the transmitters. This relay node serves only to assist the two transmitters in communicating their messages to their respective receivers. Dirty paper coding was used in this paper instead of time sharing between the users as was done in [119]. In [121], the authors introduce two types of relaying : forward the desired message to the intended destination, or forward the unwanted message by a relay so that the receiver can decode this message and eliminate interference, and then improve its own rate. Afterward, they evaluate the gains from forwarding unwanted messages, calling this scenario the 'Interference Forwarding'. In the same way, the authors in [122] detail two scenarios of relaying, called signal relaying when the desired message is forwarded, and interference forwarding in the other case. The paper presents also the in-band relay reception/transmission where the relay receives and transmits simultaneously in the same band where the sources communicate with the destinations, and the out-of-band relay reception/in-band relay transmission, where the relay receives the source signals over links that are orthogonal to each other and to the underlying interference channel. The authors focus on the first transmission model, pointing out the benefits of both scenarios of relaying. In [123], the authors evaluates the benefits of the FD mode, and shows that it can achieve better performance in terms of capacity and outperform Half-Duplex (HD) mode, even in the presence of self-interference. The authors consider two-way relay channels where two source nodes communicate with each other through the aid of a relay node, using an AF protocol over different time slots. In [124], the resource allocation problem is investigated for CR networks with relay stations where the secondary receiver can either receive data directly from the transmitter or through the help of the CR relay stations. Proportional fair scheduling is considered and different scenarios are studied depending on the transmit power. The authors in [125] consider both FD and HD Gaussian relay channels, by assuming that the noises at the relay and destination are arbitrarily correlated. The capacity upper bound as well as the achievable rates are derived for DF, AF and CF. In [126], the downlink resource allocation in an Long-Term Evolution (LTE)-Advanced cellular system with DF relay nodes is investigated. The FD relaying mode is considered and an optimal subcarrier and power allocation scheme is proposed. In [127], upper and lower bounds on the ergodic and outage capacities are studied for

a variety of wireless channel models.

Several papers consider the multi-carrier transmission with relays. In [128], the authors study an OFDM transmission with HD DF relay and investigate the problem of power allocation under both some and individual power constraints. In [109], the power allocation problem is formulated in order to maximize the sum-rate of CR users on Gaussian MAC assuming an outage constraint at the PU. Joint subcarrier pairing is considered in [129, 130].

In [131], the authors study the cooperative communication in a CR network by considering the relay assignment and channel allocation in order to maximize the transmission rate. In [132], the outage performance of a single-carrier FD relay channel is studied considering a FD protocol and taking the relay self-interference into account. An optimization method for an AF relay-assisted CR network with HD mode is developed in [100] in order to maximize the system capacity. Several constraints are considered as power budgets of the CR nodes and the interference limitations at the PU. In [133], the outage probability of a relay-assisted underlay system is evaluated. The single-carrier scenario is considered with different amounts of CSI.

5.3 System model

We consider a new uplink CR system model composed of one primary cell and one secondary cell, where the secondary BS is assumed to be working as a relay as it is represented in Fig. 5.1. A similar system model is proposed in [134, 135] for the single-carrier case, where the secondary transmitter acts as a relay node. However, neither SIC nor SC are applied at the SU. The same parameters of the system model described in Chapter 3 are used in this chapter. We denote by h_r the complex channel coefficient between the relay and the primary receiver and by P_r the relay transmitted power. We assume that both primary and secondary user, such as relay, have the same amount of power and that the noise variance at each node $n_i^k = n_0$ is the same on each subcarrier k. In a first step, we investigate the problem in the single-carrier case and then we process to the multi-carrier case resolving both subcarriers and power optimization problem.

The studied system model is given by Fig. 5.1 and its channel model is described in Fig. 5.2 where y_i is the channel output and x_i is the channel input for user i. We assume that the secondary BS is able to work as a FD relay node, where the received signal can be amplified or decoded and then relayed at the same time, with a negligible time delay. Thus, the primary receiver receives the initial signals and the signals relayed by the secondary BS at the same time as it is described in Section 2.7. In this case, the system model in subcarrier k when y_s^k relays is modeled as

$$y_p^k = h_{pp}^k x_p^k + h_{ps}^k x_s^k + h_r^k x_r^k + z_p^k \tag{5.1}$$

$$y_s^k = h_{sp}^k x_p^k + h_{ss}^k x_s^k + z_s^k \tag{5.2}$$

where x_r^k is the relay transmitted signal which depends on the relaying protocol (AF or DF) and will be defined later.

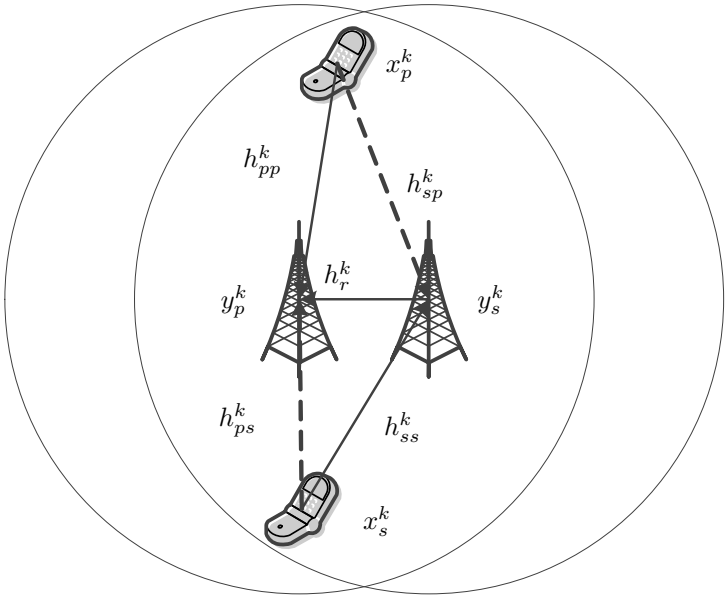

FIGURE 5.1 – Studied Scenario

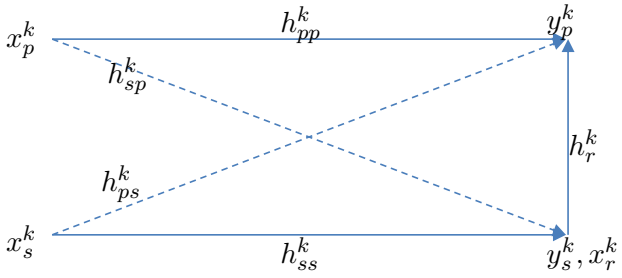

FIGURE 5.2 – CR Relay Channel Model

5.4 AF relaying protocol achievable rates

In this section, the secondary receiver is assumed to be working as an AF relay node. We detail both primary and secondary achievable rates applying this relaying protocol. For the sake of simplicity, we limit our study to two possible decoding strategies at the secondary receiver : treating the interference of the primary transmitter as noise or applying SIC by decoding the primary signal. This work can however be extended to the general dynamic decoding algorithm proposed in Chapter 3.

5.4.1 Primary achievable rate

The primary received signal is written as

$$y_p^k = h_{pp}^k x_p^k + h_{ps}^k x_s^k + h_r^k x_r^k + z_p^k \tag{5.3}$$

where x_r^k denotes the relayed signal and it is equal to $x_r^k = \beta_{AF}^k y_s^k$, where β_{AF}^k denotes the amplifier gain within subcarrier k defined by

$$\beta_{AF}^k = \sqrt{\frac{P_r^k}{|h_{sp}^k|^2 P_p^k + |h_{ss}^k|^2 P_s^k + n_0}} \tag{5.4}$$

Thus, the primary received signal can be written as

$$y_p^k = \left(h_{pp}^k + \beta_{AF}^k h_r^k h_{sp}^k\right) x_p^k + \left(h_{ps}^k + \beta_{AF}^k h_r^k h_{ss}^k\right) x_s^k + \beta_{AF}^k h_r^k z_r^k + z_p^k \tag{5.5}$$

Consequently, the primary rate in this scenario is calculated as

$$R_p^{k,AF} = \frac{B}{L} \log_2 \left(1 + \frac{|h_{pp}^k + \beta_{AF}^k h_r^k h_{sp}^k|^2 P_p^k}{|h_{ps}^k + \beta_{AF}^k h_r^k h_{ss}^k|^2 P_s^k + \beta_{AF}^k |h_r^k|^2 n_0 + n_0}\right) \tag{5.6}$$

The secondary receiver is supposed to be relaying whenever $R_p^{k,AF} > R_{p_{y_p}}^k$, with $R_{p_{y_p}}^k$ defined in eq. (3.4). If this conditions is not met, P_r^k is set to zero.

5.4.2 Secondary achievable rate

On the other hand, the secondary user can either treat the interference from the primary user as noise or apply SIC. In the latter case, a double test has to be done. Firstly, we verify if the secondary receiver is relaying or not. And then we proceed to the SIC condition detailed in Section 3.5. Consequently, four cases are studied :

1. If $R_p^{k,AF} > R_{p_{y_p}}^k$, i.e. if the secondary receiver relays, we have two possible cases.
   (a) If $R_{p_{y_p}}^k \leqslant R_{p_{y_s}}^k$, i.e. if $R_p^{k,AF} \leqslant R_{p_{y_s}}^k$, SIC can be applied. The condition to apply SIC can be written as

$$\frac{|h_{pp}^k + \beta_{AF}^k h_r^k h_{sp}^k|^2 P_p^k}{|h_{ps}^k + \beta_{AF}^k h_r^k h_{ss}^k|^2 P_s^k + \beta_{AF}^k |h_r^k|^2 n_0 + n_0} \leqslant \frac{|h_{sp}^k|^2 P_p^k}{|h_{ss}^k|^2 P_s^k + n_0} \tag{5.7}$$

In this case, the secondary achievable rate can be written as

$$R_s^k = \frac{B}{L}\log_2\left(1+\frac{|h_{ss}^k|^2 P_s^k}{n_0}\right) \tag{5.8}$$

(b) Otherwise, i.e. if $R_{p_{y_p}}^k > R_{p_{y_s}}^k$, the secondary receiver treats all interference it receives as noise. Consequently, the secondary achievable rate can be expressed by

$$R_s^k = \frac{B}{L}\log_2\left(1+\frac{|h_{ss}^k|^2 P_s^k}{|h_{sp}^k|^2 P_p^k + n_0}\right) \tag{5.9}$$

2. If $R_p^{k,AF} \leqslant R_{p_{y_p}}^k$, i.e. the secondary receiver does not relay, two cases are possible.

(a) If $R_{p_{y_p}}^k \leqslant R_{p_{y_s}}^k$, i.e. if $R_p^k \leqslant R_{p_{y_s}}^k$, SIC can be applied. The condition to apply SIC can be written as

$$\frac{|h_{pp}^k|^2 P_p^k}{|h_{ps}^k|^2 P_s^k n_0} \leqslant \frac{|h_{sp}^k|^2 P_p^k}{|h_{ss}^k|^2 P_s^k + n_0} \tag{5.10}$$

In this case, the secondary achievable rate is

$$R_s^k = \frac{B}{L}\log_2\left(1+\frac{|h_{ss}^k|^2 P_s^k}{n_0}\right) \tag{5.11}$$

(b) Otherwise, i.e. if $R_{p_{y_p}}^k > R_{p_{y_s}}^k$, the secondary receiver treats all interference it receives as noise. Consequently, the secondary achievable rate can be expressed by

$$R_s^k = \frac{B}{L}\log_2\left(1+\frac{|h_{ss}^k|^2 P_s^k}{|h_{sp}^k|^2 P_p^k + n_0}\right) \tag{5.12}$$

5.5 DF relaying protocol achievable rates

When the secondary receiver is applying the DF relaying protocol, the primary rate is given by [136]

$$R_p^{k,DF} = \max_{0\leqslant\gamma\leqslant 1} \min\left\{\frac{B}{L}\log_2\left(1+\frac{(1-\gamma)|h_{sp}^k|^2 P_p^k}{|h_{ss}^k|^2 P_s^k + n_0}\right), \frac{B}{L}\log_2\left(1+\frac{|h_{pp}^k|^2 P_p^k + |h_r^k|^2 P_r^k + 2\sqrt{\gamma|h_{pp}^k|^2 P_p^k |h_r^k|^2 P_r^k}}{|h_{ps}^k|^2 P_s^k + n_0}\right)\right\} \tag{5.13}$$

where γ is the correlation coefficient between the source and relay inputs. In the following, we assume that γ is null. This will be justified by simulations in Section 5.7.2. Thus, the primary achievable rate after DF relaying can be written as

$$R_p^{k,DF} = \min\left\{\frac{B}{L}\log_2\left(1+\frac{|h_{sp}^k|^2 P_p^k}{|h_{ss}^k|^2 P_s^k + n_0}\right), \frac{B}{L}\log_2\left(1+\frac{|h_{pp}^k|^2 P_p^k + |h_r^k|^2 P_r^k}{|h_{ps}^k|^2 P_s^k + n_0}\right)\right\} \tag{5.14}$$

As in the AF case, the secondary receiver relays only when $R_p^{k,DF} > R_{p,y_p}^k$, i.e.

$$\min\left\{\frac{B}{L}\log_2\left(1+\frac{|h_{sp}^k|^2P_p^k}{|h_{ss}^k|^2P_s^k+n_0}\right),\frac{B}{L}\log_2\left(1+\frac{|h_{pp}^k|^2P_p^k+|h_r^k|^2P_r^k}{|h_{ps}^k|^2P_s^k+n_0}\right)\right\}>\frac{B}{L}\log_2\left(1+\frac{|h_{pp}^k|^2P_p^k}{|h_{ps}^k|^2P_s^k+n_0}\right) \tag{5.15}$$

Then, if

$$\frac{|h_{sp}^k|^2P_p^k}{|h_{ss}^k|^2P_s^k+n_0}=\min\left\{\frac{|h_{sp}^k|^2P_p^k}{|h_{ss}^k|^2P_s^k+n_0},\frac{|h_{pp}^k|^2P_p^k+|h_r^k|^2P_r^k}{|h_{ps}^k|^2P_s^k+n_0}\right\} \tag{5.16}$$

the secondary receiver relays whenever

$$\frac{|h_{sp}^k|^2}{|h_{ss}^k|^2P_s^k+n_0}>\frac{|h_{pp}^k|^2}{|h_{ps}^k|^2P_s^k+n_0} \tag{5.17}$$

which means that the SIC condition given in (5.7) is always met in this case.

Otherwise, i.e. if

$$\frac{|h_{pp}^k|^2P_p^k+|h_r^k|^2P_r^k}{|h_{ps}^k|^2P_s^k+n_0}=\min\left\{\frac{|h_{sp}^k|^2P_p^k}{|h_{ss}^k|^2P_s^k+n_0},\frac{|h_{pp}^k|^2P_p^k+|h_r^k|^2P_r^k}{|h_{ps}^k|^2P_s^k+n_0}\right\} \tag{5.18}$$

the secondary receiver relays whenever

$$\frac{|h_{pp}^k|^2P_p^k+|h_r^k|^2P_r^k}{|h_{ps}^k|^2P_s^k+n_0}>\frac{|h_{pp}^k|^2P_p^k}{|h_{ps}^k|^2P_s^k+n_0} \tag{5.19}$$

which is always true if $P_r^k > 0$. From eq. (5.18) and (5.19), the SIC condition (5.7) always holds if the secondary receiver relays. Consequently, the secondary achievable rate when the secondary receiver acts as a DF relay node is given by eq. (5.11).

5.6 Power allocation procedure for multi-carrier DF relaying protocol

In this section, we present two power allocation methods for the multi-carrier case : EPA and Lagrange Multiplier methods.

5.6.1 Equal power allocation

We first assume that the power is equally allocated within subcarriers with $P_i^k = \frac{P_{i,\max}}{L}$, where $i = \{p, r\}$. For the SU, the interference threshold allowed at the primary receiver is taken into account and the per-carrier power is equal to $P_s^k = \min\{\frac{P_{s,\max}}{L}, \frac{I_{th}^k}{|h_{ps}^k|^2}\}$.

5.6.2 Power optimization

In this section, we aim to optimally allocate the transmit powers at primary and secondary transmitters as well as relay node within different subcarriers. Our algorithm is iterative and it is described at the n^{th} iteration as follows : Firstly, both primary transmitter and relay node optimize their transmit power vectors $\mathbf{p}_{p,n}$ and $\mathbf{p}_{r,n}$, respectively based on $\mathbf{p}_{s,n-1}$. The relay transmit power is optimized jointly with the primary transmit power since relaying is used in order to improve the primary rate. Similarly, the secondary system updates its power $\mathbf{p}_{s,n}$, based on $\mathbf{p}_{p,n-1}$ and $\mathbf{p}_{r,n-1}$.

Primary user

If the secondary receiver relays under DF relaying protocol in the FD mode, the power optimization problem for the PU can be written at the n^{th} iteration as

$$\begin{aligned}
&\max_{\mathbf{p}_{p,n},\mathbf{p}_{r,n}} \sum_{k=1}^{L} R_{p,n}^{k,DF} \\
&\text{s.t.} \sum_{k=1}^{L} P_{p,n}^{k} + \sum_{k=1}^{L} P_{r,n}^{k} = P_{\text{total}} \\
&\text{s.t.}\, P_{p,n}^{k} \geqslant 0 \,\forall k \\
&\text{s.t.}\, P_{r,n}^{k} \geqslant 0 \,\forall k
\end{aligned} \tag{5.20}$$

where P_{total} denotes the total maximum power to be optimized at both primary transmitter and relay node. $P_{\text{total}} = P_{p,max} + P_{r,max}$, with $P_{r,max}$ the maximum transmit power at the relay node. Moreover, the primary achievable rate with DF at iteration n is given by

$$R_{p,n}^{k,DF} = \min\left\{ \frac{B}{L}\log_2\left(1 + \frac{|h_{sp}^{k}|^2 P_{p,n}^{k}}{|h_{ss}^{k}|^2 P_{s,n-1}^{k} + n_0}\right), \frac{B}{L}\log_2\left(1 + \frac{|h_{pp}^{k}|^2 P_{p,n}^{k} + |h_{r}^{k}|^2 P_{r,n}^{k}}{|h_{ps}^{k}|^2 P_{s,n-1}^{k} + n_0}\right)\right\}$$

To solve this max-min optimization problem, let us define $\overline{R_n^k} = \min\left(R_{p,n,1}^{k,DF}, R_{p,n,2}^{k,DF}\right)$. The optimization problem can be written as

$$\max_{\mathbf{p}_{p,n},\mathbf{p}_{r,n},\overline{\mathbf{R}_n}} \sum_{k=1}^{L} \overline{R_n^k} \tag{5.21a}$$

$$\text{s.t.} \sum_{k=1}^{L} P_{p,n}^{k} + \sum_{k=1}^{L} P_{r,n}^{k} = P_{\text{total}} \tag{5.21b}$$

$$\text{s.t.}\, \overline{R_n^k} \leqslant R_{p,n,1}^{k,DF} \,\forall\, k \in \{1,\ldots,L\} \tag{5.21c}$$

$$\text{s.t.}\, \overline{R_n^k} \leqslant R_{p,n,2}^{k,DF} \,\forall\, k \in \{1,\ldots,L\} \tag{5.21d}$$

where $\overline{\mathbf{R}_n} = \left(\overline{R_n^1},\ldots,\overline{R_n^L}\right)$, $R_{p,n,1}^{k,DF} = \log_2\left(1 + A_{n-1}^{k} P_{p,n}^{k}\right)$, $R_{p,n,2}^{k,DF} = \log_2\left(1 + B_{n-1}^{k} P_{p,n}^{k} + C_{n-1}^{k} P_{r,n}^{k}\right)$,

and

$$A_{n-1}^{k} = \frac{|h_{sp}^{k}|^2}{|h_{ss}^{k}|^2 P_{s,n-1}^{k} + n_0}$$
$$B_{n-1}^{k} = \frac{|h_{pp}^{k}|^2}{|h_{ps}^{k}|^2 P_{s,n-1}^{k} + n_0}$$
$$C_{n-1}^{k} = \frac{|h_{r}^{k}|^2}{|h_{ps}^{k}|^2 P_{s,n-1}^{k} + n_0}$$

The Lagrangian of problem (4.3) can be written as

$$\mathbb{L}\left(P_{p,n}^{k}, P_{r,n}^{k}, \overline{R_n^k}, \lambda, \delta^k, \mu^k\right) = -\sum_{k=1}^{L} \overline{R_n^k} + \lambda\left[\sum_{k=1}^{L} P_{p,n}^{k} + \sum_{k=1}^{L} P_{r,n}^{k} - P_{\text{total}}\right] + \sum_{k=1}^{L} \delta^k \left(\overline{R_n^k} - R_{p,n,1}^{k,DF}\right) \tag{5.22}$$
$$+ \sum_{k=1}^{L} \mu^k \left(\overline{R_n^k} - R_{p,n,2}^{k,DF}\right)$$

where $\lambda, \delta^k, \mu^k \geqslant 0$ denote the Lagrange multipliers.

We calculate the partial derivative of the Lagrangian with respect to $P_{p,n}^{k}$, $P_{r,n}^{k}$ and $\overline{R_n^k}$, respectively.

$$\frac{\partial \mathbb{L}}{\partial P_{p,n}^{k}} = \lambda - \delta^k \frac{A_{n-1}^{k}}{1 + A_{n-1}^{k} P_{p,n}^{k}} - \mu^k \frac{B_{n-1}^{k}}{1 + B_{n-1}^{k} P_{p,n}^{k} + C_{n-1}^{k} P_{r,n}^{k}} = 0 \tag{5.23}$$
$$\frac{\partial \mathbb{L}}{\partial P_{r,n}^{k}} = \lambda - \mu^k \frac{C_{n-1}^{k}}{1 + B_{n-1}^{k} P_{p,n}^{k} + C_{n-1}^{k} P_{r,n}^{k}} = 0 \tag{5.24}$$
$$\frac{\partial \mathbb{L}}{\partial \overline{R_n^k}} = -1 + \delta^k + \mu^k = 0 \tag{5.25}$$

From these equations we get the analytical expressions of $P_{p,n}^{k}$ and $P_{r,n}^{k}$ in terms of the Lagrange multipliers. The primary transmit power is given by

$$P_{p,n}^{k} = \left[\frac{A_{n-1}^{k} C_{n-1}^{k} (1 - \mu^k)}{\lambda (C_{n-1}^{k} - B_{n-1}^{k})}\right]^{+} \tag{5.26}$$

and the relay power which is equal to

$$P_{r,n}^{k} = \left[\frac{\mu^k}{\lambda} - \frac{1 + B_{n-1}^{k} P_{p,n}^{k}}{C_{n-1}^{k}}\right]^{+} \tag{5.27}$$

can be written as

$$P_{r,n}^{k} = \left[\frac{\mu^k}{\lambda} - \frac{1}{C_{n-1}^{k}} - \frac{A_{n-1}^{k} B_{n-1}^{k} (1 - \mu^k)}{\lambda (C_{n-1}^{k} - B_{n-1}^{k})}\right]^{+} \tag{5.28}$$

The values of the Lagrange multipliers are found using the bisection method.

Secondary user

As it was said before, the secondary receiver always apply SIC when it acts as a DF relay node. Consequently, the power optimization problem for the SU can be given by

$$\max_{\mathbf{p}_{s,n}} \sum_{k=1}^{L} \log_2 \left(1 + \frac{|h_{ss}^k|^2 P_{s,n}^k}{n_0}\right) \tag{5.29a}$$

$$\text{s.t.} \sum_{k=1}^{L} P_{s,n}^k = P_{s,\max} \tag{5.29b}$$

$$\text{s.t. } P_{s,n}^k \geqslant 0 \, \forall \, k \in \{1, \ldots, L\} \tag{5.29c}$$

$$|h_{ps}^k|^2 P_{s,n}^k \leqslant I_{th}^k \, \forall \, k \in \{1, \ldots, L\} \tag{5.29d}$$

This problem can be solved using the Lagrangian method and the secondary power can be given by 3.2

$$P_{s,n}^k = \min \left\{ \left[\frac{1}{\nu^k} - \frac{n_0}{|h_{ss}^k|^2} \right]^+, \frac{I_{th}^k}{|h_{ps}^k|^2} \right\} \tag{5.30}$$

where ν^k represents the Lagrange multiplier.

5.7 Simulation results

The performance of the proposed algorithm is assessed using Monte-Carlo simulations for different schemes. The same parameters as in previous chapters are used. We assume that the total transmit power at each node $P_{p,max} = P_{s,max} = P_{r,max} = 21$ dBm and that the maximum constraint power for problem is equal to $P_{\text{total}} = 24$ dBm. First of all, we consider the single-carrier case, i.e. $L = 1$. In this case, different scenarios are studied.

5.7.1 AF in the single-carrier scenario

In this scenario, the positions of mobiles and BSs are chosen randomly and the system rates are studied according to d_{sec}, the distance between the primary and secondary BSs. Simulations results given in Figures 5.3, 5.4 and 5.5 highlight the improvement provided by the relay on the primary and total rates. The curve denoted by 'without relay' means that the secondary receiver is not allowed to relay and that it treats the interference of the primary as noise. Furthermore, 'SIC' indicates that SIC is applied at the secondary receiver and 'SIC & AF' means that the secondary receiver applies SIC and relays at the same time. Finally, we denote by 'AF' the cases where only relaying is active while SIC cannot be applied at the secondary receiver.

We can notice that the percentage of applying SIC decreases when the secondary receiver is relaying, since the condition to apply SIC is not always met due to the constraint we impose at the relay ($R_p^{k,AF} > R_{p_{y_p}}^k$). This results in a small degradation of the secondary rate.

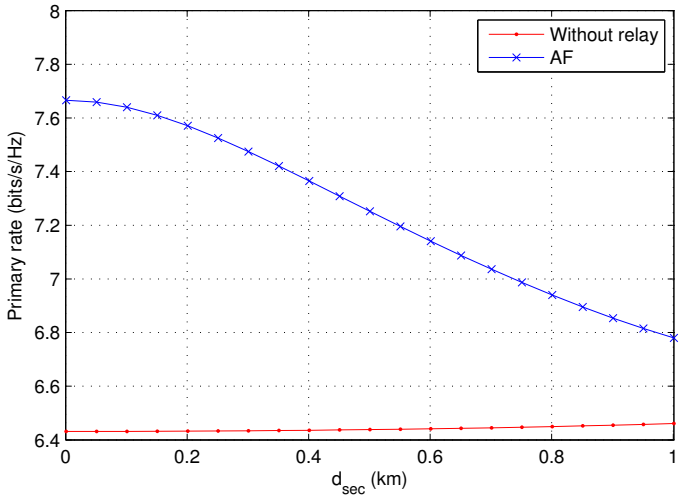

FIGURE 5.3 – Primary rate with AF relaying protocol in terms of d_{sec}

In Fig. 5.3, the primary rate without relay is compared to the primary rate when AF relaying protocol is used. An improvement of [5%, 19%] is shown, and it increases when the d_{sec} decreases.

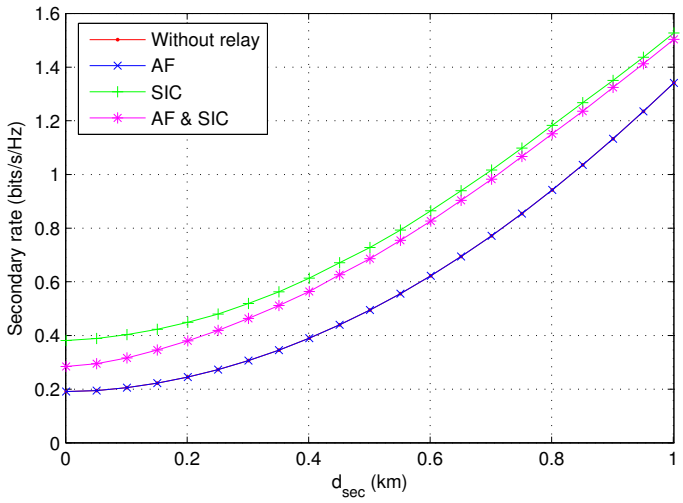

FIGURE 5.4 – Secondary rate with AF relaying protocol in terms of d_{sec}

In Fig. 5.4, we compare the secondary achievable rate for different scenarios. Without applying SIC, relaying has no impact on the secondary achievable rate, however simulations show that the probability of applying SIC at the secondary decreases when the secondary receiver relays because condition (5.7) is harder to fulfill than condition (5.10).

In Fig. 5.5, the total system rates are compared. Without applying SIC at the secondary receiver, an improvement that lies between 4.48% and 18.9% is obtained on the total rate. When SIC is applied, the total system rate increases between 3.75% and 16.9%.

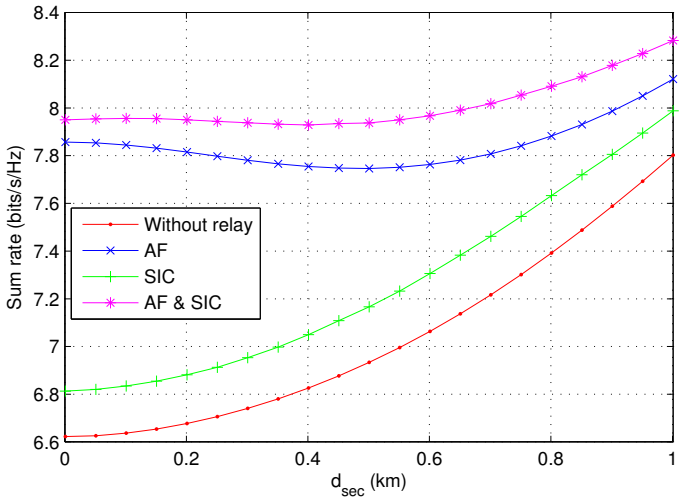

FIGURE 5.5 – Sum rate with AF relaying protocol in terms of d_{sec}

5.7.2 DF in the single-carrier scenario

As it was said in Section 5.5, the primary rate when DF is applied is given in (5.14) and it depends on factor γ. The performance of the system model for fixed positions and depending on the value of γ is given in Figures 5.7, 5.8 and 5.9 for primary, secondary and sum rates respectively. The parameters of simulations are as follows : $d_{sec} = 0.2$ km, $d_{BS_pM_p} = 0.5$ km and $d_{BS_sM_s} = 0.7$ km. The studied scenario is illustrated in Fig. 5.6.

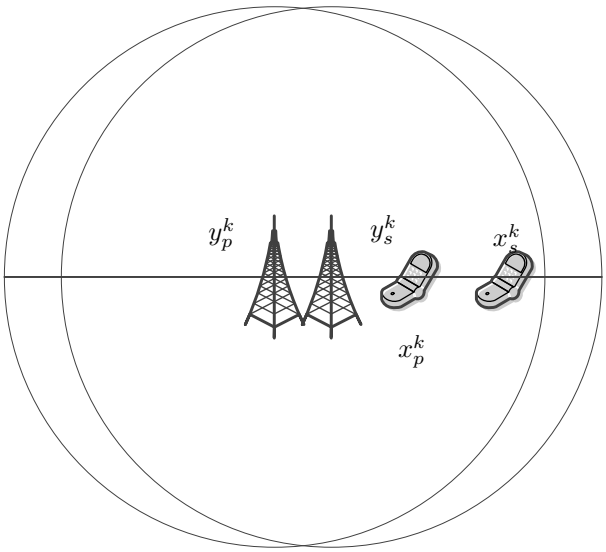

FIGURE 5.6 – Second scenario with fixed positions

Simulation results show that the optimal value of γ is zero when the relay is close to the primary transmitter and it is equal to 0.1 otherwise. We denote by 'SIC' the achievable rate where the secondary receiver decodes the primary rate but does not relay it (because it is less important than the rate achieved without relaying). Furthermore, 'DF' denotes the case where the secondary receiver relays. In this case it always applies SIC. Finally, as for AF, the label

'without relay' means that the secondary receiver does not relay and it treats the primary signal as noise. Consequently, we suppose that γ is null. Under this assumption, primary, secondary and sum rates are given in Figures 5.10, 5.11 and 5.12 respectively, to highlight the improvement of the achievable rate thanks to DF relaying.

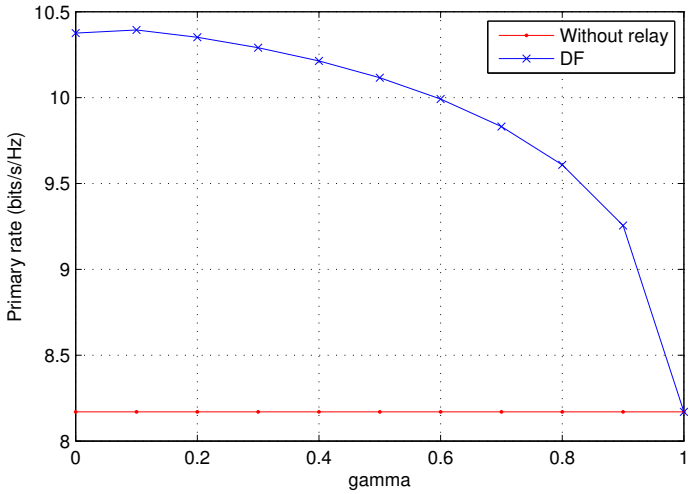

FIGURE 5.7 – Primary rate with DF in terms of γ

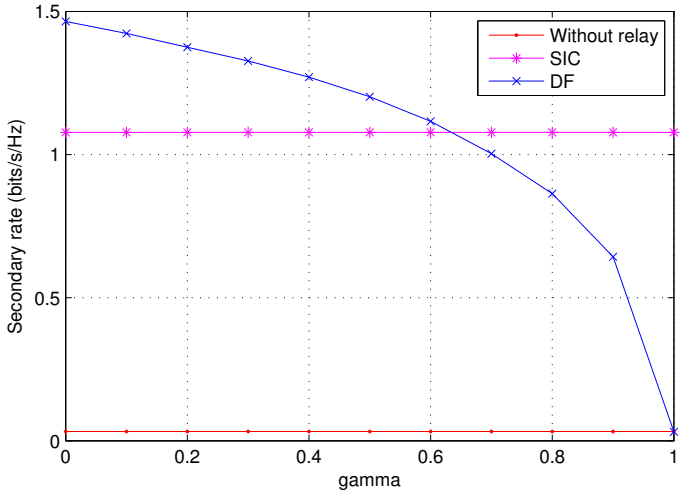

FIGURE 5.8 – Secondary rate with DF in terms of γ

Figure 5.10 shows that the primary rate increases between 2.3% and 14.8% for $d_{sec} = 1$ km and $d_{sec} = 0$ km respectively, which means that the improvement of the primary rate increases when the BSs are close to each others. In Figure 5.11, it is shown that unlike AF protocol, there is no degradation on the secondary achievable rate when the secondary receiver relays. Consequently, an improvement between 4.8% and 17.8% is obtained at the sum rate when both DF relaying and SIC are applied.

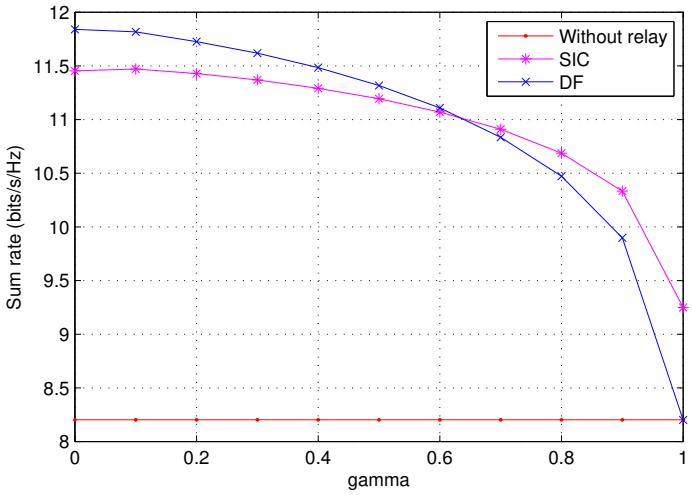

FIGURE 5.9 – Sum rate with DF in terms of γ

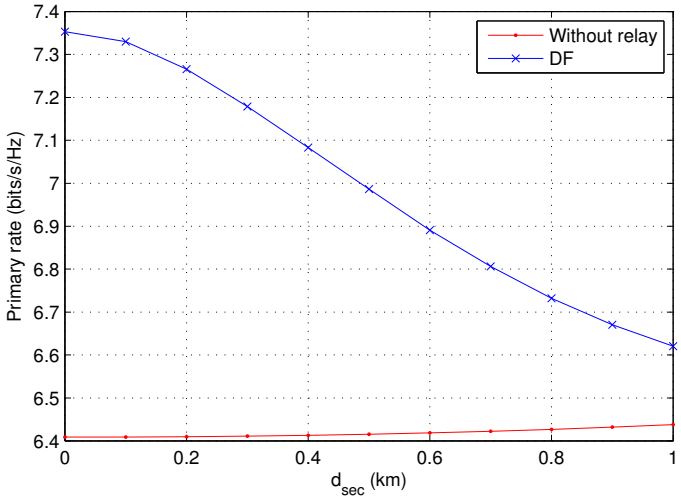

FIGURE 5.10 – Primary rate with DF relaying protocol in terms of d_{sec}

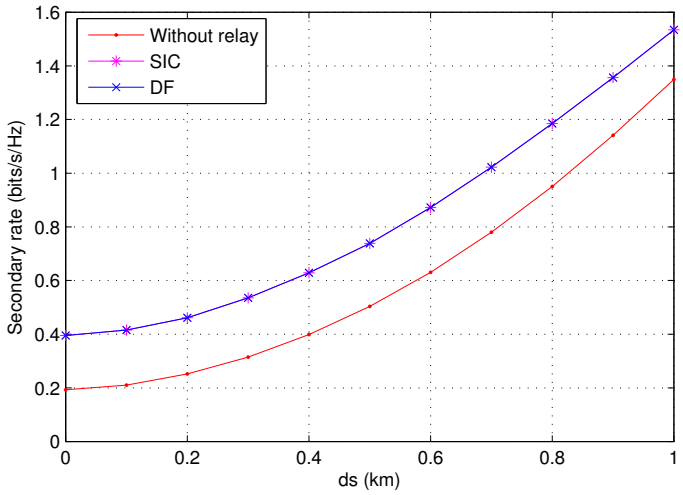

FIGURE 5.11 – Secondary rate with DF relaying protocol in terms of d_{sec}

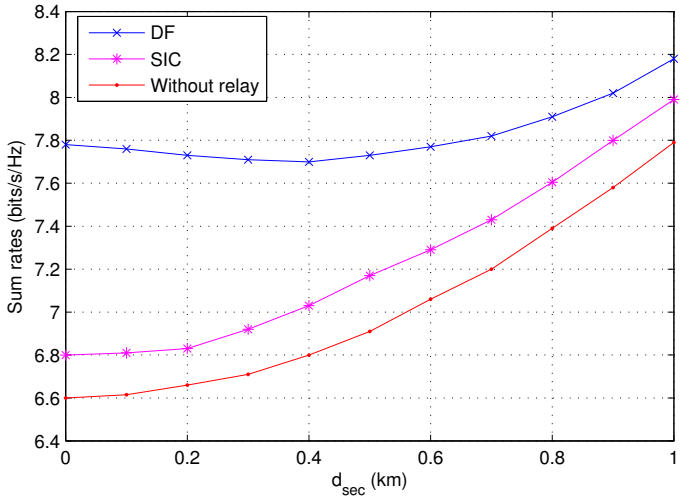

FIGURE 5.12 – Sum rate with DF relaying protocol in terms of d_{sec}

5.7.3 Comparison between AF and DF

To compare the performance of AF and DF protocols, two scenarios are considered. In the first scenario the mobiles positions are chosen randomly. The rates are plotted in Figures 5.13, 5.14 and 5.15 for primary, secondary and sum rates respectively, depending on the distance between the BSs.

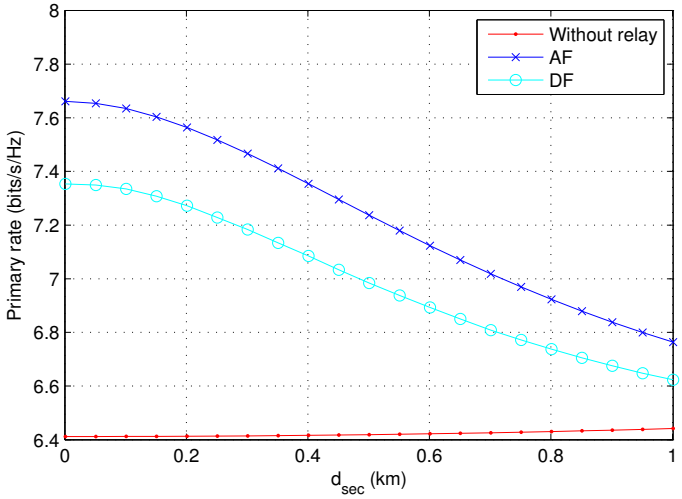

FIGURE 5.13 – Comparison between primary rates with AF and DF for random d_{sec}

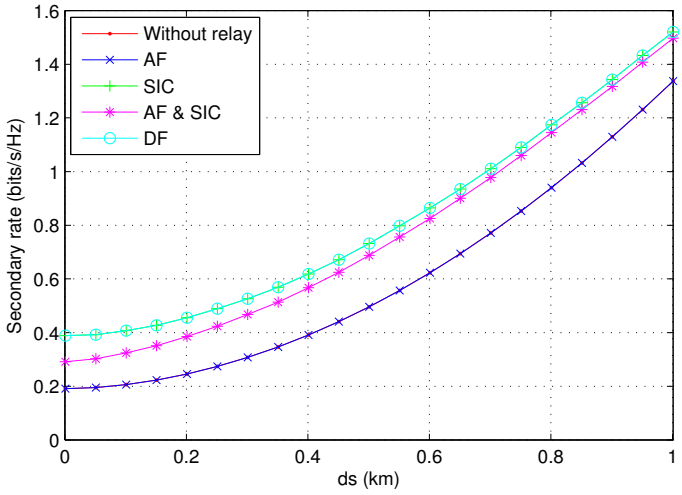

FIGURE 5.14 – Comparison between secondary rates with AF and DF for random d_{sec}

Simulation results show that AF protocol provides a larger gain for the primary rate, than DF relaying protocol. Consequently, despite the degradation of the secondary rate by AF comparing to the rate obtained when SIC is applied, the AF relaying protocol presents better results for the total sum rate as it is shown in Fig. 5.15.

In the second scenario the primary mobile is fixed at $d_{BS_pM_p} = 0.4$ km and the secondary mobile at $d_{BS_sM_s} = 0.7$ km. In Fig. 5.16, we notice that DF relaying can be better than AF

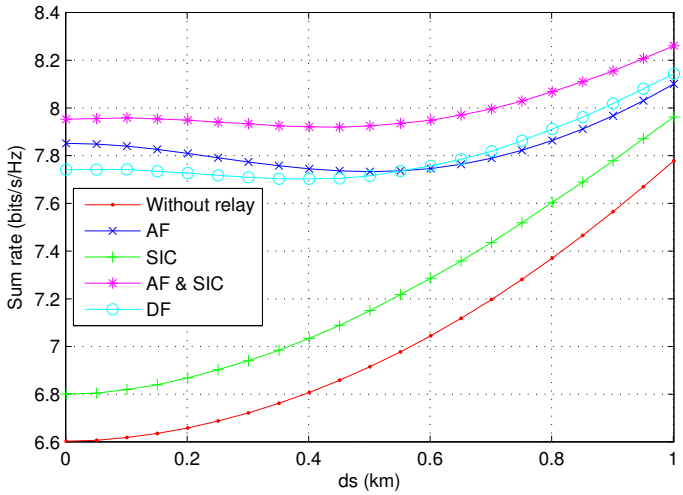

FIGURE 5.15 – Comparison between sum rates with AF and DF for random d_{sec}

for the primary rate, with d_{sec} between 0.1 and 0.2 km. Otherwise, AF always presents better improvements on the primary rate.

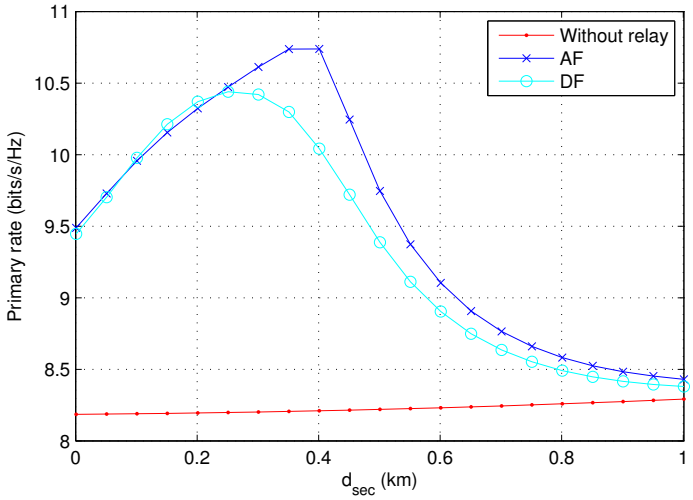

FIGURE 5.16 – Primary rate in terms of d_{sec} for special scenario

In Fig. 5.17, it is shown that concerning the secondary rate, DF outperforms AF with a gain between 11% and 66%. However, both relaying protocols have the same influence on the secondary achievable rate, and attain their maximum at $d_{sec} = 0.4$ km. Consequently, concerning the sum rate, DF outperforms AF for d_{sec} between 0 and 0.27 km, while AF presents better performance for d_{sec} between 0.27 and 0.7 km. Both relaying protocols have the same improvement on sum rate for $d_{sec} > 0.7$ km.

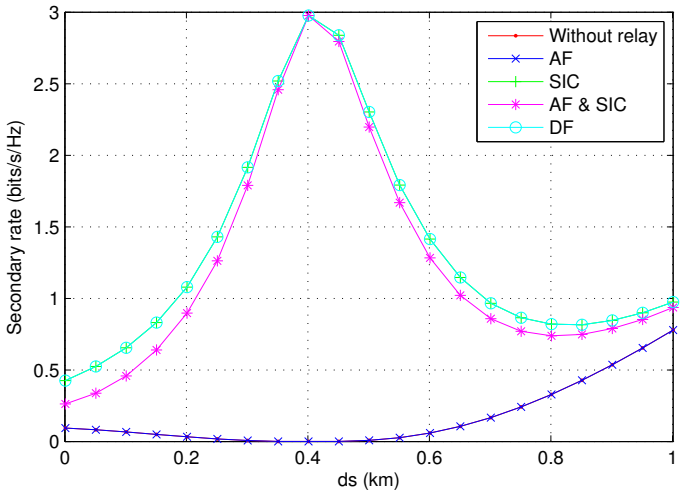

FIGURE 5.17 – Secondary rate in terms of d_{sec} for special scenario

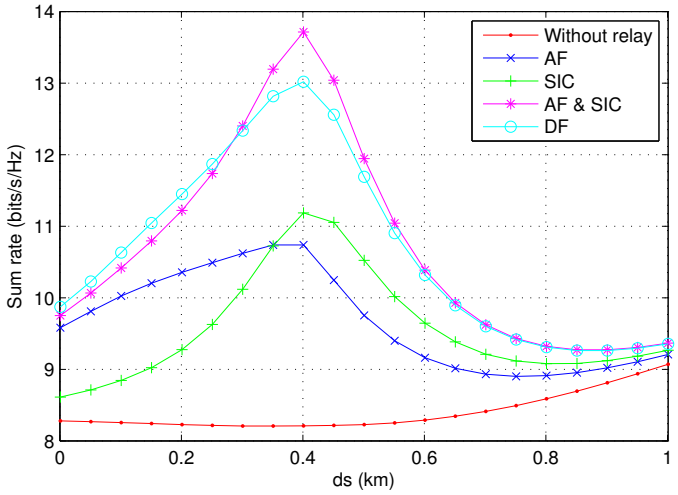

FIGURE 5.18 – Sum rate in terms of d_{sec} for special scenario

5.7.4 DF in the multi-carrier scenario

We now consider $L = 64$ subcarriers for each primary and secondary systems. We use the same parameters as in the single-user case. The performance of the DF relay node in the multi-carrier scenario is evaluated depending on d_{sec}. Simulation results given in Fig. 5.19 and Fig. 5.20 show that the proposed model insures better achievable rates in the multi-carrier case as well as in the single-carrier case. We note that the improvement of both primary and sum rates is better when the secondary BS is closer to the primary BS, i.e. when d_{sec} is small. In this case, the primary achievable rate is improved of 13.5 % while the total system rate increases of 11.9% comparing to the scenario without relaying. Relaying does not have any influence on the secondary rate since relaying is used whenever SIC takes place. As a consequence, the proposed algorithm enhances both primary and secondary rates.

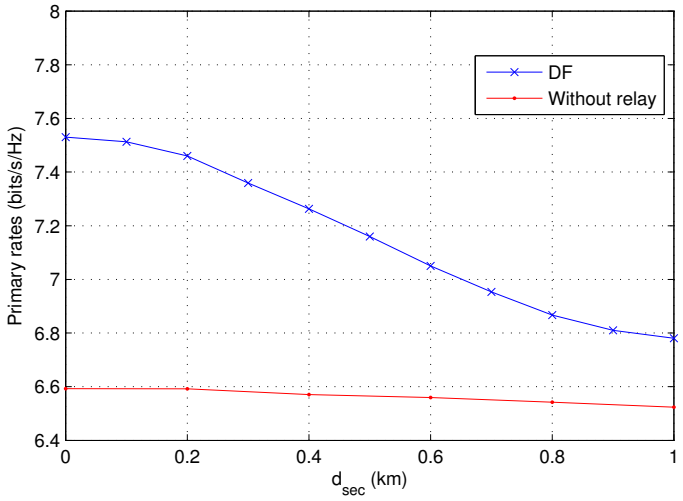

FIGURE 5.19 – Primary rate vs d_{sec} with DF relaying in the multi-carrier scenario

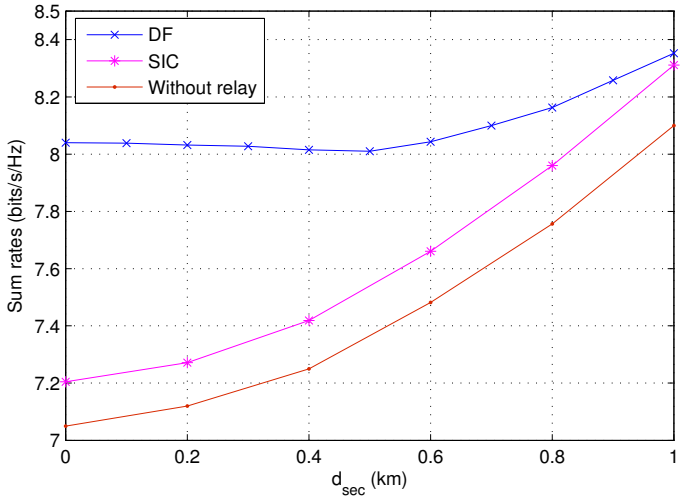

FIGURE 5.20 – Sum rate vs d_{sec} with DF relaying in the multi-carrier scenario

5.8 Conclusion

In this chapter, we proposed a new relay-assisted CR system model, where the secondary BS can serve as a relay node. We assumed that this node relays whenever the received signal after relaying is better than the received signal without relay. We investigated the single-carrier scenario for both AF and DF relaying protocols considering FD relay mode. Different possible schemes were studied and the decoding algorithm at the secondary receiver was detailed. Moreover, we investigated the resource allocation problem in the multi-carrier case for the DF relaying protocol. Both AF and DF relaying protocols were compared via simulations and for different scenarios. Simulation results have shown that the proposed model presents a major improvement of the total system rate.

Conclusion and Perspectives

5.9 Conclusion

This thesis has studied the resource allocation in an underlay OFDM cognitive radio system. Our objective was to maximize the system achievable rates at both primary and secondary systems. A dynamic resource allocation algorithm as well as a new model based on a relay-node at the secondary receiver have been proposed. First, we have presented a dynamic decoding algorithm at the SU when only on secondary mobile terminal is available in the secondary cell. By this algorithm, the SU was able to either treat the interference of the primary transmitter as noise, or use SIC or SC. We have investigated the resource allocation problem in both perfect and statistical CSI and a general solution for the uplink underlay OFDM based CR system was obtained for both scenarios.

In the first scenario insured by a band manager, all channel gains were supposed to be known at all nodes. The power optimization problem has been studied taking into account the maximum power budget at the primary and the secondary transmitter as well as the maximum allowable interference at the primary receiver. Both dual decomposition and SCA methods were applied. Simulation results have shown that the proposed algorithm achieves higher sum rate than classical algorithms, providing high-enough data rates for the secondary system at the expense of a very low degradation of the primary system's rate. In addition, we have described via statistical study the distribution of the different studied scenarios according to the users positions.

In the second scenario, we have assumed that only statistical knowledge about the primary links were available at the SU. For that, we have calculated the outage probabilities for the optimization problem and then we have studied the optimization problem in a similar way as in the full CSI scenario. Simulation results have demonstrated that the proposed algorithm is efficient and robust despite the lack of channel knowledge.

In the full CSI case, we have considered the multiuser transmission where multiple secondary mobile terminals can coexist in the secondary cell. We have proposed a multiuser resource allocation algorithm by assuming that only one secondary transmitter can be active within each subcarrier. This algorithm was composed of two steps : the subcarrier allocation which was based on the single-user scheme results, and the power allocation which was investigated once all subcarriers were allocated. Simulation results have revealed that the growth of the rates using the decoding strategy algorithm is greater in the multiuser case than in the single-user case

thanks to multiuser diversity. In addition, the achievable rates with the proposed algorithm are 4% less than those of the exhaustive search which is more complex than the heuristic proposed method.

Finally, in order to maximize the primary achievable rate, a new model based on a relay node at the secondary BS was proposed. More specifically, we have assumed that the secondary receiver can act as a FD relay node in order to help the primary transmission. Firstly, we have considered both AF and DF relaying protocols in the single-carrier case, assuming an EPA and taking into account the interference threshold at the primary receiver. Moreover, we have examined the multi-carrier scenario for the DF relaying protocol. Simulation results have shown an important growth of the primary achievable rate comparing to scenarios without relaying.

5.10 Perspectives

In this thesis, we have studied the resource allocation in OFDM based CR system in order to maximize the system achievable rates. The proposed algorithms and model can be complemented by additional studies related to the investigated problem. Some open areas and potential research directions based on this work that might be interesting to pursue in the future are listed below.

— Multiple relays : In Section 3.9, we have considered the multiuser case assuming that multiple secondary mobile terminals can coexist in the secondary cell. However, the scenario where multiple secondary cells exist is also possible. This scenario can be extended to the relay model proposed in Chapter 5 by considering all secondary BSs as relay nodes and the relay selection problem can be investigated. The multiple relay selection scheme is widely discussed in the literature [137–141]. In this thesis, we assumed perfect feasibility of FD relaying. Self-interference should however be considered in the studied model, and its influence on performance results should be evaluated.

— Multiple-Input Multiple-Output (MIMO) CR : Recent development in MIMO antenna techniques opens up a new dimension, namely space, for co-channel users to coexist without causing severe interference to each other [142]. Adopting MIMO power allocation within a CR framework was widely studied in [8, 143–147] for both theoretical and practical issues. In the general CR scenario, multiple antennas can be used to provide the secondary transmitter more degrees of freedom in space in addition to time and frequency so as to balance between increasing its own transmit rate and mitigating interference at the primary receiver. In our scenario, beamforming may be used by the secondary transmitter to mitigate interference at the primary receiver, while the secondary receiver may on the contrary aim at obtaining a high level of interference in order to use SIC or SC and thus increase its data rate.

— Different scenarios : The proposed dynamic decoding strategy algorithm can be generalized to several scenarios such as the classic interference channel, without taking into consideration the cognitive constraints. Moreover, since SIC and SC are widely studied for different channel models, as heterogeneous cellular networks [148–150], Device-to-Device (D2D) communications [151–154], the proposed algorithm can be also applied in

one of these scenarios in order to achieve higher data rates.

— Spectrum sensing : In this thesis, we have considered a perfect sensing of the primary's activity at the SU. However, this assumption is not practical and the secondary spectrum sensing system must be able to effectively detect any transmission from the primary system before transmitting its own signal. Many works have focused on the spectrum sensing issue for the CR networks [155–158]. Additionally, cooperative spectrum sensing has recently been discussed in CR networks [159, 160].

— Finite blocklength codes : in this thesis, we have assume optimal channel coding i.e. infinite length size of codewords. However, different studies have evaluated the achievable rates in the finite blocklength regime. It will be interesting to extend the obtained results to the case of the finite blocklength regime. From a practical point of view, some error correcting codes such as polar codes can be implemented to achieve performance close to these different bounds [161].

Annexe A

Typical and jointly typical sequences

A.1 Typical sequences

The typical set is a set of sequences whose probability is close to two raised to the negative power of the entropy of their source distribution. The notion of typicality is only concerned with the probability of a sequence and not the actual sequence itself.

Let $\mathbf{X}^N = (X_1, X_2, \ldots, X_N)$ be an ensemble of N i.i.d. random variables, with N sufficiently large. Let $\mathcal{A}_X$ be the alphabet of the ensemble X, and $\mathbf{x}^N$ a given realization of N independent variables x. Consequently

$$Pr\left(\mathbf{X}^N = \mathbf{x}^N\right) \approx 2^{-H(X)N} \tag{A.1}$$

which can be written as

$$-\frac{1}{N}\log_2 Pr\left(\mathbf{X}^N = \mathbf{x}^N\right) = -\frac{1}{N}\sum_{i=1}^{N}\log_2 Pr\left(X_i = x_i\right) \to H(X) \tag{A.2}$$

where $H(X)$ represents the entropy of X. That this set has total probability close to one is a consequence of the Asymptotic Equipartition Property (AEP) which is a kind of law of large numbers.

We define the typical elements of $\mathcal{A}_X^N$ to be those elements that have probability close to $2^{-NH(X)}$. We introduce a parameter ϵ that defines how close the probability has to be to $2^{-NH(X)}$ for an element to be 'typical'. The typical set $\mathcal{T}_\epsilon$ is then defined as :

$$\mathcal{T}_\epsilon = \left\{\mathbf{x}^N \in \mathcal{A}_X^N : \left|\frac{1}{N}\log_2 Pr\left(\mathbf{X}^N = \mathbf{x}^N\right) - H(X)\right| < \epsilon\right\} \tag{A.3}$$

We can prove that whatever value of ϵ we choose, the typical set contains almost all the probability as N increases, i.e.

$$Pr\left(\mathbf{x}^N \in \mathcal{T}_\epsilon\right) \underset{N\to\infty}{\longrightarrow} 1 \tag{A.4}$$

and that the number of typical sets $|\mathcal{T}_\epsilon|$ has an upper-bound

$$|\mathcal{T}_\epsilon| \leqslant 2^{N(H(X)+\epsilon)} \tag{A.5}$$

In summary, for a sequence X^N with N sufficiently large, the outcome $\mathbf{x}^N = (x_1, x_2, \ldots, x_N)$ is almost certain to belong to $\mathcal{T}_\epsilon$ having only $2^{NH(X)}$ members, each having probability close to $2^{-NH(X)}$.

A.1.1 Typical sequence properties

1.

$$Pr\{\mathbf{x}^N \in \mathcal{A}_X^N\} \geqslant 1-\epsilon \tag{A.6}$$

2.

$$(1-\epsilon)2^{n(H(X)-\epsilon)} \leqslant \left|\mathcal{A}_X^N\right| \leqslant 2^{n(H(X)+\epsilon)} \tag{A.7}$$

3.

$$\mathbf{x}^N \in \mathcal{A}_X^N \Rightarrow \left|-\frac{1}{N}\log_2 Pr(\mathbf{X}^N = \mathbf{x}^N) - H(X)\right| < \epsilon \tag{A.8}$$

4.

$$\left|\frac{1}{N}\mathcal{N}(x_i) - Pr(x_i)\right| < \epsilon \parallel \mathbf{X}^N \parallel \tag{A.9}$$

where $\mathcal{N}(x_i)$ indicates the number of occurrences of x_i in $\mathbf{X}^N$ and $\parallel \mathbf{X}^N \parallel$ the cardinality of $\mathbf{X}^N$. This property is called strong typicality.

A.2 Jointly typical sequences

The set of all jointly-typical sequence pairs of length N can be defined by :

$$\mathcal{J}_\epsilon = \Bigg\{\mathbf{x}^N \in \mathcal{A}_X^N : \left|\frac{1}{N}\log_2 Pr\left(\mathbf{X}^N = \mathbf{x}^N\right) - H(X)\right| < \epsilon \tag{A.10}$$

$$\left|\frac{1}{N}\log_2 Pr\left(\mathbf{Y}^N = \mathbf{y}^N\right) - H(Y)\right| < \epsilon \tag{A.11}$$

$$\left|\frac{1}{N}\log_2 Pr\left((\mathbf{X}^N, \mathbf{Y}^N) = (\mathbf{x}^N, \mathbf{y}^N)\right) - H(X,Y)\right| < \epsilon\Bigg\} \tag{A.12}$$

where $(\mathbf{x}^N, \mathbf{y}^N)$ is a sequence of N i.i.d. random variables with jointly probability

$$Pr\left(\mathbf{X}^N = \mathbf{x}^N, \mathbf{Y}^N = \mathbf{y}^N\right) = \prod_{i=1}^{N} Pr\left(X_i = x_i, Y_i = y_i\right) \tag{A.13}$$

A.2.1 Jointly typical sequence properties

1.

$$Pr\left((\mathbf{x}^N, \mathbf{y}^N) \in \mathcal{J}_\epsilon\right) \underset{N\to\infty}{\longrightarrow} 1 \tag{A.14}$$

2.

$$|\mathcal{J}_\epsilon| \leqslant 2^{N(H(X,Y)+\epsilon)} \tag{A.15}$$

3. If $\mathbf{x}' \sim X^N$ and $\mathbf{y}' \sim Y^N$, i.e. $\mathbf{x}'$ and $\mathbf{y}'$ are independent samples with the same marginal distribution as $P(\mathbf{x}, \mathbf{y})$, then

$$Pr\left((\mathbf{x}', \mathbf{y}') \in \mathcal{J}_\epsilon\right) \leqslant 2^{-N(I(X;Y)-3\epsilon)} \tag{A.16}$$

where $I(X;Y)$ represents the mutual information of X and Y.

Consequently, there exist $2^{N(H(X,Y))}$ jointly typical sequences each having probability close to $2^{-N(I(X;Y))}$.

A.3 General properties

Let $\{\mathbf{X}, \mathbf{Y}, \mathbf{X_r}\}$ be a finite collection of discrete random variables with joint distribution $Pr\left(\mathbf{x}, \mathbf{y}, \mathbf{x_r}\right)$. Let N be the number of independent subsets $\mathbf{S}$ of these random variables, which means that

$$\begin{aligned} Pr\left(\mathbf{S} = \mathbf{s}\right) &= \prod_{i=1}^{N} Pr\left(S_i = s_i\right) \\ &= Pr\left((\mathbf{X}, \mathbf{Y}, \mathbf{X_r}) = (\mathbf{x}, \mathbf{y}, \mathbf{x_r})\right) \\ &= \prod_{i=1}^{N} Pr(x_i, y_i, x_{r_i}) \end{aligned} \tag{A.17}$$

By the law of large numbers, for a given subset $\mathbf{S}$ of random variables

$$-\frac{1}{N}\log_2 Pr\left(S_1, S_2, \ldots, S_n\right) = -\sum_{i=1}^{N} \log_2 Pr(S_i) \to H(S) \tag{A.18}$$

with probability one. We define $\mathcal{A}_\epsilon$ as the set of all jointly ϵ-typical sequences, and $\mathcal{A}_\epsilon(S)$ denote the restriction of $\mathcal{A}_\epsilon$ to the coordinates corresponding to S.

One can prove that if $(\mathbf{x},\mathbf{y}) \in \mathcal{A}_\epsilon(X,Y)$, then

$$2^{-N(H(X|Y)+\epsilon)} \leqslant Pr(\mathbf{x}|\mathbf{y}) \leqslant 2^{-N(H(X|Y)-\epsilon)} \tag{A.19}$$

This property follows from (A.12) and $Pr(\mathbf{x}|\mathbf{y}) = Pr(\mathbf{x},\mathbf{y})/Pr(\mathbf{y})$.

A.4 Conditionally independent sequences

Let the discrete random variables $\mathbf{X},\mathbf{Y},\mathbf{X}_r$ have joint distribution $Pr(\mathbf{x},\mathbf{y},\mathbf{x}_r)$. Let $\mathbf{X}',\mathbf{Y}'$ be conditionally independent given $\mathbf{X}_r$, with marginals

$$\begin{aligned} Pr(\mathbf{x}|\mathbf{x}_r) &= \sum_{\mathbf{y}} Pr\left(\mathbf{x},\mathbf{y},\mathbf{x}_r\right)/Pr(\mathbf{x}_r) \\ Pr(\mathbf{y}|\mathbf{x}_r) &= \sum_{\mathbf{x}} Pr\left(\mathbf{x},\mathbf{y},\mathbf{x}_r\right)/Pr(\mathbf{x}_r) \end{aligned} \tag{A.20}$$

Let $(\mathbf{X},\mathbf{Y},\mathbf{X_r}) \sim \prod_{i=1}^N Pr\left(x_i,y_i,x_{ri}\right)$, and $(\mathbf{X}',\mathbf{Y}',\mathbf{X_r}) \sim \prod_{i=1}^N Pr\left(x_i|x_{ri}\right) Pr\left(y_i|x_{ri}\right) Pr\left(x_{ri}\right)$.

For $(\mathbf{x},\mathbf{y},\mathbf{x_r}) \in \mathcal{A}_\epsilon(X,Y,X_r)$, we have

$$2^{-N(H(X|X_r)+H(Y|X_r)+H(X_r)+6\epsilon)} \leqslant Pr(\mathbf{x}|\mathbf{x_r})Pr(\mathbf{y}|\mathbf{x_r})Pr(\mathbf{x_r}) \leqslant 2^{-N(H(X|X_r)+H(Y|X_r)+H(X_r)-6\epsilon)} \tag{A.21}$$

from (A.19), and

$$2^{-N(H(X,Y,X_r)+\epsilon)} \leqslant Pr(\mathbf{x},\mathbf{y},\mathbf{x_r}) \leqslant 2^{-N(H(X,Y,X_r)-\epsilon)} \tag{A.22}$$

from (A.12).

Note that

$$\begin{aligned} H(X|X_r) + H(Y|X_r) + H(X_r) - H(X,Y,X_r) &= H(X|X_r) + H(Y|X_r) - H(X,Y|X_r) \\ &= I(X;Y|X_r) \end{aligned} \tag{A.23}$$

Consequently,

$$Pr(\mathbf{x},\mathbf{y},\mathbf{x_r})2^{-N(I(X;Y|X_r)+7\epsilon)} \leqslant Pr(\mathbf{x}|\mathbf{x_r})Pr(\mathbf{y}|\mathbf{x_r})Pr(\mathbf{x_r}) \leqslant Pr(\mathbf{x},\mathbf{y},\mathbf{x_r})2^{-N(I(X;Y|X_r)-7\epsilon)} \tag{A.24}$$

Now summing the terms in the preceding equation over $\mathcal{A}_\epsilon$,

$$\begin{aligned} (1-\epsilon)2^{-N(I(X;Y|X_r)+7\epsilon)} &\leqslant \sum_{\mathcal{A}_\epsilon} 2^{-N(I(X;Y|X_r)+7\epsilon)} Pr(\mathbf{x},\mathbf{y},\mathbf{x_r}) \\ &\leqslant \sum_{\mathcal{A}_\epsilon} Pr(\mathbf{x}|\mathbf{x_r})Pr(\mathbf{y}|\mathbf{x_r})Pr(\mathbf{x_r}) \\ &= Pr\left\{\left(\mathbf{X}',\mathbf{Y}',\mathbf{X_r}\right) \in \mathcal{A}_\epsilon(X,Y,X_r)\right\} \\ &\leqslant 2^{-N(I(X;Y|X_r)-7\epsilon)} \sum_{\mathcal{A}_\epsilon} Pr(\mathbf{x},\mathbf{y},\mathbf{x_r}) \\ &\leqslant 2^{-N(I(X;Y|X_r)-7\epsilon)} \end{aligned} \tag{A.25}$$

By conclusion,

$$(1-\epsilon)2^{-N(I(X;Y|X_r)+7\epsilon)} \leqslant Pr\left\{\left(\mathbf{X}', \mathbf{Y}', \mathbf{X_r}\right) \in \mathcal{A}_\epsilon(X,Y,X_r)\right\} \leqslant 2^{-N(I(X;Y|X_r)-7\epsilon)} \qquad \text{(A.26)}$$

Bibliographie

[1] F. C. Commission, "All-digital television is coming (and sooner than you think !)," http ://www.fcc.gov/cgb/consumerfacts/digitaltv.html, Tech. Rep.

[2] U. F. C. Commission, "Notice of proposed rule making and order, fcc 03-322, in the matter of facilitating opportunities for flexible, efficient, and reliable spectrum use employing cognitive radio technologies," FCC ET Docket, Tech. Rep. 03-322, Dec 2003.

[3] "Ieee 802.22 working group on wireless regional area network," http ://standards.ieee.org/news/2011/802.22.htmlsthash.c9cOrGds.dpuf, Tech. Rep.

[4] J. Jiang and Y. Xin, "On the achievable rate regions for interference channels with degraded message sets," *Information Theory, IEEE Transactions on*, vol. 54, pp. 4707–4712, Oct. 2008.

[5] A. M. Wyglinski, M. Nekovee, and Y. T. Hou, Eds., *Cognitive Radio Communications and Networks - Principles and Practice.* ELSEVIER, 2010.

[6] G. Bansal, M. J. Hossain, and V. K. Bhargava, "Optimal and suboptimal power allocation schemes for ofdm-based cognitive radio systems," *IEEE Transactions on Wireless Communications*, vol. 7, no. 11, p. 4710 ?4718, Nov 2008.

[7] Q. Qu, L. Milstein, and D. Vaman, "Cognitive radio based multi-user resource allocation in mobile ad hoc networks using multi-carrier cdma modulation," *IEEE Journal on Selected Areas in Communications*, vol. 26, no. 1, pp. 70–82, Jan 2008.

[8] R. Zhang and Y.-C. Liang, "Exploiting multi-antennas for opportunistic spectrum sharing in cognitive radio networks," *IEEE Journal of Selected Topics in Signal Processing*, vol. 2, no. 1, pp. 88–102, Feb 2008.

[9] U. S. Jha and R. Prasad, *OFDM Towards Fixed and Mobile Broadband Wireless Access.* Norwood, MA, USA : Artech House, Inc., 2007.

[10] A. Attar, O. Holland, M. Nakhai, and A. Aghvami, "Interference-limited resource allocation for cognitive radio in orthogonal frequency-division multiplexing networks," *IET Communications*, vol. 2, no. 6, pp. 806–814, July 2008.

[11] J. Mitola and J. Maguire, G.Q., "Cognitive radio : making software radios more personal," *IEEE Personal Communications*, vol. 6, no. 4, pp. 13–18, Aug 1999.

[12] J. Mitola, "Cognitive radio for flexible mobile multimedia communications," *IEEE International Workshop on Mobile Multimedia Communications, 1999 (MoMuC '99)*, pp. 3–10, 1999.

[13] N. Devroye, T. Vahid, and V. Mai, "Cognitive radio networks : Highlights of information theoretic limits, models and design," *IEEE Signal Processing Magazine*, pp. 12–23, 2008.

[14] N. Devroye, P. Mitran, and V. Tarokh, "Achievable rates in cognitive radio channels," *IEEE Transaction on Information Theory*, vol. 52, pp. 1813–1827, May 2006.

[15] A. Goldsmith, S. Jafar, I. Maric, and S. Srinivasa, "Breaking spectrum gridlock with cognitive radios : An information theoretic perspective," *Proceedings of the IEEE*, vol. 97, pp. 894–914, May 2009.

[16] R. Blasco-Serrano, J. Lv, R. Thobaben, E. Jorswieck, and M. Skoglund, "Multi-antenna transmission for underlay and overlay cognitive radio with explicit message-learning phase," *EURASIP Journal on Wireless Communications and Networking*, July 2013.

[17] H. Mahmoud, T. Yucek, and H. Arslan, "Ofdm for cognitive radio : merits and challenges," *IEEE Transactions on Wireless Communications*, vol. 16, no. 2, pp. 6–15, April 2009.

[18] R. W. Chang, "Synthesis of band-limited orthogonal signals for multichannel data transmission," *Bell system Technical Journal*, vol. 45, pp. 1775–1796, Dec 1966.

[19] L. Nithyanandan, R. Saravanaprabu, and P. Dananjayan, "Hybrid interference cancellation receiver for mc-cdma system," in *2005 IEEE International Conference on Personal Wireless Communications, 2005. ICPWC 2005.*, Jan 2005, pp. 465–469.

[20] J. Blomer and N. Jindal, "Transmission capacity of wireless ad hoc networks : Successive interference cancellation vs. joint detection," in *IEEE International Conference on Communications, 2009. ICC '09*, June 2009, pp. 1–5.

[21] F. Baccelli, A. El Gamal, and D. Tse, "Interference networks with point-to-point codes," *IEEE Transactions on Information Theory*, vol. 57, no. 5, pp. 2582–2596, May 2011.

[22] X. Zhang and M. Haenggi, "The performance of successive interference cancellation in random wireless networks," *IEEE Transactions on Information Theory*, vol. 60, no. 10, pp. 6368–6388, Oct 2014.

[23] J. Andrews, "Interference cancellation for cellular systems : a contemporary overview," *IEEE Wireless Communications*, vol. 12, no. 2, pp. 19–29, April 2005.

[24] S. Vanka, S. Srinivasa, Z. Gong, P. Vizi, K. Stamatiou, and M. Haenggi, "Superposition coding strategies : Design and experimental evaluation," *IEEE Transactions on Wireless Communications*, vol. 11, no. 7, pp. 2628–2639, July 2012.

[25] T. Cover and J. Thomas, *Elements of Information Theory.* John Wiley and Sons, 1991.

[26] R. Rimoldi, B. ; Urbanke, "A rate-splitting approach to the gaussian multiple-access channel," *IEEE Transactions on Information Theory*, vol. 42, pp. 364–375, Mar 1996.

[27] T. Cover, "Broadcast channels," *Information Theory, IEEE Transactions on*, 1972.

[28] S. Verdu, *Multiuser Detection*, 1st ed. New York, NY, USA : Cambridge University Press, 1998.

[29] P. Patel and J. Holtzman, "Analysis of a simple successive interference cancellation scheme in a ds/cdma system," *IEEE Journal on Selected Areas in Communications*, vol. 12, no. 5, pp. 796–807, Jun 1994.

[30] P. Bergmans, "Random coding theorem for broadcast channels with degraded components," *IEEE Transactions on Information Theory*, vol. 19, no. 2, pp. 197–207, Mar 1973.

[31] A. Grant, B. Rimoldi, R. Urbanke, and P. Whiting, "Rate-splitting multiple access for discrete memoryless channels," *IEEE Transactions on Information Theory*, vol. 47, no. 3, pp. 873–890, Mar 2001.

[32] A. Carleial, "Interference channels," *IEEE Transactions on Information Theory*, vol. 24, no. 1, pp. 60–70, 1978.

[33] T. Han and K. Kobayashi, "A new achievable rate region for the interference channel," vol. 27, pp. 49–60, Jan 1981.

[34] H.-F. Chong, M. Motani, H. K. Garg, and H. El Gamal, "On the han kobayashi region for theinterference channel," *IEEE Transactions on Information Theory*, vol. 54, no. 7, pp. 3188–3195, July 2008.

[35] T. Cover and A. Gamal, "Capacity theorems for the relay channel," *Information Theory, IEEE Transactions on*, vol. 25, no. 5, pp. 572–584, Sep 1979.

[36] L. Wang, E. Sasoglu, B. Bandemer, and Y.-H. Kim, "A comparison of superposition coding schemes," in *2013 IEEE International Symposium on Information Theory Proceedings (ISIT)*, July 2013, pp. 2970–2974.

[37] C. Shannon, "A mathematical theory of communication," *Bell System Technical Journal, The*, vol. 27, no. 3, pp. 379–423, July 1948.

[38] R. Ahlswede, "Multi-way communication channels," *2nd Internatioanl Symposium on Information Theory*, pp. 23–52, 1971.

[39] H. Liao, "A coding theorem for multiple access communications," in *International Symposium on Information Theory*, 1972.

[40] T. Cover, R. McEliece, and E. C. Posner, "Asynchronous multiple-access channel capacity," *IEEE Transactions on Information Theory*, vol. 27, no. 4, pp. 409–413, Jul 1981.

[41] D. Tse and P. Viswanath, *Fundamentals of Wireless Communication*. Cambridge University Press, 2005.

[42] T. Cover, "An achievable rate region for the broadcast channel," *Information Theory, IEEE Transactions on*, vol. 21, no. 4, pp. 399–404, Jul 1975.

[43] A. Carleial, "Interference channels," *IEEE Transactions on Information Theory*, vol. 24, no. 1, pp. 60–70, Jan 1978.

[44] ——, "A case where interference does not reduce capacity," *IEEE Transactions on Information Theory*, vol. 21, no. 5, pp. 569–570, Sep 1975.

[45] H. Sato, "The capacity of the gaussian interference channel under strong interference (corresp.)," *IEEE Transactions on Information Theory*, vol. 27, no. 6, pp. 786–788, Nov 1981.

[46] M. Costa, "On the gaussian interference channel," *IEEE Transactions on Information Theory*, vol. 31, no. 5, pp. 607–615, Sep 1985.

[47] A. Motahari, A.S. ; Khandani, "Capacity bounds for the gaussian interference channel," *IEEE Transactions on Information Theory*, 2009.

[48] G. . B. C. Xiaohu S. ; Kramer, "A new outer bound and the noisy-interference sum-rate capacity for gaussian interference channels," *Information Theory, IEEE Transactions on*, 2009.

[49] H. Chong, M. Motani, H. K. Garg, and H. E. Gamal, "On the han-kobayashi region for theinterference channel," *IEEE Transactions on Information Theory*, vol. 54, no. 7, pp. 3188–3195, July 2008.

[50] G. Kramer, "Review of rate regions for interference channels," in *2006 International Zurich Seminar on Communications*, 2006, pp. 162–165.

[51] ——, "Outer bounds on the capacity of gaussian interference channels," *IEEE Transactions on Information Theory*, vol. 50, no. 3, pp. 581–586, March 2004.

[52] R. Etkin, D. Tse, and H. Wang, "Gaussian interference channel capacity to within one bit," *Information Theory, IEEE Transactions on*, vol. 54, no. 12, pp. 5534–5562, Dec 2008.

[53] A. Goldsmith, *Wireless communications*. f Cambridge University Press, 2005.

[54] E. van der Meulen, *Transmission of Information in a T-terminal Discrete Memoryless Channel*, u. o. C. Department of statistics, Ed. Berkeley, 1968.

[55] ——, "Three terminal communication channels," *Adv. Appl. Prob*, vol. 3, pp. 120–154, 1971.

[56] M. Khojastepour, A. Sabharwal, and B. Aazhang, "On capacity of gaussian 'cheap' relay channel," in *Global Telecommunications Conference, 2003. GLOBECOM '03. IEEE*, vol. 3, Dec 2003, pp. 1776–1780 vol.3.

[57] Y. Liang and V. Veeravalli, "Gaussian orthogonal relay channels : Optimal resource allocation and capacity," *Information Theory, IEEE Transactions on*, vol. 51, no. 9, pp. 3284–3289, Sept 2005.

[58] M. Janani, A. Hedayat, T. Hunter, and A. Nosratinia, "Coded cooperation in wireless communications : space-time transmission and iterative decoding," *Signal Processing, IEEE Transactions on*, vol. 52, no. 2, pp. 362–371, Feb 2004.

[59] J. Laneman, D. Tse, and G. W. Wornell, "Cooperative diversity in wireless networks : Efficient protocols and outage behavior," *IEEE Transactions on Information Theory*, vol. 50, no. 12, pp. 3062–3080, Dec 2004.

[60] R. Nabar, H. Bolcskei, and F. Kneubuhler, "Fading relay channels : performance limits and space-time signal design," *Selected Areas in Communications, IEEE Journal on*, vol. 22, no. 6, pp. 1099–1109, Aug 2004.

[61] Y.-S. Choi and H. Shirani-Mehr, "Simultaneous transmission and reception : Algorithm, design and system level performance," *IEEE Transactions on Wireless Communications*, vol. 12, no. 12, pp. 5992–6010, December 2013.

[62] Z. Zhan, G. Villemaud, F. Hutu, and J.-M. Gorce, "Full-Duplex Dual-Band Radio Dedicated to Flexible Radio Communications," INRIA, Research Report RR-8558, Jul. 2014. [Online]. Available : https://hal.inria.fr/hal-01018429

[63] D. Kim, H. Lee, and D. Hong, "A survey of in-band full-duplex transmission : From the perspective of phy and mac layers," *IEEE Communications Surveys Tutorials*, vol. 17, no. 4, pp. 2017–2046, Fourthquarter 2015.

[64] S. Boyd and L. Vandenberghe, *Convex Optimization*. Cambridge University Press, 2004.

[65] T. Wang, "Resource allocation in ofdm-based wireless communication systems," Ph.D. dissertation, Vandendorpe, Luc, 2012.

[66] W. Yu and R. Lui, "Dual methods for nonconvex spectrum optimization of multicarrier systems," *IEEE Transactions on Communications*, vol. 54, no. 7, pp. 1310–1322, July 2006.

[67] G. Munz, S. Pfletschinger, and J. Speidel, "An efficient waterfilling algorithm for multiple access ofdm," in *IEEE Global Telecommunications Conference, 2002. GLOBECOM '02.*, vol. 1, Nov 2002, pp. 681–685 vol.1.

[68] D. Yu and J. Cioffi, "Spc10-2 : Iterative water-filling for optimal resource allocation in ofdm multiple-access and broadcast channels," in *IEEE Global Telecommunications Conference, 2006. GLOBECOM '06*, Nov 2006, pp. 1–5.

[69] R. Soundararajan and S. Vishwanath, "Adaptive sum power iterative waterfilling for mimo cognitive radio channels," in *IEEE International Conference on Communications, 2008. ICC '08*, May 2008, pp. 1060–1064.

[70] Q. Qi, A. Minturn, and Y. Yang, "An efficient water-filling algorithm for power allocation in ofdm-based cognitive radio systems," in *International Conference on Systems and Informatics (ICSAI), 2012*, May 2012, pp. 2069–2073.

[71] J. Mao, G. Xie, J. Gao, and Y. Liu, "Energy efficiency optimization for ofdm-based cognitive radio systems : A water-filling factor aided search method," *IEEE Transactions on Wireless Communications*, vol. 12, no. 5, pp. 2366–2375, May 2013.

[72] Y.-C. Liang, K.-C. Chen, G. Li, and P. Mahonen, "Cognitive radio networking and communications : an overview," *IEEE Transactions on Vehicular Technology*, vol. 60, no. 7, pp. 3386–3407, Sept 2011.

[73] A. Jovicic and P. Viswanath, "Cognitive radio : An information-theoretic perspective," *IEEE Transaction on Information Theory*, 2006.

[74] S. Sun, J. Di, and W. Ni, "Distributed power control based on convex optimization in cognitive radio networks," *Wireless Communications and Signal Processing*, pp. 1–6, Oct 2010.

[75] J. Rui Z. ; Cioffi, "Iterative spectrum shaping with opportunistic multiuser detection," *IEEE Transactions on Communications*, 2012.

[76] P. Popovski, H. Yomo, K. Nishimori, and R. D. Taranto, "Opportunistic interference cancellation in cognitive radio systems," *New Frontiers in Dynamic Spectrum Access Networks, 2007. DySPAN 2007. 2nd IEEE International Symposium on*, pp. 472–475, April 2007.

[77] W. Wang, W. Wang, Q. Lu, K. Shin, and T. Peng, "Geometry-based optimal power control of fading multiple access channels for maximum sum-rate in cognitive radio networks," *IEEE Transactions on Wireless Communications*, vol. 9, no. 6, pp. 1843–1848, June 2010.

[78] L. Zhang, Y. Xin, and Y.-C. Liang, "Weighted sum rate optimization for cognitive radio mimo broadcast channels," *IEEE Transactions on Wireless Communications*, vol. 8, no. 6, pp. 2950–2959, June 2009.

[79] A. Tajer, N. Prasad, and X. Wang, "Beamforming and rate allocation in miso cognitive radio networks," *IEEE Transactions on Signal Processing*, vol. 58, no. 1, pp. 362–377, Jan 2010.

[80] K.-J. Lee and I. Lee, "Mmse based block diagonalization for cognitive radio mimo broadcast channels," *IEEE Transactions on Wireless Communications*, vol. 10, no. 10, pp. 3139–3144, October 2011.

[81] H. Park and T. Hwang, "Optimal beamforming and power allocation for cognitive femto base stations based on soft decision," *IEEE Journal on Selected Areas in Communications*, vol. 33, no. 5, pp. 878–895, May 2015.

[82] S. Asghari, V. ; Aissa, "Adaptive time-sharing and power allocation for cognitive radio fading broadcast channels," *2010 IEEE International Conference on Communications (ICC)*, pp. 1–5, May 2010.

[83] V. Asghari and S. Aissa, "Resource management in spectrum-sharing cognitive radio broadcast channels : Adaptive time and power allocation," *IEEE Transactions on Communications*, vol. 59, no. 5, pp. 1446 – 1457, 2011.

[84] X. Hong, Z. Chen, C.-X. Wang, S. Vorobyov, and J. Thompson, "Cognitive radio networks," *IEEE Vehicular Technology Magazine*, vol. 4, no. 4, pp. 76–84, December 2009.

[85] R. Datta, N. Michailow, M. Lentmaier, and G. Fettweis, "Gfdm interference cancellation for flexible cognitive radio phy design," in *IEEE Vehicular Technology Conference (VTC Fall), 2012*, Sept 2012, pp. 1–5.

[86] S. Rini, E. Kurniawan, and A. Goldsmith, "Combining superposition coding and binning achieves capacity for the gaussian cognitive interference channel," *Information Theory Workshop (ITW), 2012 IEEE*, pp. 227 – 231, Sept. 2012.

[87] D. Chatterjee, T. Wong, and O. Oyman, "Achievable rates in cognitive radio networks," *Signals, Systems and Computers, 2009 Conference Record of the Forty-Third Asilomar Conference on*, pp. 35 – 39, Nov. 2009.

[88] S. Bopping and J. Shea, "Superposition coding in the downlink of cdma cellular systems," in *IEEE Wireless Communications and Networking Conference, 2006. WCNC 2006.*, vol. 4, April 2006, pp. 1978–1983.

[89] S. Sadr, A. Anpalagan, and K. Raahemifar, "Radio resource allocation algorithms for the downlink of multiuser ofdm communication systems," *IEEE Communication Survey & Tutorials*, vol. 11, no. 3, p. 92 ?106, Sep 2009.

[90] R. Zhang, Y. Liang, and S. Cui, "Dynamic resource allocation in cognitive radio networks," *IEEE Signal Processing Magazine*, vol. 27, no. 3, pp. 102 – 114, May 2010.

[91] S. Wang, F. Huang, and Z.-H. Zhou, "Fast power allocation algorithm for cognitive radio networks," *IEEE Communication letters*, vol. 15, no. 8, p. 845 ?847, Aug 2011.

[92] Y. Zhang and C. Leung, "Resource allocation in an ofdm-based cognitive radio system," *IEEE Transactions on Communications*, vol. 57, no. 7, pp. 1928–1931, July 2009.

[93] S. Almalfouh and G. Stuber, "Interference-aware radio resource allocation in ofdma-based cognitive radio networks," *IEEE Transactions on Vehicular Technology*, vol. 60, no. 4, pp. 1699–1713, May 2011.

[94] X. Kang, Y.-C. Liang, A. Nallanathan, H. Garg, and R. Zhang, "Optimal power allocation for fading channels in cognitive radio networks : Ergodic capacity and outage capacity," *IEEE Transactions on Wireless Communications*, vol. 8, no. 2, pp. 940–950, Feb 2009.

[95] X. Kang, H. Garg, Y.-C. Liang, and R. Zhang, "Optimal power allocation for ofdm-based cognitive radio with new primary transmission protection criteria," *IEEE Transactions on Wireless Communications*, vol. 9, no. 6, pp. 2066–2075, June 2010.

[96] S. Ekin, M. M. Abdallah, K. A. Qarage, and E. Serpedin, "Random subcarrier allocation in ofdm-based cognitive networks," *IEEE Transactions on Signal processing*, vol. 60, no. 9, pp. 4758–4774, Feb 2012.

[97] M. Khoshkholgh, N. Yamchi, K. Navaie, H. Yanikomeroglu, V. Leung, and K. Shin, "Radio resource allocation for ofdm-based dynamic spectrum sharing : Duality gap and time averaging," *IEEE Journal onSelected Areas in Communications*, vol. 33, no. 5, pp. 848–864, May 2015.

[98] M. Pischella and D. L. Ruyet, "Cooperative allocation for underlay cognitive radio systems," *International Workshop on Signal Processing Advances in Wireless Communications (SPAWC 2013)*, pp. 1–5, June 2013.

[99] R. Zhang and Y.-C. Liang, "Investigation on multiuser diversity in spectrum sharing based cognitive radio networks," *IEEE Communications Letters*, vol. 14, no. 2, pp. 133–135, Feb 2010.

[100] S. Wang, F. Huang, M. Yuan, and S. Du, "Resource allocation for multiuser cognitive ofdm networks with proportional rate constraints," *International Journal of Communication Systems*, vol. 25, no. 2, pp. 254–269, 2012.

[101] J. pyo Hong and W. Choi, "Capacity scaling law by multiuser diversity in cognitive radio systems," in *2010 IEEE International Symposium on Information Theory Proceedings (ISIT)*, June 2010, pp. 2088–2092.

[102] M. Ge and S. Wang, "Fast optimal resource allocation is possible for multiuser ofdm-based cognitive radio networks with heterogeneous services," *IEEE Transactions on Wireless Communications*, vol. 11, no. 4, pp. 1500–1509, Apr 2012.

[103] S. Wang, F. Huang, , and C. Wang, "Adaptive proportional fairness resource allocation for ofdm-based cognitive radio networks," *IEEE Transactions on Wireless Communications*, vol. 19, no. 3, p. 273 ?284, Mar 2013.

[104] S. Wang, Z.-H. Zhou, M. Ge, and C. Wang, "Resource allocation for heterogeneous cognitive radio networks with imperfect spectrum sensing," *IEEE Journal on Selected Areas in Communications*, vol. 31, no. 3, p. 464 ?475, 2013.

[105] A. Ghasemi and E. Sousa, "Spectrum sensing in cognitive radio networks : requirements, challenges and design trade-offs," *IEEE Communications Magazine*, vol. 46, no. 4, pp. 32–39, April 2008.

[106] M. Pischella and D. L. Ruyet, "Adaptive resource allocation and decoding strategy for underlay multi-carrier cooperative cognitive radio systems," *Transactions on Emerging Telecommunications Technologies*, vol. 24, pp. 748–761, Dec 2013.

[107] G. Scutari, D. Palomar, and S. Barbarossa, "Asynchronous iterative water-filling for gaussian frequency-selective interference channels," *Information Theory and Applications Workshop, 2007*, 2007.

[108] S. Boyd and A. Mutapcic, *Subgradient methods*, Winter 2006-07, ch. notes for EE364.

[109] B. Maham, P. Popovski, X. Zhou, and A. Hjorungnes, "Cognitive multiple access network with outage margin in the primary system," *IEEE Transactions on Wireless Communications*, vol. 10, no. 10, pp. 3343–3353, October 2011.

[110] D. Palomar and J. Fonollosa, "Practical algorithms for a family of waterfilling solutions," *Signal Processing, IEEE Transactions on*, vol. 53, no. 2, pp. 686–695, Feb 2005.

[111] L. Musavian and S. Aissa, "Fundamental capacity limits of cognitive radio in fading environments with imperfect channel information," *IEEE Transactions on Communications*, vol. 57, no. 11, pp. 3472–3480, Nov 2009.

[112] X. Xie and W. Guo, "Fundamental effective capacity limits of cognitive radio in fading environments with imperfect channel information," in *2011 International Conference on Computational Problem-Solving (ICCP)*, Oct 2011, pp. 232–235.

[113] H. Suraweera, P. Smith, and M. Shafi, "Capacity limits and performance analysis of cognitive radio with imperfect channel knowledge," *IEEE Transactions on Vehicular Technology*, vol. 59, no. 4, pp. 1811–1822, May 2010.

[114] Y. He and S. Dey, "Throughput maximization in cognitive radio under peak interference constraints with limited feedback," *IEEE Transactions on Vehicular Technology*, vol. 61, no. 3, pp. 1287–1305, March 2012.

[115] Z. Rezki and M.-S. Alouini, "Ergodic capacity of cognitive radio under imperfect channel-state information," *IEEE Transactions on Vehicular Technology*, vol. 61, no. 5, pp. 2108–2119, Jun 2012.

[116] A. Shojaeifard, H. Saki, M. Mahyari, and M. Shikh-Bahaei, "Resource allocation and interference management for adaptive modulation and coding-based ofdma cognitive radio networks," in *2014 IEEE International Conference on Communications (ICC)*, June 2014, pp. 5908–5913.

[117] P. Smith, P. Dmochowski, H. Suraweera, and M. Shafi, "The effects of limited channel knowledge on cognitive radio system capacity," *IEEE Transactions on Vehicular Technology*, vol. 62, no. 2, pp. 927–933, Feb 2013.

[118] P. Dmochowski, H. Suraweera, P. Smith, and M. Shafi, "Impact of channel knowledge on cognitive radio system capacity," in *2010 IEEE 72nd Vehicular Technology Conference Fall (VTC 2010-Fall)*, Sept 2010, pp. 1–5.

[119] O. Sahin and E. Erkip, "On achievable rates for interference relay channel with interference cancelation," *Conference Record of the Forty-First Asilomar Conference on Signals, Systems and Computers, 2007. ACSSC 2007.*, pp. 805 – 809, 2007.

[120] S. Sridharan, S. Vishwanath, S. A. Jafar, and S. Shamai, "On the capacity of cognitive relay assisted gaussian interference channel," *IEEE International Symposium on Information Theory, 2008. ISIT 2008.*, pp. 549 – 553, 2008.

[121] I. Maric, R. Dabora, and A. Goldsmith, "On the capacity of the interference channel with a relay," *ISIT 2008. IEEE International Symposium on Information Theory, 2008.*, pp. 554 – 558, 2008.

[122] O. Sahin, E. Erkip, and O. Simeone, "Interference channel with a relay : Models, relaying strategies, bounds," *Information Theory and Applications Workshop*, pp. 90 – 95, 2009.

[123] R. Hu, C. Hu, J. Jiang, X. Xie, and L. Song, "Full-duplex mode in amplify-and-forward relay channels : Outage probability and ergodic capacity," *International Journal of Antennas and Propagation*, vol. 2014, p. 8, 2014.

[124] L. Jui-Chi and C. Jyh-Cheng, "Resource allocation in cognitive radio relay networld," *IEEE Journal on Selected aread in Communications*, vol. 31, no. 12, pp. 476 488–3080, March 2013.

[125] L. Zhang, J. Jiang, A. J. Goldsmith, and S. Cui, "Study of gaussian relay channels with correlated noises," *IEEE Transactions on Communications*, vol. 59, no. 3, pp. 863–876, March 2011.

[126] X. Zhang, X. S. Shen, and L.-L. Xie, "Joint subcarrier and power allocation for cooperative communications in lte-advanced networks," *IEEE Transactions on Wireless Communications*, vol. 13, no. 2, pp. 658–668, February 2014.

[127] A. Host-Madsen and J. Zhang, "Capacity bounds and power allocation for wireless relay channels," *IEEE Transactions on Information Theory*, vol. 51, no. 6, pp. 2020–2040, June 2005.

[128] L. Vandendorpe, R. T. Duran, J. Louveaux, and A. Zaidi, "Power allocation for ofdm transmission with df relaying," in *IEEE International Conference on Communications, 2008. ICC '08*, May 2008, pp. 3795–3800.

[129] W. Dang, M. Tao, H. Mu, and J. Huang, "Subcarrier-pair based resource allocation for cooperative multi-relay ofdm systems," *IEEE Transactions on Wireless Communications*, vol. 9, no. 5, pp. 1640–1649, May 2010.

[130] X. Li, Q. Zhang, G. Zhang, and J. Qin, "Joint power allocation and subcarrier pairing for cooperative ofdm af multi-relay networks," *IEEE Communications Letters*, vol. 17, no. 5, pp. 872–875, May 2013.

[131] P. Li, S. Guo, W. Zhuang, and B. Ye, "On efficient resource allocation for cognitive and cooperative communications," *IEEE Journal on Selected Areas in Communications*, vol. 32, no. 2, pp. 264–273, February 2014.

[132] M. Khafagy, A. Ismail, M. S. Alouini, and S. Aissa, "On the outage performance of full-duplex selective decode-and-forward relaying," *IEEE Communications Letters*, vol. 17, no. 6, pp. 1180–1183, June 2013.

[133] K. Tourki, K. A. Qaraqe, and M. S. Alouini, "Outage analysis for underlay cognitive networks using incremental regenerative relaying," *IEEE Transactions on Vehicular Technology*, vol. 62, no. 2, pp. 721–734, Feb 2013.

[134] F. Verde, A. Scaglione, D. Darsena, and G. Gelli, "An amplify-and-forward scheme for cognitive radios," in *2014 IEEE International Conference on Acoustics, Speech and Signal Processing (ICASSP)*, May 2014, pp. 2724–2728.

[135] ——, "An amplify-and-forward scheme for spectrum sharing in cognitive radio channels," *IEEE Transactions on Wireless Communications*, vol. 14, no. 10, pp. 5629–5642, Oct 2015.

[136] G. Kramer, M. Gastpar, and P. Gupta, "Cooperative strategies and capacity theorems for relay networks," *IEEE Transactions on Information Theory*, vol. 51, no. 9, pp. 3037–3063, Sept 2005.

[137] M. Naeem, D. C. Lee, and U. Pareek, "An efficient multiple relay selection scheme for cognitive radio systems," in *2010 IEEE International Conference on Communications Workshops (ICC)*, May 2010, pp. 1–5.

[138] T. Wang and L. Vandendorpe, "Wsr maximized resource allocation in multiple df relays aided ofdma downlink transmission," *IEEE Transactions on Signal Processing*, vol. 59, no. 8, pp. 3964–3976, Aug 2011.

[139] M. Choi, J. Park, and S. Choi, "Low complexity multiple relay selection scheme for cognitive relay networks," in *2011 IEEE Vehicular Technology Conference (VTC Fall)*, Sept 2011, pp. 1–5.

[140] M. Shaat and F. Bader, "Joint resource optimization in decode and forward multi-relay cognitive network with direct link," in *2012 IEEE Wireless Communications and Networking Conference (WCNC)*, April 2012, pp. 1398–1403.

[141] H. Al-Tous and I. Barhumi, "Resource allocation for multiple-user af-ofdma systems using the auction framework," *IEEE Transactions on Wireless Communications*, vol. 14, no. 5, pp. 2377–2393, May 2015.

[142] D. Gesbert, M. Shafi, D. shan Shiu, P. J. Smith, and A. Naguib, "From theory to practice : an overview of mimo space-time coded wireless systems," *IEEE Journal on Selected Areas in Communications*, vol. 21, no. 3, pp. 281–302, Apr 2003.

[143] G. Scutari and D. P. Palomar, "Mimo cognitive radio : A game theoretical approach," *IEEE Transactions on Signal Processing*, vol. 58, no. 2, pp. 761–780, Feb 2010.

[144] Y. J. A. Zhang and A. M. C. So, "Optimal spectrum sharing in mimo cognitive radio networks via semidefinite programming," *IEEE Journal on Selected Areas in Communications*, vol. 29, no. 2, pp. 362–373, February 2011.

[145] K. Wang, Y. Xiao, and Y. An, "Mimo cognitive radio system interference cancellation based on protograph ldpc codes," in *2012 IEEE 11th International Conference on Signal Processing (ICSP)*, vol. 2, Oct 2012, pp. 1283–1286.

[146] R. Iwata, V. Va, K. Sakaguchi, and K. Araki, "Experiment on mimo cognitive radio using tx/rx beamforming," in *2013 IEEE 24th International Symposium on Personal Indoor and Mobile Radio Communications (PIMRC)*, Sept 2013, pp. 2871–2875.

[147] Y. Liu and L. Dong, "Spectrum sharing in mimo cognitive radio networks based on cooperative game theory," *IEEE Transactions on Wireless Communications*, vol. 13, no. 9, pp. 4807–4820, Sept 2014.

[148] Q. Du and X. Zhang, "Effective capacity of superposition coding based mobile multicast in wireless networks," in *IEEE International Conference on Communications, 2009. ICC '09.*, June 2009, pp. 1–5.

[149] F. Hou, Z. Chen, J. Huang, Z. Li, and A. K. Katsaggelos, "Multimedia multicast service provisioning in cognitive radio networks," in *9th International Wireless Communications and Mobile Computing Conference (IWCMC), 2013*, July 2013, pp. 1175–1180.

[150] X. Zhang and M. Haenggi, "Successive interference cancellation in downlink heterogeneous cellular networks," in *2013 IEEE Globecom Workshops (GC Wkshps)*, Dec 2013, pp. 730–735.

[151] C. Ma, G. Sun, X. Tian, K. Ying, Y. Hui, and X. Wang, "Cooperative relaying schemes for device-to-device communication underlaying cellular networks," in *IEEE Global Communications Conference (GLOBECOM), 2013*, Dec 2013, pp. 3890–3895.

[152] S. Shalmashi and S. B. Slimane, "Cooperative device-to-device communications in the downlink of cellular networks," in *IEEE Wireless Communications and Networking Conference (WCNC), 2014*, April 2014, pp. 2265–2270.

[153] N. K. Pratas and P. Popovski, "Underlay of low-rate machine-type d2d links on downlink cellular links," in *IEEE International Conference on Communications Workshops (ICC), 2014*, June 2014, pp. 423–428.

[154] C. Ma, W. Wu, Y. Cui, and X. Wang, "On the performance of successive interference cancellation in d2d-enabled cellular networks," in *2015 IEEE Conference on Computer Communications (INFOCOM)*, April 2015, pp. 37–45.

[155] T. Yucek and H. Arslan, "A survey of spectrum sensing algorithms for cognitive radio applications," *IEEE Communications Surveys Tutorials*, vol. 11, no. 1, pp. 116–130, First 2009.

[156] Y. E. Lin, K. H. Liu, and H. Y. Hsieh, "On using interference-aware spectrum sensing for dynamic spectrum access in cognitive radio networks," *IEEE Transactions on Mobile Computing*, vol. 12, no. 3, pp. 461–474, March 2013.

[157] P. R. Parekh and M. B. Shah, "Spectrum sensing in wideband ofdm based cognitive radio," in *International Conference on Communications and Signal Processing (ICCSP), 2014*, April 2014, pp. 1476–1481.

[158] J. Jiang, H. Sun, D. Baglee, and H. V. Poor, "Achieving autonomous compressive spectrum sensing for cognitive radios," *IEEE Transactions on Vehicular Technology*, vol. 65, no. 3, pp. 1281–1291, March 2016.

[159] J. Shen, T. Jiang, S. Liu, and Z. Zhang, "Maximum channel throughput via cooperative spectrum sensing in cognitive radio networks," *IEEE Transactions on Wireless Communications*, vol. 8, no. 10, pp. 5166–5175, October 2009.

[160] M. J. Saber and S. M. S. Sadough, "Multiband cooperative spectrum sensing for cognitive radio in the presence of malicious users," *IEEE Communications Letters*, vol. 20, no. 2, pp. 404–407, Feb 2016.

[161] Y. Polyanskiy, H. V. Poor, and S. Verdu, "Channel coding rate in the finite blocklength regime," *IEEE Transactions on Information Theory*, vol. 56, no. 5, pp. 2307–2359, May 2010.

le cnam

Marwa CHAMI

Optimization in cognitive radio systems with successive interference cancellation and relaying

le cnam

Abstract :
In this thesis, we investigate the resource allocation problem for an uplink multi-user underlay Cognitive Radio system where the SU is allowed to coexist with the PU under the interference threshold constraint. First, we evaluate the performance of the single-user scenario, assuming perfect CSI at the SU. We propose an adaptive decoding algorithm where the SU can either treat the interference as noise or perform SIC or SC. We investigate the power allocation problem under some constraints. Secondly, the secondary multi-user scenario is investigated. Power and subcarrier allocation problems are detailed. Then, we study the single-user scenario where only statistical CSI is available at the SU. We detail the outage probabilities expressions and solve the non-convex optimization problem. Finally, we propose a new system model where the secondary receiver acts as a Full-Duplex relay node to maximize the primary rate. The proposed scenario is studied for AF and DF relaying protocols.

Keywords :
Cognitive radio, Optimization, OFDM, CSI, Relay, Full-Diplex

Résumé :
Dans cette thèse, nous étudions le problème d'allocation de ressources pour un système de radio cognitive où le SU est autorisé à coexister avec le PU sous la contrainte de seuil d'interférence. Tout d'abord, nous évaluons la performance du scénario à un seul utilisateur, avec une CSI parfaite à SU. Nous proposons un algorithme adaptatif où le SU peut traiter l'interférence comme du bruit ou appliquer SIC ou SC. Nous étudions le problème d'allocation de puissance sous certaines contraintes. Puis, le scénario multi-utilisateurs secondaires est étudié. Les problèmes d'allocation de puissance et de sous-porteuse sont détaillés. Ensuite, nous supposons que seule la CSI statistique est disponible à SU. Nous détaillons les expressions de probabilité d'interruption et résolvons le problème d'optimisation non convexe. Enfin, nous proposons un nouveau modèle où le récepteur secondaire agit comme un nœud de relais Full-Duplex. Le scénario proposé est étudié pour les protocoles AF et DF.

Mots clés :
Radio Cognitive, Optimisation, OFDM, CSI, Relais, Full-Diplex